



UNIVERSIDAD NACIONAL AUTÓNOMA
DE MÉXICO

FACULTAD DE CIENCIAS

Fermion Masses and Dark Matter

T E S I S

QUE PARA OBTENER EL TÍTULO DE:

Físico

PRESENTA:

Stefan Daniel Nellen Mondragón

TUTOR

Dr. Eduardo Peinado Rodríguez





Universidad Nacional
Autónoma de México

Dirección General de Bibliotecas de la UNAM

Biblioteca Central



UNAM – Dirección General de Bibliotecas
Tesis Digitales
Restricciones de uso

DERECHOS RESERVADOS ©
PROHIBIDA SU REPRODUCCIÓN TOTAL O PARCIAL

Todo el material contenido en esta tesis esta protegido por la Ley Federal del Derecho de Autor (LFDA) de los Estados Unidos Mexicanos (México).

El uso de imágenes, fragmentos de videos, y demás material que sea objeto de protección de los derechos de autor, será exclusivamente para fines educativos e informativos y deberá citar la fuente donde la obtuvo mencionando el autor o autores. Cualquier uso distinto como el lucro, reproducción, edición o modificación, será perseguido y sancionado por el respectivo titular de los Derechos de Autor.

A mis abuelos, Alfonso y Bernd.

A mis padres, Myriam y Lukas.

Y a mi hermana, Katia.

Agradecimientos

Agradezco al Dr. Eduardo Peinado por haberme asesorado durante de la escritura la tesis, y antes de eso durante la realización de mi servicio social. Fueron los dos cursos de teoría del campo que tomé con el que me llevaron a escoger un tema de investigación en física de altas energías. Así también agradezco su enorme apoyo y su guía, sin los cuales este trabajo no hubiera sido posible.

También agradezco al Dr. Newton Nath y al M.Sc. León García por su paciencia y apoyo durante la investigación y la escritura del artículo, y además por las diversas discusiones de las que, sin duda, aprendí muchísimo.

Agradezco a los sinodales, el Dr. Mariano Chernicoff, el Dr. Ángel Sánchez, el Dr. Eric Vázquez, y el Dr. Newton Nath, por haber leído esta tesis, y por sus comentarios y correcciones.

Agradezco a todos mis amigos que leyeron, o escucharon, partes de este trabajo. En particular, agradezco a Andrés por haber leído la tesis, y por su ayuda puliendo este trabajo. Además, agradezco las diversas conversaciones que he mantenido con él, de física y otros temas, las que me han mantenido motivado durante la carrera y me han impulsado a aprender más.

Agradezco a mis padres, a mi hermana, y a mi abuela, que tuvieron paciencia durante el periodo que realicé mi trabajo, y tuvieron que escuchar, voluntariamente o no, mis problemas y mi progreso, les agradezco mucho. También les agradezco haberme ayudado a mantenerme motivado, sobre todo durante el casi año y medio que llevamos de pandemia.

Por último, quiero agradecer a mis abuelos, Alfonso y Bernd, que, junto con mis padres, me inspiraron el amor por la física. Que en paz descansen.

Investigación realizada gracias al proyecto CONACyT CB-2017-2018/A1-S-13051, al Programa de Apoyo a Proyectos de Investigación e Innovación Tecnológica (PAPIIT) de la UNAM IN107118 e IN107621, y a la beca de colaboración en investigación alemán-mexicana SP 778/4-1 (DFG) y 278017 (CONACyT). Agradezco a la DGAPA-UNAM la beca recibida.

Resumen

En este trabajo se presenta y estudia un modelo de axión sabroso. Se derivan restricciones fenomenológicas a bajas energías, que permiten que el axión sabroso sea un candidato a materia oscura. Este axión surge mediante la identificación de la simetría de Peccei-Quinn con la simetría de Froggatt-Nielsen. En el primer capítulo se identifican los problemas que el modelo pretende resolver, estos son la ausencia de masa de neutrinos en el Modelo Estándar, la jerarquía en los valores de las masas de los fermiones, la existencia de materia oscura, y la posibilidad de que esta esté compuesta por un nuevo tipo de partícula. En el siguiente capítulo se discuten las masas en el Modelo Estándar y algunas extensiones simples, mientras que en el tercer capítulo los aspectos necesarios de física de axiones se presentan, tal que el modelo de axión sabroso pueda ser entendido. Luego, en el cuarto capítulo se construye el modelo partiendo del sector de quarks, donde a orden principal las matrices de masas adquieren una estructura de interacción a primeros vecinos (*Nearest-Neighbour-Interaction*). Los neutrinos obtienen masas de Majorana, con una estructura del tipo A_2 en su matriz de masas, por medio del mecanismo sube y baja (*seesaw*) tipo-I. El axión se extrae de los bosones de Goldstone de la teoría, y se compara contra el axión de la teoría de gran unificación de $SU(5)$. Posteriormente, se realiza un estudio numérico detallado de las masas y parámetros de mezcla de los quarks y leptones. Esto permite estudiar decaimientos que violan el sabor con axiones, al igual que violación del sabor mediada por corrientes neutras. Por último, el axión se propone como candidato a materia oscura, donde es producido por el mecanismo de desalineación (*misalignment mechanism*). Este modelo se desarrolló en colaboración con el Dr. Eduardo Peinado, el Dr. Newton Nath, y el M.Sc. León García.

Abstract

In this work a flavourful axion model is presented and studied. Constraints, derived from the low-energy phenomenology, on the parameters of this model permit the axion to be a dark matter candidate. This axion arises through an identification of the Froggat-Nielsen symmetry with the Peccei-Quinn symmetry. In the first chapter the problems which are to be solved are identified, mainly the lack of neutrino masses in the Standard Model and the hierarchy of the fermion mass values, the existence of dark matter, and the possibility that it is a new type of particle. Following this, in the next chapter the masses in the Standard Model and some very simple extensions are discussed, while in the third chapter the necessary aspects of axion physics are presented so that the flavourful axion model can be understood. Next, in the fourth chapter the model is constructed by parting from the quark sector, where at leading order the mass matrices acquire the Nearest-Neighbour-Interaction structure. The neutrinos get Majorana masses, with an A_2 structure of the mass matrix, by way of the type-I seesaw mechanism. The axion is extracted from the theory's Goldstone bosons, and is benchmarked against the $SU(5)$ grand unified theory axion. Following this, a detailed numerical study of the masses and mixing parameters of the quarks and leptons is done. This allows studying flavour violating decays with axions, as well as flavour violation mediated by flavour changing neutral currents. Finally, the axion is poised as a dark matter candidate through the misalignment mechanism. This model was developed in collaboration with Dr. Eduardo Peinado, Dr. Newton Nath, and M.Sc. León García.

Contents

Abstract	vi
List of Figures	xi
List of Tables	xiii
1 Introduction	1
1.1 Fermion Masses	2
1.2 Dark Matter	2
2 Masses in the Standard Model and Beyond	7
2.1 Masses in the Standard Model	7
2.1.1 Standard Model Lagrangian	7
2.1.2 Higgs Mechanism	11
2.1.3 Gauge Boson Masses	13
2.1.4 Higgs Boson Mass	16
2.1.5 Fermion Masses	16
2.1.6 Quark Masses and Mixings	18
2.1.7 Summary of Standard Model Parameters	20
2.2 Massive Neutrinos	21
2.2.1 Dirac and Majorana Masses	21
2.2.2 Seesaw Mechanism	23
2.2.3 Lepton Masses and Mixings	24
2.3 Froggatt-Nielsen Mechanism	26
2.3.1 Mass Hierarchy through $U(1)_{FN}$ and the Flavon Field	26
2.3.2 UV Completion	27
3 Axions	30
3.1 QCD Axions	30
3.1.1 The Strong CP Problem	31

3.1.2	Solving the Strong CP Problem: Axions and the Peccei-Quinn Symmetry	33
3.1.3	Axion Mass and Couplings	35
3.1.3.1	Axion Mass	37
3.1.3.2	Axion-Photon Coupling	39
3.1.4	Invisible Axion Models	40
3.2	Axions as Dark Matter Candidates	43
4	A Flavourful Axion Model	45
4.1	The Model	45
4.1.1	Overview of the Model	45
4.1.2	The Quark Sector	47
4.1.3	UV-Completion of the Quark Sector	48
4.1.3.1	Type-I Seesaw	48
4.1.3.2	Type-II Seesaw	51
4.1.4	The Lepton Sector	52
4.1.5	The Scalar Sector	54
4.1.6	The Axion	55
4.2	Numerical Analysis	57
4.2.1	Masses and Mixing Parameters of Fermions	57
4.2.1.1	Quark Masses and Mixing Parameters	59
4.2.1.2	Lepton Masses and Mixing Parameters	59
4.2.2	Flavour Violating Decays with Axions	61
4.2.3	Flavour Violating Higgs Couplings	64
4.2.4	Flavourful Axion as a Dark Matter Candidate	67
5	Conclusion	68
A	Why a New Particle?	70
B	Derivation of some Cosmological Quantities	72
B.1	Virial Mass of the Coma Cluster	72
B.2	Misalignment Mechanism	73
C	The Origin of the Strong CP Problem and two Axion Models	80
C.1	From the $U(1)$ Problem to the Strong CP Problem	80
C.2	PQWW Axion	84
C.3	KSVZ Axion	85
D	Redefinition of Phases in Mass Matrices	87

Bibliography

89

List of Figures

1.1	Galaxy rotation curves from Vera Rubin and her collaborators [1].	4
2.1	Graph showing the Higgs couplings to masses of some Standard Model particles as measured by the CMS collaboration [2].	17
2.2	Dimension five type-I Froggatt-Nielsen UV completion.	28
2.3	Dimension six type-I Froggatt-Nielsen UV completion.	29
2.4	Dimension five type-II Froggatt-Nielsen UV completion.	29
3.1	Chiral anomalies due to triangle diagrams.	32
3.2	Passing from the axion-anomaly coupling in the UV-complete theory to the effective axion-gluon coupling. The same applies to the axion-photon coupling. . .	41
4.1	UV-complete diagram within the DFSZ type-I seesaw framework from Eqs. (4.7) and (4.8).	49
4.2	UV-complete diagram within the DFSZ type-II seesaw framework from Eqs. (4.16), and (4.17).	51
4.3	UV complete diagram for a dimension-6 operator within the DFSZ type-I seesaw framework in presence of flavon field σ' as follows from Eqs. (4.27), and (4.28). . . .	54
4.4	Different axion models, including this flavourful axion, and bounds in the $g_{a\gamma} - m_a$ plane. Current bounds are solid, while future projections are transparent. The exception to this rule is the bound coming from Kaon decay (light brown), which is model dependent and only applicable for the flavourful axion (see Section 4.2.2). This plot was adapted from [3].	58

4.5	Exclusion region plot in the $(\tan \alpha - \tan \beta)$ plane obtained from the non-observation of the $t \rightarrow hc$ flavor violating decay. The gray colored region is excluded by ATLAS data [4], the purple colored region is expected to be probed in the future by the HL-LHC experiment [5] and the orange region will be further probed by ILC or CLIC [6]. The uncolored region (see white thin band) predicts a branching ratio beyond the sensitivity of these experiments. The dashed line indicates limit of no flavor violation in light Higgs Yukawa couplings.	65
-----	--	----

List of Tables

2.1	Representations and charges of the SM fields.	8
2.2	Standard Model free parameters.	20
2.3	Lepton masses and mixing parameters from [7, 8]. Normal mass ordering is assumed here.	26
4.1	Field content and transformation properties of the PQ-symmetry under the DFSZ type-I seesaw model, where $i = 1, 2, 3$ represent families of three quarks. The PQ charges of the quarks are given in the order of the families' masses, with the lightest as the first.	47
4.2	Vector like fermions and their transformation properties of the PQ-symmetry under the DFSZ type-I seesaw model, where $C = L, R$	49
4.3	Field content and transformation properties of the leptonic fields and the scalar field σ' , where $i = 1, 2, 3$ represent the three lepton families.	52
4.4	Best-fit values of the model parameters in the quark sector are shown in the upper table. The global best-fit as well as their 1σ error [8, 9] for the various observables are given in the second and third columns of the lower table. Also, the best-fit values of the various observables are listed in the last column of the lower table.	60
4.5	Best-fit values of the model parameters in the lepton sector are shown in the upper table. The global best-fit as well as their 1σ error [7, 8, 9] for the various observables are given in the second and third columns of the lower table. Also, the best-fit values of the various observables are listed in the last column of the lower table.	61

Introduction

The consolidation of the Standard Model of Particle Physics (SM) during the 1970s can be considered one of the greatest scientific achievements of the past century. This model explains three fundamental forces of nature, the electromagnetic force, the weak force, and the strong force, with gravity notably absent. Although the model has been tested to varying degrees of accuracy, most of which agree with the SM, there still exist unanswered questions. Besides the fact that gravity is missing from the SM, the masses of the fermions pose some of the most important open questions. For example, the masses and nature of the neutrinos, as well as the wide range of the values of the fermion masses, which span many orders of magnitude, are some of the problems which can be considered unanswered by the SM in its current state.

Moving on to a much greater scale, of the order of at least Mpc, unanswered questions in cosmology regarding the nature of dark matter open the SM for extensions that must be consistent with cosmology, the so-called dark sector. There is the possibility (or necessity, depending on one's point of view) to explain minimally and concisely the phenomena at short distances (or high energies) with those at cosmological scales.

In this work a model addressing the mass hierarchies of the SM fermions (including neutrinos), and the strong CP problem, while at the same time giving a possible dark matter candidate, a flavourful axion, is presented. The name *flavourful axion* stems from the fact the Peccei-Quinn and Froggatt-Nielsen symmetries are identified, whereupon the Peccei-Quinn symmetry is treated as a flavour symmetry, and its Goldstone boson, the axion, becomes flavourful.

The aim of this chapter is to motivate the problem from the particle physics point of view (Section 1.1), and also to give an historical motivation to the dark matter problem (Section 1.2). Before the model is presented, an overview of the theoretical framework behind it is given. In Chapter 2 masses and mass generation in the Standard Model are discussed (Section 2.1), including the simplest realizations of massive neutrinos (Section 2.2). A possible solution to the mass hierarchy problem is given by the Froggatt-Nielsen mechanism, which is the topic of Section 1.1. Chapter 3 deals

with the fundamentals of axion physics, with an emphasis on parameters studied in the model (Chapter 4), including the dark matter relic density. Longer calculations and some minor topics not directly related to the model are relegated to the different appendices, in a way that the main body of this work is mostly self-contained.

1.1 Fermion Masses

Regarding fermions, the most obvious issue in the SM are the massless neutrinos. Although the possibility of neutrinos having non-zero masses has been proposed at least since Pontecorvo's work in the 1950s (see for example [10]), wherein the possibility of flavour oscillations occurring between neutrinos was studied. Nevertheless, almost 50 years had to pass for the experimental confirmation of neutrino oscillations, for which a Nobel Prize was awarded in 2015 to Takaaki Kajita and Arthur B. McDonald for the work of the Super-Kamiokande [11] and SNO [12] experiments, respectively. Since these oscillations can only occur if the neutrinos are massive, there is clear incentive to extend the SM by allowing for massive neutrinos. Interestingly, neutrinos masses are not as clearly defined as those of the other fermions. Neutrinos in the SM are chiral, and only left-handed neutrinos (and hence right-handed anti-neutrinos) appear in this model. In particular, it is unclear whether they are Majorana fermions or Dirac fermions, the latter case would also imply the existence of right-handed neutrinos (see Section 2.2).

Another problem, more philosophical in nature, is the fermion mass-hierarchy. The fermion masses in the SM are generated by the Higgs mechanism (see Section 2.1.2), and thus depend on the vacuum expectation value and the Yukawa couplings between the Higgs doublet and the fermions. The mass of the electron is $m_e \approx 0.511$ MeV, while that of the top quark is $m_t \approx 172$ GeV. There is a difference of six orders of magnitude between these two fermions, and hence between the biggest and smallest Yukawa coupling. This wide range in the values of the couplings can be considered unnatural¹. Therefore, extensions of the SM explaining this hierarchy are proposed. These can range from minimal extensions like that presented here (Froggatt-Nielsen) to explanations coming from string theory (for example [13]).

1.2 Dark Matter

Dark matter (DM) is matter that interacts gravitationally at long range, but otherwise very weakly. The *dark* comes from the fact that this kind of matter interacts very weakly, if at all, with the electromagnetic field, thus making it very elusive and

¹Where *naturalness* should be considered as the property of all the couplings to be of order 1.

practically invisible to direct electromagnetism based observation. There is compelling evidence for its existence using indirect observations, as will be seen in this section and Appendix A. DM has been, and continues to be, a strong motivator for extending the SM. Arguments in favour of DM composed of a new kind of particle are presented in Appendix A, in contrast with baryonic DM or modifications of gravitational dynamics without DM.

The first appearance of the modern concept of DM is often attributed to Fritz Zwicky [14]¹. What Zwicky did is apply the virial theorem to the Coma galaxy cluster [15], finding an upper bound for its mass², M_C , of

$$M_c > 9 \times 10^{43} \text{ kg.} \quad (1.1)$$

With the former in mind and an estimation of the number of sun-like stars he found a mass-to-light ratio of 500³, one of the conclusions of this unusually high number was that there exists a large amount of non-radiating matter in the cluster, i.e. DM. Nowadays it is known that clusters of the size of Coma do actually have an asymptotical mass-to-light ratio of about 400, which somewhat agrees with Zwicky's result. His calculation was not correct due to a value for the Hubble constant (to infer the speed of the cluster) that was an order of magnitude too large [15]. Nevertheless, his conclusion of the existence of unseen matter is one of the early suggestions of DM.

Contemporary to Zwicky (actually a bit earlier, in 1932), Jan Oort found that the amount of observable mass in a galaxy was only about a third of the total mass, by analyzing the dynamics of stars of varying sizes [16, 17]. This did not garner much attention at the time (for that matter, neither did Zwicky's work on the subject), but a general method of identifying these discrepancies arose in the form of the rotation curves of galaxies. A rotation curve of a galaxy is a plot of the rotational velocity, v_c , of the stars and gas in the galaxy against the galactic radius r , where this means the distance to the symmetry axis of the galaxy. The expectation for such a curve is Keplerian in the limit $r \rightarrow \infty$, this means $v \propto r^{-\frac{1}{2}}$. This expectation stems from the form of the Newtonian potential. An axisymmetric galaxy has the following speed profile

$$v_c = \sqrt{\frac{G_N M(r)}{r}}, \quad (1.2)$$

with $M(r)$ the mass enclosed by a sphere of radius r centred on the galactic centre. Outside the sphere M is constant and v_c declines as $r^{-\frac{1}{2}}$. Notice this holds even for

¹Zwicky's original paper stems from 1933, and was written in German, the cited paper is a review of that work from 1937.

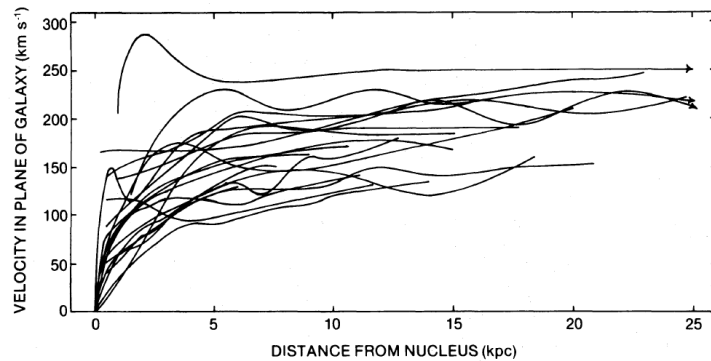
²See Appendix B.1 for an outline of the derivation of this result.

³This quantity is adimensional, since it is normalized to the Sun's mass-to-light-ratio.

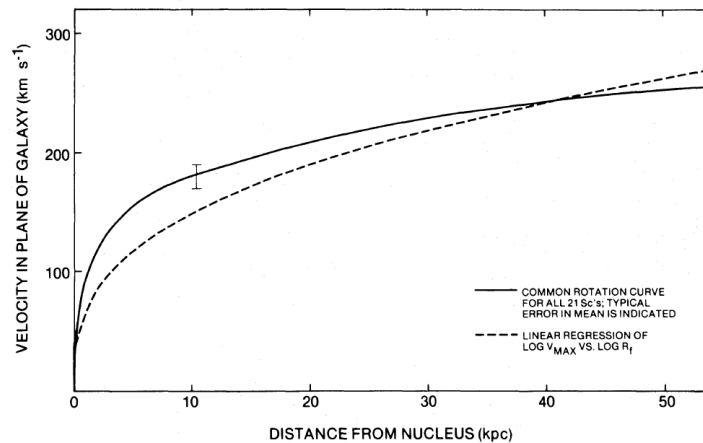
non-uniform mass distributions, ρ . In general, a spherically symmetrical distribution satisfies

$$\rho(r) = \frac{1}{4\pi r^2} \frac{dM(r)}{dr}. \quad (1.3)$$

The density distribution will only affect rotation when $r < R$, with R the galactic radius.



(a) Rotation curves of 21 light galaxies.



(b) Mean rotation curve for the 21 galaxies (solid line) and least-squares fit to a model presented in [1].

Figure 1.1: Galaxy rotation curves from Vera Rubin and her collaborators [1].

By the 1970s and 1980s, in great part because of Vera Rubin's work [1], it was clear that the Keplerian limit was not satisfied, in fact in the limit of large radial distances the rotation curves become constant, what is now called a flat rotation curve (see Fig. 1.1). An explanation for this phenomenon is the existence of a *dark halo*, a distribution of matter, that interacts gravitationally with the rest of the galaxy, but is not observable,

in other words, a DM distribution. The mass density, ρ , can be written as

$$\rho(r) = \rho_v(r) + \rho_D(r) \quad (1.4)$$

the sum of the visible matter and DM densities. The visible matter will experience Keplerian falloff as r increases, after a maximum r_m at $0 < r_m < R$, but if the galactic halo is large enough (i.e. at least $R_h \geq R$), the falloff will not be observed. Take as an example a simplified scenario, where the dark halo is spherical and the contribution of visible matter can be neglected (i.e. in the limit $r \sim R$). From Eq. (1.2) it can be seen that to get flat rotation curves $M(r) \propto r$, therefore combining Eq. (1.2) and Eq. (1.3) one arrives at the mass distribution in presence of this halo

$$\rho(r) = \frac{v_c^2}{4\pi G_N r^2}. \quad (1.5)$$

This is obviously an idealized result, but it shows that the density should have a factor of $r^{-\gamma}$, with $\gamma \sim 2$, as $r \gg 0$ ¹. As a sidenote, the inclusion of a dark halo stabilizes the galaxy. Numerical simulations show that galactic disks are unstable and tend to form bars, unless there is a large enough dispersion of velocities (see for example [18]).

Another indication for the existence of DM is the gravitational lensing of light [15]. As postulated by General Relativity, massive objects bend the trajectory of light, causing a lensing effect. This lensing can manifest either as the appearance of multiple images of the same object (strong lensing) or the distortion of said object (weak lensing). Measuring the deflection of light it is possible to estimate the mass of galaxies and other celestial bodies.

If DM is not baryonic or composed of massive objects, then it must indeed be a new type of matter, a *new particle*. Based on Λ CDM (Lambda Cold Dark Matter), the standard cosmological model, and some of the phenomena mentioned in this section and Appendix A, where many arguments in favour of particle dark matter are laid out, there are some properties a DM candidate should have. These are [15]:

- **Dark:** This means roughly that the DM candidate should interact very weakly, if at all with the electromagnetic field. An important aspect of this is that the DM candidate would radiate photons very inefficiently, rendering it dissipationless².
- **Collisionless:** What should be understood exactly is that the self-interaction to mass ratio is small $\frac{\sigma_{xx}}{m_x} \ll 1$. Or equivalently, that the mean free path of these particles should be of the order of galaxy cluster sizes, i.e. Mpc.

¹A common parametrization is $\rho(r) = \frac{\rho_0}{1+(\frac{r}{a})^\gamma}$, where a is a characteristic linear scale of the galaxy.

²Consequences of this are that the DM particle would not accrete nor collapse to the center of gravity as easily as baryons do [15].

- **Classical:** In the sense that the particles' de Broglie wavelength should not be larger than a dwarf galaxy's scale (of the order of kpc), so that the dark halo can be coherent.
- **Fluid:** The DM candidate should mostly behave as a fluid. If this were not the case, i.e. if it was granular, forming massive particles of considerable mass, the effect of the DM would destabilize and disrupt present structures, for example by heating galactic disks. Also, it would result in more microlensing than is observed.

These characteristics are not as constraining as they seem. The particle should interact weakly compared to its mass, it should be optically opaque and its distribution should correspond to Λ CDM. A very popular category of DM candidates are the WIMPs (Weakly Interacting Massive Particles), particles that are coupled at least as weakly as the weak interaction, therefore at large scales its main interaction is gravitational. Another popular candidate, and the focus of this work, are axions and axion-like particles (see Chapter 3), these are very light scalar particles, that originally were postulated as a solution to the Strong CP problem (see Section 3.1.2).

SM extensions, which account for DM, can also serve to guide other, different SM extensions, with the aim to solve different problems within the same framework. For example, in Chapter 4, a model is presented where an axion arises as a DM candidate, while simultaneously explaining the fermion mass hierarchy, and solving the strong CP problem. In this regard, it is also necessary to understand the problem from the point of view of particle physics, in particular how the SM works, and how to extend it consistently. This is the aim of the next chapter.

Masses in the Standard Model and Beyond

In this chapter the tree-level masses in the Standard Model are introduced (Section 2.1). Since initially, all the particles in the Standard Model are massless, the Higgs mechanism, which gives the SM particles their mass, is also explained (Section 2.1.2). With this mechanism the masses of all the particles are derived at tree-level from massless Lagrangian. Later, two simple extensions of the Standard Model are explained, regarding neutrino masses (Section 2.2), and the fermion mass hierarchy (Section 2.3).

2.1 Masses in the Standard Model

Masses in the Standard Model (SM) do not appear in the Lagrangian until the Electroweak (EW) symmetry breaks, through a mechanism known as the Higgs Mechanism (see Section 2.1.2). After this, the charged fermions, the weak gauge bosons, and the Higgs boson become massive. At the end of this section, in table section 2.1.7, the free parameters of the SM, including the masses, are summarized. The approach taken here follows mostly from the textbooks [19, 20].

2.1.1 Standard Model Lagrangian

To understand how masses appear in the SM it is useful to know the structure of its Lagrangian. The SM is a $SU(3)_C \times SU(2)_L \times U(1)_Y$ Yang-Mills theory [19], where $SU(3)_C$ is the Quantum Chromodynamics (QCD) gauge group and $SU(2)_L \times U(1)_Y$ is the EW gauge group, which is spontaneously broken down to $U(1)_Q$, the electromagnetic (EM) gauge group. As will be shown in Section 2.1.3 this is not the same as $U(1)_Y$, which corresponds to (weak) hypercharge. The group $SU(2)_L$ corresponds to the weak isospin. It is worth noting that $SU(2)_L \times U(1)_Y$ is a chiral theory, which means left- and right-handed fermions transform differently. Before symmetry breaking all fields

	G_μ^a	W_μ^a	B_μ	Q^n	u_R^n	d_R^n	L^n	e_R^n	H
$SU(3)_C$ representation	8	1	1	3	3	3	1	1	1
$SU(2)_L$ representation	1	3	1	2	1	1	2	1	2
Hypercharge Y	0	0	0	1/6	2/3	-1/3	-1/2	-1	1/2

Table 2.1: Representations and charges of the SM fields.

in the SM are massless. The mechanism through which the symmetry breaking occurs and the fields acquire mass is explained in section 2.1.2.

For $SU(3)_C$ there are eight gauge bosons called gluons, G_μ^a , with a running from 1 to 8. The gauge bosons belonging to $SU(2)_L$ are W_μ^a , here a runs from 1 to 3¹. Finally, the $U(1)_Y$ gauge boson is B_μ . Fermions are usually separated into two categories: quarks and leptons. Quarks carry colour charge and thus couple to gluons, whereas leptons do not. In other words, quarks of each flavour transform under $SU(3)_C$ as triplets, whereas leptons transform trivially. This means that a quark field q is represented as

$$q = \begin{pmatrix} q_R \\ q_G \\ q_B \end{pmatrix}. \quad (2.1)$$

The three entries represent the three colour charges a quark can have: red, green, and blue, or anti-red, anti-green, and anti-blue, for quarks and anti-quarks, respectively. For $SU(2)_L$ the situation is somewhat different as it distinguishes between left and right fields. Left-handed fermions transform as doublets, while right-handed fermions transform as singlets. Therefore, the fermions can be written as

$$Q^n = \begin{pmatrix} u_L^n \\ d_L^n \end{pmatrix}, \quad L^n = \begin{pmatrix} \nu_L^n \\ e_L^n \end{pmatrix}, \quad u_R^n, \quad d_R^n, \quad \nu_R^n, \quad e_R^n, \quad (2.2)$$

where n runs from 1 to 3 and represents the generation the fermion belongs to. Thus each fermion can actually be one of the following $u^n \in \{u, c, t\}$, $d^n \in \{d, s, b\}$, $e^n \in \{e, \mu, \tau\}$ and $\nu^n \in \{\nu_e, \nu_\mu, \nu_\tau\}$. Lastly, there is a complex scalar $SU(2)_L$ doublet, H , which can be written as

$$H = \begin{pmatrix} H^+ \\ H^0 \end{pmatrix}. \quad (2.3)$$

A summary of the representations and charges of the SM fields is given in Table 2.1.

The Standard Model Lagrangian, before symmetry breaking, can be written as follows

$$\mathcal{L}_{SM} = \mathcal{L}_G + \mathcal{L}_F + \mathcal{L}_S + \mathcal{L}_Y, \quad (2.4)$$

¹For any $SU(N)$, there will be $N^2 - 1$ gauge bosons, as these transform in the adjoint representation.

\mathcal{L}_G represents the gauge boson kinetic Lagrangian, \mathcal{L}_F the fermion kinetic Lagrangian, \mathcal{L}_S the scalar Lagrangian, and \mathcal{L}_Y the Yukawa terms.

The gauge boson kinetic Lagrangian is given by

$$\mathcal{L}_G = -\frac{1}{4}G_{\mu\nu}^a G_a^{\mu\nu} - \frac{1}{4}W_{\mu\nu}^a W_a^{\mu\nu} - \frac{1}{4}B_{\mu\nu} B^{\mu\nu}, \quad (2.5)$$

where

$$\begin{aligned} G_{\mu\nu}^a &= \partial_\mu G_\nu^a - \partial_\nu G_\mu^a + g_s f_{bc}^a G_\mu^b G_\nu^c, \\ W_{\mu\nu}^a &= \partial_\mu W_\nu^a - \partial_\nu W_\mu^a + g \epsilon_{bc}^a W_\mu^b W_\nu^c, \\ B_{\mu\nu} &= \partial_\mu B_\nu - \partial_\nu B_\mu, \end{aligned} \quad (2.6)$$

are the field strength tensors for gluons, and the W^a and B bosons, respectively. Additionally, g_s is the strong coupling constant, g the weak coupling constant, $f_{bc}^a = f^{abc}$ are the $SU(3)$ structure constants, and $\epsilon_{bc}^a = \epsilon^{abc}$ the $SU(2)$ structure constants.

The fermion Lagrangian is

$$\mathcal{L}_F = \sum_{\Psi} \bar{\Psi} i \gamma^\mu D_\mu \Psi, \quad (2.7)$$

where the sum runs over all fermions Ψ . One has to take care with D_μ , the covariant derivative, since different fermions do not necessarily transform in the same way. In general it can be written as

$$D_\mu \Psi = \left(\partial_\mu - i F_{SU(3)_C} g_s \frac{1}{2} \lambda_a G_\mu^a - i F_{SU(2)_L} g \frac{1}{2} \sigma_a W_\mu^a - i Y g' B_\mu \right) \Psi. \quad (2.8)$$

The factors $F_{SU(3)_C}$ and $F_{SU(2)_L}$ are dependent on the representation of the field under the gauge group. For an arbitrary $SU(N)$ they are

$$F_{SU(N)}(\Psi) = \begin{cases} 1, & \text{if } \Psi \text{ is in the fundamental representation} \\ 0, & \text{if } \Psi \text{ is in the trivial representation} \\ -1, & \text{if } \Psi \text{ is in the anti-fundamental representation} \end{cases} \quad (2.9)$$

For $SU(N)$ the N representation is fundamental and 1 is trivial. Conjugate fields transform in the conjugate representation. It is also worth noting that the hypercharge Y is field dependent as well, the hypercharge of the conjugate of a field also changes sign. Also, it should be kept in mind that when numbers are summed with matrices, it is understood that these represent the identity matrix multiplied by said number, for example $\sigma_a + Y = \sigma_a + Y I_{2 \times 2}$. All charges and representations can be read off from Table 2.1. The hypercharge coupling constant, g' was introduced, as well as σ_a , the

three Pauli matrices, and λ_a , the eight Gell-Mann matrices.

The scalar Lagrangian is

$$\mathcal{L}_S = (D_\mu H)^\dagger (D^\mu H) - \mu^2 H^\dagger H - \lambda (H^\dagger H)^2, \quad (2.10)$$

where μ and λ are the quadratic and quartic couplings, respectively. The quartic coupling can be interpreted as a mass, but in order for the Higgs Mechanism to work it must be imaginary. From Eq. (2.8) it follows by replacing Ψ with H , that

$$D_\mu H = \left(\partial_\mu - ig \frac{1}{2} \sigma_a W_\mu^a - ig' \frac{1}{2} B_\mu \right) H. \quad (2.11)$$

It is common to write the Lagrangian as

$$\mathcal{L}_S = (D_\mu H)^\dagger (D^\mu H) - V(H), \quad V(H) = \mu^2 H^\dagger H + \lambda (H^\dagger H)^2, \quad (2.12)$$

especially when the scalar potential, $V(H)$, is more complicated.

The last part of the SM Lagrangian contains the Yukawa interactions. These are the couplings of fermions to H . A general Lorentz invariant Yukawa term is proportional to

$$\bar{\Psi}_i H \Psi_j. \quad (2.13)$$

This is not $SU(2)_L \times U(1)_Y$ invariant in general, though. Also, the fermion mass terms are proportional to

$$\bar{\Psi} \Psi = \bar{\Psi}_L \Psi_R + \bar{\Psi}_R \Psi_L, \quad (2.14)$$

which is also not invariant under $SU(2)_L \times U(1)_Y$ in general. This means that the most general $SU(2)_L \times U(1)_Y$ invariant Yukawa term must contract the left-handed doublet Ψ_L with H , and then multiply Ψ_R . As a consequence, there will be no mixing between leptons and quarks, and neutrinos will not possess Yukawa terms. The lepton Yukawa terms take the form

$$\mathcal{L}_{Y,l} = -y_{ij}^e \bar{L}^i H e_R^j, \quad (2.15)$$

where the indexes i, j run over the three generations and a sum is implied. In the SM y^e is diagonal. For quarks there is a small complication, since $U(1)_Y$ must also be conserved. For this to happen the sum of hypercharges in the Yukawa term must be 0. This is not a problem for the down-type quarks, since the hypercharges in

$$\mathcal{L}_{Y,d} = -y_{ij}^d \bar{Q}^i H d_R^j \quad (2.16)$$

are $-1/6 + 1/2 - 1/3 = 0$. The analogue for up-type quarks would sum $-1/6 + 1/2 + 2/3 = 1$, which is not $U(1)_Y$ invariant. It would be if $1/2$ was exchanged to $-1/2$,

i.e. H would have to be replaced by its $U(1)_Y$ conjugate, while also being an $SU(2)_L$ doublet. This is most easily realized by defining

$$\tilde{H} \equiv i\sigma_2 H^*, \quad (2.17)$$

which transforms as a doublet under $SU(2)_L$, but has the opposite $U(1)_Y$ charge. Thus, the Yukawa term for up-type quarks is

$$\mathcal{L}_{Y,u} = -y_{ij}^u \bar{Q}^i \tilde{H} u_R^j. \quad (2.18)$$

Lastly, \mathcal{L}_Y is the sum of Eqs. (2.15), (2.16), and (2.18) and their hermitian conjugates (h.c.), since the Lagrangian has to be real (so that the action is real). Thus the Yukawa Lagrangian of the SM is

$$\mathcal{L}_Y = -y_{ij}^e \bar{L}^i H e_R^j - y_{ij}^u \bar{Q}^i \tilde{H} u_R^j - y_{ij}^d \bar{Q}^i H d_R^j + h.c. \quad (2.19)$$

2.1.2 Higgs Mechanism

As mentioned before, the SM gauge group, $SU(3)_C \times SU(2)_L \times U(1)_Y$, is spontaneously broken down to $SU(3)_C \times U(1)_Q$. This happens because the Higgs doublet acquires a vacuum expectation value (vev), characterized by

$$v = \sqrt{\frac{-\mu^2}{\lambda}}, \quad (2.20)$$

which is possible when the $\mu^2 < 0$ and $\lambda > 0$ in the scalar potential of Eq. (2.12). Goldstone's Theorem [21, 22, 23] states that in a spontaneously broken continuous symmetry, a massless scalar boson, known as a *Goldstone boson*, arises for every broken generator of the symmetry. This is not observed in a gauge symmetry, as the Goldstone bosons are absorbed by the gauge bosons, which become massive. The mechanism through which this occurs is called the *Higgs Mechanism*.

This mechanism is more easily illustrated in an Abelian gauge theory, as the process is conceptually the same. Consider a $U(1)$ gauge theory with a complex scalar field, ϕ . The Lagrangian of this is

$$\mathcal{L} = -\frac{1}{4} F_{\mu\nu} F^{\mu\nu} + (D_\mu \phi)^\dagger (D^\mu \phi) - \mu^2 \phi^\dagger \phi - \lambda (\phi^\dagger \phi)^2, \quad (2.21)$$

where $F_{\mu\nu} = \partial_\mu A_\nu - \partial_\nu A_\mu$, and A_μ is the theory's gauge boson, and $D_\mu = \partial_\mu - ieA_\mu$, with e being the scalar coupling to the gauge field. If $\mu^2 < 0$, $\langle 0|\phi|0\rangle = 0$ is not a minimum of the potential (here it is a local maximum), thus the field acquires a vev ,

spontaneously breaking $U(1)$. After symmetry breaking the field can be written as

$$\phi(x) = \frac{v + h(x)}{\sqrt{2}} e^{i\frac{\pi(x)}{v}}, \quad (2.22)$$

here h is a real scalar field, which satisfies $\langle 0|h|0\rangle = 0$, and π a Goldstone boson. The factors of $\frac{1}{\sqrt{2}}$ and $\frac{1}{v}$ preserve canonical normalization in the kinetic terms. Substituting Eq. (2.22) in the Lagrangian of Eq. (2.21)

$$\begin{aligned} \mathcal{L} = & -\frac{1}{4}F_{\mu\nu}F^{\mu\nu} \\ & + \frac{1}{2}\left(\partial_\mu h - i\frac{1}{v}(v+h)\partial_\mu\pi - ie(v+h)A_\mu\right)\left(\partial^\mu h + i\frac{1}{v}(v+h)\partial^\mu\pi + ie(v+h)A^\mu\right) \\ & - \frac{\mu^2}{2}(v+h)^2 - \frac{\lambda}{4}(v+h)^4, \end{aligned} \quad (2.23)$$

where the exponentials have canceled. The field h has mass given by the quadratic terms in the Lagrangian, while π is massless. To see what happens to the gauge field it is useful to focus only on its kinetic terms, i.e. in

$$\mathcal{L}_A = -\frac{1}{4}F_{\mu\nu}F^{\mu\nu} + \frac{e^2v^2}{2}\left(A_\mu + \frac{1}{ev}\partial_\mu\pi\right)\left(A^\mu + \frac{1}{ev}\partial^\mu\pi\right). \quad (2.24)$$

The field A_μ has acquired mass $m_A = ev$, but there is also kinetic mixing between A_μ and π in the form of an $evA_\mu\partial^\mu\pi$ term. This term can be removed by the gauge transformation

$$A_\mu \rightarrow A_\mu - \frac{1}{ev}\partial_\mu\pi. \quad (2.25)$$

This gauge is called the *unitary gauge*. Therefore, the gauge boson has absorbed the Goldstone boson and as such has now three degrees of freedom, which means it has acquired mass (the new degree of freedom corresponds to longitudinal polarization). It is often said that *the gauge boson eats the Goldstone boson, thus acquiring mass*.

Returning to the SM, after symmetry breaking the Higgs doublet can be written as

$$H(x) = \exp\left(2i\frac{\tau_a\pi^a(x)}{v}\right)\begin{pmatrix} 0 \\ \frac{1}{\sqrt{2}}(v+h(x)) \end{pmatrix}, \quad (2.26)$$

where h is a real scalar, called the Higgs boson, and $\tau_a = \frac{\sigma_a}{2}$ are the $SU(2)$ generators, with $a = 1, 2, 3$. As in the Abelian case, the factors of $\frac{1}{\sqrt{2}}$ and $\frac{2}{v}$ are included to preserve canonical normalization of the fields. The *vev* of the Higgs doublet is

$$\langle H \rangle = \langle 0|H|0 \rangle = \begin{pmatrix} 0 \\ \frac{v}{\sqrt{2}} \end{pmatrix}. \quad (2.27)$$

In the unitary gauge $\pi^a = 0$, thus

$$H(x) = \begin{pmatrix} 0 \\ \frac{1}{\sqrt{2}}(v + h(x)) \end{pmatrix}. \quad (2.28)$$

This simplifies the Lagrangian considerably, but as in the abelian case, one can do the entire calculation explicitly and then remove π^a with a gauge transformation. The Lagrangian after symmetry breaking becomes quite complicated, as three of the EW gauge bosons become massive (as well as the fermions, which will be discussed in 2.1.5) and 3- and 4-point interactions appear between gauge bosons themselves, as well as with the Higgs boson, which can no longer be written in a somewhat compact Lagrangian.

2.1.3 Gauge Boson Masses

Through the Higgs Mechanism the weak gauge bosons acquire mass. Since there remains an unbroken $U(1)_Q$, one boson must remain massless. This corresponds to the massless photon of QED. To focus on the masses of the vector bosons it is enough to look at $(D_\mu \langle H \rangle)^\dagger (D^\mu \langle H \rangle)$, taking D_μ as in Eq. (2.12) and noticing that $\partial_\mu \langle H \rangle = 0$, it follows that

$$(D_\mu \langle H \rangle)^\dagger (D^\mu \langle H \rangle) = \frac{v^2}{8} \begin{pmatrix} 0 & 1 \end{pmatrix} \begin{pmatrix} gW_\mu^3 + g'B_\mu & g(W_\mu^1 - iW_\mu^2) \\ g(W_\mu^1 + iW_\mu^2) & -g'B_\mu + gW_\mu^3 \end{pmatrix}^2 \begin{pmatrix} 0 \\ 1 \end{pmatrix}. \quad (2.29)$$

Defining

$$W_\mu^\pm \equiv \frac{1}{\sqrt{2}}(W_\mu^1 \mp iW_\mu^2), \quad (2.30)$$

it follows that

$$(D_\mu \langle H \rangle)^\dagger (D^\mu \langle H \rangle) = \frac{v^2}{8} (2g^2 W_\mu^+ W^{-\mu} + (gW_\mu^3 - g'B_\mu)^2). \quad (2.31)$$

The W^+ and W^- bosons are two of the massive vector bosons, whose mass can be read from Eq. (2.31) as $m_W = \frac{gv}{2}$, the photon and the third massive vector boson must come from $(gW_\mu^3 - g'B_\mu)^2$. This term can be expressed as

$$(gW_\mu^3 - g'B_\mu)^2 = \begin{pmatrix} B^\mu & W^{3\mu} \end{pmatrix} \begin{pmatrix} g'^2 & -gg' \\ -gg' & g^2 \end{pmatrix} \begin{pmatrix} B_\mu \\ W_\mu^3 \end{pmatrix}. \quad (2.32)$$

This matrix must be diagonalized to give the masses of the new bosons. The matrix is orthogonal, so it must be diagonalized by a rotation, which is to be expected, as the

fields are canonically normalized. The matrix that diagonalizes is given by

$$O = \frac{1}{\sqrt{g^2 + g'^2}} \begin{pmatrix} g & -g' \\ g' & g \end{pmatrix} = \begin{pmatrix} \cos \theta_W & -\sin \theta_W \\ \sin \theta_W & \cos \theta_W \end{pmatrix}, \quad (2.33)$$

where θ_W is the Weinberg angle and is a free parameter of the SM. It follows from this that $\tan \theta_W = \frac{g'}{g}$, i.e. $g \sin \theta_W = g' \cos \theta_W$. After diagonalization Eq. (2.32) becomes

$$(gW_\mu^3 - g'B_\mu)^2 = \begin{pmatrix} A^\mu & Z^\mu \end{pmatrix} \begin{pmatrix} 0 & 0 \\ 0 & g^2 + g'^2 \end{pmatrix} \begin{pmatrix} A_\mu \\ Z_\mu \end{pmatrix}, \quad (2.34)$$

where

$$\begin{aligned} A_\mu &\equiv \sin \theta_W W_\mu^3 + \cos \theta_W B_\mu \\ Z_\mu &\equiv \cos \theta_W W_\mu^3 - \sin \theta_W B_\mu. \end{aligned} \quad (2.35)$$

Lastly, Eq. (2.31) takes the following form

$$(D_\mu \langle H \rangle)^\dagger (D^\mu \langle H \rangle) = \frac{g^2 v^2}{4} W_\mu^+ W^{-\mu} + \frac{(g^2 + g'^2)v^2}{8} Z_\mu Z^\mu + 0 \cdot A_\mu A^\mu. \quad (2.36)$$

As a consequence of this, the last massive vector boson, the Z boson, has a mass $m_Z = \frac{v}{2} \sqrt{g^2 + g'^2} = \frac{gv}{2 \cos \theta_W} = \frac{m_W}{\cos \theta_W}$, implying that the mass of the W bosons is smaller than that of the Z boson. Another result is that the photon, A_μ , is massless and therefore it must be the gauge boson of $U(1)_Q$.

To get the full vector boson kinetic terms it is necessary to rewrite

$$-\frac{1}{4} W_\mu^a W_a^\mu - \frac{1}{4} B_\mu B^\mu. \quad (2.37)$$

Using the definitions of Eqs. (2.30) and (2.35) it follows directly that

$$\begin{aligned} \mathcal{L}_{V,EW} &= -\frac{1}{4} F_{\mu\nu} F^{\mu\nu} - \frac{1}{4} Z_{\mu\nu} Z^{\mu\nu} - \frac{1}{2} W_{\mu\nu}^+ W^{-\mu\nu} + \frac{m_W^2}{2} W_\mu^+ W^{-\mu} + \frac{m_Z^2}{2} Z_\mu Z^\mu \\ &+ ie \cot \theta_W (Z_{\mu\nu} W^{+\mu} W^{-\nu} - W_{\mu\nu}^+ Z^\mu W^{-\nu} + W_{\mu\nu}^- Z^\mu W^{+\nu}) \\ &+ ie (F_{\mu\nu} W^{+\mu} W^{-\nu} - W_{\mu\nu}^+ A^\mu W^{-\nu} + W_{\mu\nu}^- A^\mu W^{+\nu}) \\ &+ e^2 (A_\mu W^{+\mu} A_\nu W^{-\nu} - A_\mu A^\mu W_\nu^+ W^{-\nu}) \\ &+ \frac{e^2}{2 \sin^2 \theta_W} (W_\mu^+ W^{+\mu} W_\nu^- W^{-\nu} - W_\mu^+ W^{-\mu} W_\nu^+ W^{-\nu}) \\ &+ e^2 \cot^2 \theta_W (Z_\mu W^{+\mu} Z_\nu W^{-\nu} - Z_\mu Z^\mu W_\nu^+ W^{-\nu}) \\ &+ W_\mu^+ W_\nu^- A^\mu Z^\nu + W_\mu^- W_\nu^+ A^\mu Z^\nu - 2W_\mu^+ W^{-\mu} A_\nu Z^\nu. \end{aligned} \quad (2.38)$$

The field strength tensors for the photon, the W^\pm bosons, and the Z boson are defined as $F_{\mu\nu} \equiv \partial_\mu A_\nu - \partial_\nu A_\mu$, $W_{\mu\nu}^\pm = \partial_\mu W_\nu^\pm - \partial_\nu W_\mu^\pm$, and $Z_{\mu\nu} \equiv \partial_\mu Z_\nu - \partial_\nu Z_\mu$, respectively. Most of the Lagrangian describes interactions between 3 and 4 gauge bosons. The W^\pm bosons are directly coupled to the photon (having electric charge ± 1 , respectively), while the Z boson is not.

To understand how the electromagnetic charge arises from symmetry breaking it is useful to look at D_μ from Eq. (2.8). Rewriting it using $\tau_a = \frac{1}{2}\sigma_a$ (and ignoring QCD), the covariant derivative becomes

$$D_\mu = \partial_\mu - iF_{SU(2)_L} g \tau_a W_\mu^a - iY g' B_\mu. \quad (2.39)$$

Defining $\tau_\pm \equiv \frac{1}{\sqrt{2}}(\tau_1 \pm i\tau_2)$ it is possible to write

$$\tau_a W_\mu^a = \tau_+ W_\mu^+ + \tau_- W_\mu^- + \tau_3 W_\mu^3. \quad (2.40)$$

Using this, the covariant derivative can be expanded as

$$D_\mu = \partial_\mu - iF_{SU(2)_L} g \tau_+ W_\mu^+ - iF_{SU(2)_L} g \tau_- W_\mu^- - iF_{SU(2)_L} g \tau_3 W_\mu^3 - iY g' B_\mu. \quad (2.41)$$

Next, using Eq. (2.35) it is possible to write D_μ in terms of the mass eigenstates, which results in

$$\begin{aligned} D_\mu = & \partial_\mu - iF_{SU(2)_L} g \tau_+ W_\mu^+ - iF_{SU(2)_L} g \tau_- W_\mu^- \\ & - i(F_{SU(2)_L} g \cos \theta_W \tau_3 - Y g' \sin \theta_W) Z_\mu \\ & - i(F_{SU(2)_L} g \sin \theta_W \tau_3 + Y g' \cos \theta_W) A_\mu. \end{aligned} \quad (2.42)$$

Using the fact that $g \sin \theta_W = g' \cos \theta_W \equiv e$, the electric charge, the covariant derivative finally becomes

$$\begin{aligned} D_\mu = & \partial_\mu - iF_{SU(2)_L} g \tau_+ W_\mu^+ - iF_{SU(2)_L} g \tau_- W_\mu^- \\ & - i \frac{g}{\cos \theta_W} (F_{SU(2)_L} \tau_3 - Q \sin^2 \theta_W) Z_\mu - iQe A_\mu, \end{aligned} \quad (2.43)$$

where

$$Q = T_3 + Y \quad (2.44)$$

is the $U(1)_Q$ charge. The matrix τ_3 has been changed to the more general T_3 which is the diagonal element of a given $SU(2)$ representation, e.g. τ_3 for the fundamental representation, and $\frac{1}{2}\text{diag}(1, 0, -1)$ for the adjoint (triplet) a representation. By doing this it can be easily seen that the electric charge of the W^\pm boson is in fact $Q_{W^\pm} = \pm 1$. This makes it clear that $SU(2)_L \times U(1)_Y$ breaks down to $U(1)_Q$, which is not $U(1)_Y$

as the charge Q is a mixture of Y and the $SU(2)_L$ generator T_3 .

2.1.4 Higgs Boson Mass

It is worth briefly discussing the Higgs boson, h . The terms in the Lagrangian only including the Higgs boson are

$$\mathcal{L}_h = \frac{1}{2}\partial_\mu h \partial^\mu h - \frac{\mu^2}{2}(v+h)^2 - \frac{\lambda}{4}(v+h)^4, \quad (2.45)$$

which are the same as in the Abelian case. Expanding (2.45), while using the value for v from Eq. (2.20) and $m_W = \frac{gv}{2}$, leads to

$$\mathcal{L}_h = \frac{1}{2}\partial_\mu h \partial^\mu h - \frac{1}{2}m_h^2 h^2 - g\frac{m_h^2}{4m_W}h^3 - g^2\frac{m_h^2}{32m_W^2}h^4, \quad (2.46)$$

where the constant term has been dropped, which can be done since it does not contribute to the Euler-Lagrange equations, and it also factors out of the path integral (and can thus be normalized away)¹. From this equation it is clear that the Higgs boson mass m_h , is given by $m_h^2 = -2\mu^2$.

The complete (boson) Lagrangian includes interactions with the gauge bosons as well, this means there are 3 and 4 particle interactions between gauge bosons and the Higgs boson, in addition to self interactions of the aforementioned bosons. The fate of the fermions after symmetry breaking is discussed in Section 2.1.5.

2.1.5 Fermion Masses

The SM fermions couple to the Higgs doublet through the Yukawa interactions described by Eq. (2.19). Again, using the unitary gauge, the doublet can be separated into two parts: the vev and the Higgs boson. The part with the Higgs boson generates Yukawa couplings between this boson and the fermions, where the Yukawa matrices are scaled by a factor of $\frac{1}{\sqrt{2}}$.

The fermion masses, as well as (kinetic) mixings, are generated by the Higgs vev . It is helpful to explicitly write the $SU(2)$ conjugate of the vev , as was done for the vev in Eq. (2.27), which is

$$\langle \tilde{H} \rangle = i\sigma_2 \langle H^* \rangle = \begin{pmatrix} \frac{v}{\sqrt{2}} \\ 0 \end{pmatrix}. \quad (2.47)$$

¹It is worth noting that a constant term will contribute to the Hamiltonian density nonetheless.

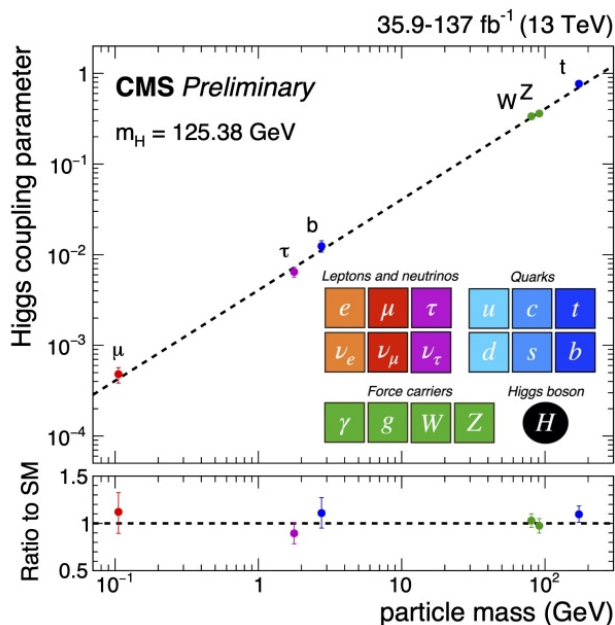


Figure 2.1: Graph showing the Higgs couplings to masses of some Standard Model particles as measured by the CMS collaboration [2].

This leads to the following products:

$$\begin{aligned}\overline{L^i}\langle H\rangle &= \frac{v}{\sqrt{2}}\overline{e^i}L, \\ \overline{Q^i}\langle\tilde{H}\rangle &= \frac{v}{\sqrt{2}}\overline{u^i}L, \\ \overline{Q^i}\langle H\rangle &= \frac{v}{\sqrt{2}}\overline{d^i}L,\end{aligned}\tag{2.48}$$

from which it is possible to write the fermion mass terms as

$$\mathcal{L}_{M,f} = -M_{ij}^e\overline{e^i}L_R^j - M_{ij}^u\overline{u^i}L_R^j - M_{ij}^d\overline{d^i}L_R^j + h.c.,\tag{2.49}$$

where the mass matrices, M^f , are defined as

$$M^f \equiv \frac{v}{\sqrt{2}}y^f\tag{2.50}$$

following Eq. (2.19). As can be seen in Fig. 2.1 current measurements of the masses and the Higgs boson couplings agree to a high degree with the Higgs Mechanism, as the masses of different particles accommodate themselves in a line in the Yukawa coupling-mass term.

2.1.6 Quark Masses and Mixings

The charged lepton mass matrix is usually taken to be diagonal and thus extracting the masses of the leptons is pretty straightforward. This is not the case for quarks. One can naively think that these matrices can also be taken to be diagonal, but this is not the case. The reason for this is that it is possible to diagonalize either the up- or the down-type quark matrix, but since they also interact through a charged current there is no assurance that they will be simultaneously diagonalizable. This is not a problem for the leptons, since only the charged lepton mass matrix needs to be diagonalized, thus it can be taken to be diagonal beforehand. This will become a problem with the introduction of massive neutrinos in Section 2.2.

The mass matrices are, in general, complex and lack any symmetry, as there is no underlying symmetry or physical principle in the SM which limits the Yukawa interactions [19]. To get the masses from the quarks a technique called *biunitary diagonalization* [19, 20] is used. By employing this technique left- and right-handed, as well as up- and down-type quarks, are transformed independently, which allows to bypass the issues that arise while using standard diagonalization. The procedure is general for an arbitrary matrix (which has a diagonal basis), essentially, it is possible to construct two hermitian matrices from the product of a matrix and its hermitian conjugate. These are diagonalized by unitary transformations, which then can be used to diagonalize the original matrix.

In this case the hermitian matrices are

$$\begin{aligned} U_L^{u\dagger} M^u M^{u\dagger} U_L^u &= M_D^{u2} = U_R^{u\dagger} M^{u\dagger} M^u U_R^u \\ U_L^{d\dagger} M^d M^{d\dagger} U_L^d &= M_D^{d2} = U_R^{d\dagger} M^{d\dagger} M^d U_R^d, \end{aligned} \quad (2.51)$$

the D subscript signifies that the matrix is diagonal. This allows the quark mass terms to be written as

$$\sum_q -\bar{q}_L U_L^q M_D^q U_R^{q\dagger} q_R + h.c., \quad (2.52)$$

here $q_{L/R}$ is a column vector containing either the three generations of the up- or the down-type quarks, $\bar{q}_{L/R}$ is implicitly transposed. Finally, transforming the quarks as

$$q_{L/R} \rightarrow q'_{L/R} = U_{L/R}^q q_{L/R}, \quad (2.53)$$

where the primed fields are in the mass basis, the mass terms become

$$-\mathcal{L}_{M,f} = \bar{l}_L M^e l_R + \bar{u}'_L M_D^u u'_R + \bar{d}'_L M_D^d d'_R + h.c., \quad (2.54)$$

$l_{L/R}$ is a column vector of charged leptons, analogous to $q_{L/R}$.

Apart from the six quark masses, there are mixing parameters, though these are only four, which is much less than one would expect from the 36 parameters of the two quark mass matrices. The entire mixing can be codified in a unitary matrix, called the *CKM matrix* (Cabibbo-Kobayashi-Maskawa) [24, 25]. This matrix is defined as

$$V_{CKM} \equiv U_L^{u\dagger} U_L^d \quad (2.55)$$

and has 9 parameters. If this matrix were completely real it would be orthogonal (i.e. a 3D rotation), thus it has 3 angles, and 6 phases as its parameters. Many of these can be removed by a phase transformation the quark fields, i.e. $q^i \rightarrow q^i e^{i\alpha^i}$, where α^i is the phase corresponding to the i -th quark. This is equivalent to multiplying the CKM matrix by a diagonal matrix of phases by both sides. In principle, this would allow one to remove the six phases, but this is not the case, as the transformation where all phases are equal leaves the matrix invariant, i.e. it is possible to factorize one of the phases from the phase matrices without transforming the CKM matrix. Therefore, only five phases can be set to 0, and the CKM matrix is left with four parameters, the three angles and one phase. The most common parametrization is the *PDG parametrization* [8], where

$$V_{CKM} = \begin{pmatrix} c_{12}c_{13} & s_{12}c_{13} & s_{13}e^{-i\delta} \\ -s_{12}c_{23} - c_{12}s_{23}s_{13}e^{i\delta} & c_{12}c_{23} - s_{12}s_{23}s_{13}e^{i\delta} & s_{23}c_{13} \\ s_{12}s_{23} - c_{12}c_{23}s_{13}e^{i\delta} & -c_{12}s_{23} - s_{12}c_{23}s_{13}e^{i\delta} & c_{23}c_{13} \end{pmatrix}, \quad (2.56)$$

with $c_{ij} = \cos \theta_{ij}$ and $s_{ij} = \sin \theta_{ij}$. The parameters are the angles θ_{12} , θ_{23} , θ_{13} , and the CP violating phase δ . The angle $\theta_{12} = \theta_C$ is often called the *Cabibbo angle*. The angles θ_{ij} can be taken between 0 and $\frac{\pi}{2}$ (due to phase redefinition), while δ can be any value between 0 and 2π . Currently they can be taken as [8]

$$\begin{aligned} \sin \theta_{12} &= 0.22650 \pm 0.00048, & \sin \theta_{13} &= 0.00361_{-0.00009}^{+0.00011} \\ \sin \theta_{23} &= 0.04053_{-0.00061}^{+0.00083}, & \delta &= 1.196_{-0.043}^{+0.045}. \end{aligned} \quad (2.57)$$

2.1.7 Summary of Standard Model Parameters

Table 2.2 summarizes the 19 free parameters of the SM. When relevant, the 1σ uncertainty range¹ is given. The parameter $\bar{\theta}$ quantifies strong CP violation and will be discussed in Section 3.1.

Parameter	Central value	1σ range
g'	0.345369	0.345360 \rightarrow 0.345378
g	0.629773	0.629720 \rightarrow 0.629827
g_s	1.2172	1.2120 \rightarrow 1.2224
v/GeV	246.21965	246.21957 \rightarrow 246.21971
m_h/GeV	125.10	124.96 \rightarrow 125.24
m_e/MeV	0.5109989461	0.5109989430 \rightarrow 0.5109989492
m_μ/MeV	105.6583745	105.6583721 \rightarrow 105.6583769
m_τ/MeV	1776.86	1776.74 \rightarrow 1776.98
m_u/MeV	2.16	1.90 \rightarrow 2.65
m_d/MeV	4.67	4.50 \rightarrow 5.15
m_s/MeV	92.9	92.2 \rightarrow 93.6
m_c/GeV	1.27	1.25 \rightarrow 1.29
m_b/GeV	4.18	4.16 \rightarrow 4.21
m_t/GeV	172.76	172.46 \rightarrow 175.06
$\theta_{12}/^\circ$	13.091	13.063 \rightarrow 13.119
$\theta_{13}/^\circ$	0.207	0.201 \rightarrow 0.213
$\theta_{23}/^\circ$	2.323	2.288 \rightarrow 2.370
$\delta/^\circ$	68.53	66.06 \rightarrow 71.10
$\bar{\theta}$	$< 10^{-10}$	

Table 2.2: Standard Model free parameters.

All masses and mixings are taken from the 2020 PDG review [8]. The five lightest quarks are taken from lattice calculations and have their masses given in the $\overline{\text{MS}}$ scheme, where for the three lightest the scale is taken as $\mu = 2\text{ GeV}$, while the charm and bottom quark have them at their pole mass $\mu = m_c, m_b$, respectively. The top quark mass reported corresponds to direct measurements. The vev v is calculated as $v = (\sqrt{2}G_F)^{-\frac{1}{2}}$, with $G_F = 1.1663788(7) \times 10^{-5}\text{ GeV}^{-2}$ the Fermi constant measured by the MuLan collaboration [26]. The gauge couplings are taken from [8], where they are given in the $\overline{\text{MS}}$ scheme at $\mu = M_Z = 91.1876(21)\text{ GeV}$. Lastly, $\bar{\theta}$ is bound by neutron electric dipole moment measurements [27, 28].

¹The 1σ uncertainty is the range corresponding to the values with one standard deviation centered around the mean (assuming a normal distribution). The probability that a value falls in this range is about 68.3%.

2.2 Massive Neutrinos

Since the observation of neutrino oscillations [29], confirming that neutrinos have mass, there has been the need to extend the SM to accommodate these developments. The decay width of the Z boson constrains the number of active neutrinos to three families [30]. An *active* neutrino is a neutrino, which takes part in weak interactions, this is contrasted to a *sterile* neutrino, which does not, and as of now the number of families of sterile neutrinos is unconstrained (but will be taken to be at least three). Therefore, when constructing neutrino masses the number of left (active) neutrinos must be the same as in the SM, but it is possible to include many more sterile neutrinos (at least three are needed to accommodate cosmological observations [31]).

2.2.1 Dirac and Majorana Masses

The most direct way to produce a mass term for neutrinos is by including a right-handed neutrino and coupling it to the left-handed neutrinos in a Yukawa term, which generates the neutrino masses after EW symmetry breaking, as was done for the other fermions [32, 33]. This leads to a Yukawa term of the form

$$-y_{ij}^e \bar{L}^i \tilde{H} \nu_R^j, \quad (2.58)$$

where the maximum value j takes is not necessarily 3. After symmetry breaking this becomes a Dirac mass term, which can be written in matrix form as

$$-\bar{\nu}_L M \nu_R, \quad (2.59)$$

where ν are neutrino column vectors.

Unlike the other fermions, it is possible to construct Majorana masses for neutrinos. A Majorana mass term violates charge conservation (because it mixes terms with the same charge), so this means that quarks and charged leptons can not have a Majorana mass. To write the Majorana mass it is useful to remember the charge conjugation, in this case the neutrino $\nu_{L/R}$,

$$\nu_{L/R}^c = C \overline{\nu_{L/R}} = i\gamma^2 \gamma^0 \bar{\nu}_{L/R}. \quad (2.60)$$

Since the Majorana mass term combines a left or right handed fermion with its charge conjugate, this term is only permitted if the fermion is self-conjugate, i.e. all the quantum numbers of this term must be 0. This means that a Majorana term for left-handed neutrinos is prohibited, since they carry weak isospin and hypercharge¹. But sterile

¹This restriction can be circumvented by introducing an $SU(2)_L$ Higgs triplet [32].

neutrinos are self conjugate, thus a Majorana mass term is permitted, which takes the form

$$-\frac{m_R}{2}\bar{\nu}_R^c\nu_R + h.c., \quad (2.61)$$

here the factor of $\frac{1}{2}$ comes from the fact that these terms are self conjugate. If these neutrinos carry lepton number $L = 1$, the existence of a Majorana mass would result in lepton number violation by $|\Delta L| = 2$. This is also true for $B - L$, which is anomaly free. Actually, one of the ways to look for Majorana masses is by lepton number violating processes, for example neutrinoless double-beta decay (also called $0\nu\beta\beta$ decay). Lepton number violation by ± 2 can be seen directly from the dimension 5 Weinberg operator [34]

$$\mathcal{L}_W = \frac{1}{2}\frac{C_{ij}}{\Lambda}(\bar{L}_L^i\tilde{H}^*)(\tilde{H}^\dagger L_L^j) + h.c., \quad (2.62)$$

where Λ is the scale at which this operator becomes significant and C_{ij} a dimensionless coupling constant. The Weinberg operator also serves to classify the three seesaw mechanisms by the way of its UV completions. The type-I seesaw mechanism is presented in this and the next section, and is done by couplings to $SU(2)_L$ singlet heavy fermions (the sterile neutrinos). In the type-II seesaw mechanism the UV completion is done with heavy scalar $SU(2)_L$ doublets, an implementation of this can be seen in Section 4.1.3.2, albeit for a dimension 5 operator in the quark sector. In the type-III seesaw mechanism the UV completion follows from the inclusion of $SU(2)_L$ triplet fermions, and is not discussed here.

Combining the right-handed Majorana mass terms with the Dirac mass term, where $m_{L/R}$ are now matrices, leads to the most general SM compatible neutrino mass Lagrangian

$$\mathcal{L}_{m,\nu} = -\bar{\nu}_L m_D \nu_R - \bar{\nu}_R^c \frac{m_R}{2} \nu_R + h.c. \quad (2.63)$$

This Lagrangian can be written in matrix form as

$$\mathcal{L}_{m,\nu} = -\frac{1}{2} \begin{pmatrix} \bar{\nu}_L^c & \bar{\nu}_R \end{pmatrix} \begin{pmatrix} 0 & M^{\nu T} \\ m_D & m_R \end{pmatrix} \begin{pmatrix} \nu_L \\ \nu_R^c \end{pmatrix} + h.c. = \begin{pmatrix} \bar{\nu}_L^c & \bar{\nu}_R \end{pmatrix} \mathcal{M} \begin{pmatrix} \nu_L \\ \nu_R^c \end{pmatrix} + h.c., \quad (2.64)$$

where $\nu_{L/R}$ is a column vector of neutrinos. Unlike the charged fermions these are not necessarily of the same size, ν_L contains three neutrinos, but ν_R contains at least three. It is worth noting that diagonalization of \mathcal{M} will lead to Majorana masses for the eigenstates, if $m_R \neq 0$. Hence, if $m_R = 0$, neutrino masses will be Dirac and only m_D will have to be diagonalized to get the mass eigenstates. As an abbreviation, it is often said that neutrinos are Dirac or Majorana, if they have Dirac or Majorana masses.

2.2.2 Seesaw Mechanism

Although no direct measurements of neutrinos masses exist, the squared mass difference of the three active neutrinos has been measured. The sum of the three neutrino masses gets a cosmological upper bound of about 0.1 eV [35, 36, 37]. Current direct measurements by KATRIN give an upper bound to the neutrinos mass of $m_\nu < 0.8$ eV [38], which translates to a bound to the sum of the neutrino masses as $\sum m_\nu < 2.4$ eV. This mass, or sum of masses, is multiple orders of magnitude lighter than the next lightest fermion, the electron at $m_e \approx 0.5 \times 10^6$ eV (see Table 2.2). Also, these measurements come from relativistic neutrinos, where it is as of now impossible to determine if they are Dirac or Majorana. Therefore, if neutrinos were Dirac and their masses generated through the Higgs mechanism, their Yukawa couplings would be of the order $y^\nu \propto 0.5 \times 10^{-12}$, which is seven orders of magnitude smaller than the electron Yukawa $y^e \propto 0.3 \times 10^{-5}$, and can thus be considered unnatural.

On the other hand, if neutrinos are Majorana the smallness of their masses can be readily explained, provided the sterile neutrinos are heavy, i.e. $m_R \gg m_D$. One mechanism which generates these small masses is called the *Seesaw mechanism*. As an example, it is easiest consider the case of just one neutrino generation. In such case the mass Lagrangian from Eq. (2.64) is given by

$$\mathcal{L}_{m,\nu} = -\frac{1}{2} \begin{pmatrix} \bar{\nu}_L^c & \bar{\nu}_R \end{pmatrix} \begin{pmatrix} 0 & m_D \\ m_D & m_R \end{pmatrix} \begin{pmatrix} \nu_L \\ \nu_R^c \end{pmatrix} + h.c., \quad (2.65)$$

where m_D and m_R , in principle, are complex numbers. They can be made real phase by a redefinition of ν_R and ν_L . The eigenvalues of \mathcal{M} are

$$m_{1/2} = \frac{m_R}{2} \pm \sqrt{\frac{m_R^2}{4} + m_D^2} = \frac{m_R}{2} \left(1 \pm \sqrt{1 + 4 \frac{m_D^2}{m_R^2}} \right). \quad (2.66)$$

Taking the limit $m_R \gg m_D$ (meaning that the order of magnitude of the elements of m_R is much greater than those in m_D), leads to

$$\begin{aligned} m_1 &= -\frac{M_D^2}{m_R}, \\ m_2 &= m_R. \end{aligned} \quad (2.67)$$

Thus $m_1 \ll m_2$, since $m_R \gg m_D$. This explains the small neutrino masses without needing Yukawa couplings many orders of magnitude smaller than the charged lepton's Yukawas.

In a more realistic case, with three active neutrino generations, the process is very

similar. In this case it is not necessary to obtain all the eigenvalues, but to compute a block-diagonal matrix of the form

$$\mathcal{M} = \begin{pmatrix} m_L & 0 \\ 0 & m'_R \end{pmatrix}. \quad (2.68)$$

The matrix m_L is a 3×3 matrix corresponding to the active neutrinos, while m'_R is an $m \times m$ matrix corresponding to the sterile neutrinos. The matrix eigenvalues are given analogous to Eq. (2.67), in the $m_R \gg m_D$ limit, thus

$$\begin{aligned} m_L &= -m_D^T m_R^{-1} m_D, \\ m'_R &= m_R. \end{aligned} \quad (2.69)$$

It is worth noting that m_L is a symmetric matrix, i.e. $m_L^T = m_L$. Also, it is common to denote the active neutrinos after separation as ν_i , with $i = 1, 2, 3$.

2.2.3 Lepton Masses and Mixings

Combining the neutrino masses from Eq. (2.63) with the charged lepton mass given by (2.54), leads to

$$\mathcal{L}_{m,l} = -\bar{e}_L M^e e_R - \bar{\nu}_L m_D \nu_R - \bar{\nu}_R^c \frac{m_R}{2} \nu_R + h.c.. \quad (2.70)$$

Unlike the SM with massless neutrinos, it is no longer possible to suppose beforehand that the charged lepton mass matrix is diagonal, since it will no longer be possible to diagonalize both matrices simultaneously. Like in Section 2.1.6, it will be possible to diagonalize the matrices through biunitary diagonalization. It is worth noting that as of now the measured parameters are the difference of the squared masses $\Delta m_{ij}^2 = m_i^2 - m_j^2$, where $\Delta m_{21}^2 > 0$, but the sign of Δm_{32}^2 is unknown [8]. This allows for two orderings of the masses, the so called normal ordering (NO) $m_3 > m_2 > m_1$ and $m_2 \gtrsim m_1 > m_3$, the inverted ordering (IO).

If the neutrinos are Dirac everything is exactly the same as with the quarks. That is, the squared mass matrices are diagonalized by

$$\begin{aligned} U_L^{e\dagger} M^e M^{e\dagger} U_L^e &= M_D^{e2} = U_R^{e\dagger} M^{e\dagger} M^e U_R^e \\ U_L^{\nu\dagger} m_D m_D^\dagger U_L^\nu &= M_D^{\nu2} = U_R^{\nu\dagger} m_D^\dagger m_D U_R^\nu, \end{aligned} \quad (2.71)$$

where $U_{L/R}^l$ are unitary matrices. By transforming

$$l_{L/R} \rightarrow l'_{L/R} = U_{L/R}^l l_{L/R}, \quad (2.72)$$

the Dirac mass matrices become diagonal. Furthermore, also as with the quarks the entire mixing of leptons can be expressed in a unitary matrix, the *PMNS matrix* (Pontecorvo-Maki-Nakagawa-Sakata) [39, 40]. This matrix is defined as

$$V_{PMNS} \equiv U_L^{e\dagger} U_L^\nu. \quad (2.73)$$

If there are three generations of active neutrinos, it takes the same form as the CKM matrix, where five of the six phases can be absorbed by the lepton fields. In the PDG parametrization it is given by

$$V_{PMNS} = \begin{pmatrix} c_{12}c_{13} & s_{12}c_{13} & s_{13}e^{-i\delta} \\ -s_{12}c_{23} - c_{12}s_{23}s_{13}e^{i\delta} & c_{12}c_{23} - s_{12}s_{23}s_{13}e^{i\delta} & s_{23}c_{13} \\ s_{12}s_{23} - c_{12}c_{23}s_{13}e^{i\delta} & -c_{12}s_{23} - s_{12}c_{23}s_{13}e^{i\delta} & c_{23}c_{13} \end{pmatrix}. \quad (2.74)$$

Once again, like the CKM matrix, θ_{ij} take values between 0 and $\frac{\pi}{2}$, and δ , also called the CP violating phase or Dirac phase, takes values between 0 and 2π . The values of these parameters are given in Table 2.3.

If neutrinos are Majorana there is a slight difference when compared to the Dirac case. After generating the left-handed neutrino Majorana masses following the same procedure as in Section 2.2.2, it is possible to diagonalize through biunitary transformations as

$$\begin{aligned} U_L^{e\dagger} M^e M^{e\dagger} U_L^e &= M_D^e{}^2 = U_R^{e\dagger} M^{e\dagger} M^e U_R^e, \\ U_L^{\nu\dagger} m_l m_L^\dagger U_L^\nu &= m_L^D{}^2 = U_R^{\nu\dagger} m_L^\dagger m_L U_R^\nu, \end{aligned} \quad (2.75)$$

which is like Eq. (2.71), but the Dirac mass has been replaced by a Majorana mass. The resulting mixing matrix is defined by,

$$V_l \equiv U_L^{e\dagger} U_L^\nu. \quad (2.76)$$

The only difference to the Dirac case is the number of phases. While for Dirac masses it was possible to redefine five of the six phases, a Majorana mass term prohibits the redefinition of phases, since a phase transformation of

$$-\frac{1}{2} m_L^i \bar{\nu}_i^c \nu_i \quad (2.77)$$

would result in a complex mass, as m_L^i would map to $m_L^i e^{2i\phi}$. Consequently, only the phases of the charged leptons can be redefined. This means that 3 phases can be taken out of the matrix. The most common parametrization is to take one of the three phases to the orthogonal matrix, giving the PMNS matrix, while multiplying the other two in

Parameter	Central value	1σ range
$\Delta m_{21}^2/10^{-5}\text{eV}^2$	7.55	7.39 \rightarrow 7.75
$\Delta m_{32}^2/10^{-3}\text{eV}^2$	2.424	2.421 \rightarrow 2.427
$\theta_{12}/^\circ$	34.5	33.5 \rightarrow 35.7
$\theta_{13}/^\circ$	8.45	8.32 \rightarrow 8.61
$\theta_{23}/^\circ$	47.7	46.0 \rightarrow 48.9
$\delta/^\circ$	218	191 \rightarrow 256

Table 2.3: Lepton masses and mixing parameters from [7, 8]. Normal mass ordering is assumed here.

a Majorana phase matrix P_M . Thus the mixing matrix is

$$V_{PMNS} = V_{PMNS}^D P_M, \quad (2.78)$$

where $P_M = \text{diag}(1, e^{i\alpha}, e^{i\beta})$ is a diagonal phase matrix, and V_{PMNS}^D is the Dirac PMNS matrix of Eq. (2.74). The phases α and β are called the Majorana phases. The majorana phases are as of now undetermined¹ and thus are also not reported in Table 2.3.

2.3 Froggatt-Nielsen Mechanism

Another open question in the SM is the fermion mass hierarchy. The Froggatt-Nielsen (FN) Mechanism [42] generates the hierarchy by a spontaneously broken global $U(1)$ flavour symmetry, called the Froggatt-Nielsen Symmetry $U(1)_{FN}$. A flavour symmetry is a symmetry of the Lagrangian that distinguishes the different flavours. This means, for example, that fermions of a different flavour possess a different charge under a $U(1)$ symmetry. The main idea of the FN Mechanism is to dynamically generate the mass hierarchy by a minimal extension of the SM [43]. Nevertheless, the mechanism is robust enough to also be applied to more complicated extensions of the SM, one of such scenarios being supersymmetry.

2.3.1 Mass Hierarchy through $U(1)_{FN}$ and the Flavon Field

In the Froggatt-Nielsen approach to mass hierarchy, the $U(1)_{FN}$ flavour symmetry is introduced, along with a scalar field, σ , which is called the flavon field. It is common that the flavon field only carries $U(1)_{FN}$ charge (also called FN charge), but is otherwise a SM singlet. The flavon acquires a vev , breaking the flavour symmetry spontaneously, while at the same time generating the mass hierarchy.

¹The only observable effect would be $m_{\beta\beta}$, coming from $0\nu\beta\beta$ [41].

The flavon couples to Yukawa terms like

$$-y_{ij}^{f^1} \overline{F_L^i} H f_R^{1j} \frac{\sigma^n}{\Lambda^n} - y_{ij}^{f^2} \overline{F_L^i} \tilde{H} f_R^{2j} \frac{\sigma^m}{\Lambda^m}, \quad (2.79)$$

where F_L^i is the $SU(2)_L$ fermion doublet, while $f^{1/2}$ are the singlets. The powers m and n are non-negative integers and Λ is the scale at which the FN operators become relevant, sometimes taken to be a GUT scale [43]. The values of m and n are not arbitrary, since the requirement for the Yukawa terms to be $U(1)_{FN}$ invariant constrains them. The flavon acquires a vev , $\langle \sigma \rangle$, which is then introduced in the Yukawa terms as a power. It is often more useful to introduce the parameter ϵ [43], which is defined as

$$\epsilon \equiv \frac{\langle \sigma \rangle}{\Lambda}. \quad (2.80)$$

As Λ will heavily suppress terms which are of the form $\frac{\langle \sigma \rangle^k}{\Lambda^n}$, with $k < n$, Eq. (2.79) will become

$$-y_{ij}^{f^1} \overline{F_L^i} H f_R^{1j} \epsilon^n - y_{ij}^{f^2} \overline{F_L^i} \tilde{H} f_R^{2j} \epsilon^m + \mathcal{O}(\Lambda^{-1}) \quad (2.81)$$

after symmetry breaking. The $\mathcal{O}(\Lambda^{-1})$ signifies the remaining terms, which are Yukawa interactions with the flavon, or powers of it smaller than k , after symmetry breaking.

If ϵ is of the correct order of magnitude, the Yukawa couplings can be taken all to be of similar size and the wide range of orders of magnitude of the Yukawa couplings in the SM can be explained. This means that by choosing m and n appropriately for the Yukawa couplings it is possible to build a model where all Yukawa couplings are all of the same (or similar) order of magnitude, and the hierarchies in the mass matrices (or equivalently, the Yukawa matrices) are generated by powers of ϵ . Commonly, ϵ is taken to be

$$\epsilon \sim 0.2 \sim \sin(\theta_C), \quad (2.82)$$

as this value works phenomenologically [43].

2.3.2 UV Completion

As can be seen from Eq. (2.79) the FN terms before symmetry breaking are not renormalizable, as they have dimension $4 + n$, here n represents the power of the fermion-flavon interaction. To have a renormalizable theory the FN terms must be UV-completed. It is standard to do the UV completion of the theory by including heavy vector-like $SU(2)_L$ singlet fermions, called the *FN fields*. This UV completion will be denoted in this work as type-I seesaw, since the topology of the UV-complete dimension 5 diagrams corresponds to the type-I seesaw mechanism for neutrinos. There are also more possible UV completions, though these tend to be model dependent. For

example in Section 4.1.3.2 a FN UV completion is done by including heavy $SU(2)_L$ doublet scalars.

The UV completion using heavy fermions is relatively straightforward. Such fermions, when they couple to the SM fermions have to satisfy the requirement that their charge assignment corresponds to that of the charge conjugate of the SM fields in a given operator. However, it is not necessary that they form $SU(2)_L$ singlets. To UV-complete the theory it is necessary to include the interaction of the FN fields with the Yukawa terms and with the flavons. For example the UV completion of a dimension five term like

$$-y_{ij}\overline{Q}_L^i H q_R^j \frac{\sigma}{\Lambda} \quad (2.83)$$

is achieved by introducing the heavy fermion F_{ij} , with mass M_{ij} . The UV completion of this term is

$$-y_{ij}^H \overline{Q}_L^i H F_{ijR} - M_{ij} \overline{F}_{ijR} F_{ijL} - y_{ij}^\sigma \overline{F}_{ijL} \sigma q_R^j. \quad (2.84)$$

By combining mass terms and Yukawa couplings between the FN fields and the flavon, as well as to the SM fermions and the Higgs doublet(s) it is possible to generate higher dimension terms, with the inclusion of Yukawa couplings between the flavon and the FN fields like

$$C_{kl}^{ij} \overline{F}_{ijL} F_{klR}. \quad (2.85)$$

A diagrammatic example of the UV completions is given in Fig. 2.2 and Fig. 2.3, where a dimension five and six diagram can be observed. All higher order diagrams can be drawn like the dimension six diagram (but with more flavon couplings). These diagrams are usually called *spaghetti diagrams* [43].

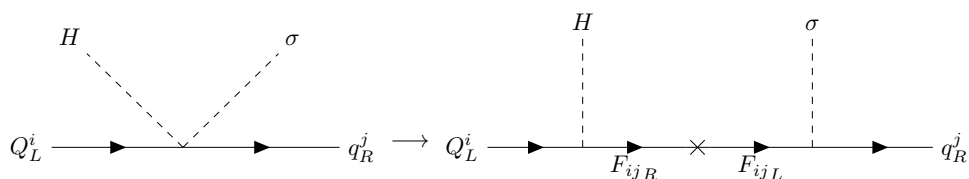


Figure 2.2: Dimension five type-I Froggatt-Nielsen UV completion.

Another way to UV-complete the theory is by including a heavy $SU(2)_L$ scalar, Φ . This scalar forms Yukawa couplings to the SM fields, as well as to the Higgs doublet and the flavon through a three scalar interaction. The UV completion of Eq. (2.83) takes the form

$$-y_{ij}\overline{Q}_L^i \Phi q_R^j - \mu H \Phi^\dagger \sigma. \quad (2.86)$$

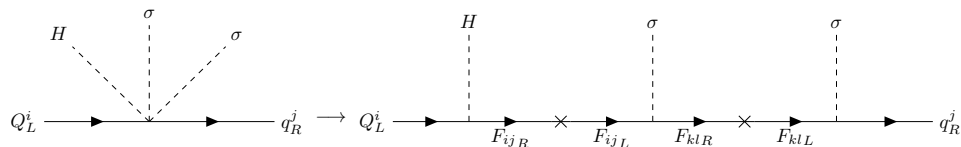


Figure 2.3: Dimension six type-I Froggatt-Nielsen UV completion.

This type of UV completion will be called type-II seesaw, since the topology of the diagrams correspond to those of the type-II seesaw mechanism for neutrinos. A diagram corresponding to this UV completion can be seen in Fig. 2.4.

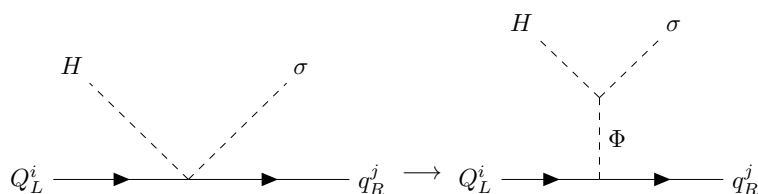


Figure 2.4: Dimension five type-II Froggatt-Nielsen UV completion.

The FN mechanism is a simple framework for extending the SM, which accounts for the mass hierarchy, in both quarks and leptons, by the inclusion of the flavour symmetry $U(1)_{FN}$. Moving on from masses, the next chapter discusses the strong CP problem, which concerns the smallness of strong CP violation, and the Peccei-Quinn solution to this problem, which implies the existence of a pseudoscalar particle, the axion.

Since the late 1970s, when axions arose as a consequence of the Peccei-Quinn (PQ) solution to the strong CP problem, axions and axion-like particles (ALPs) have caught the interest of many physicists not only because they solve the strong CP problem, but also because if their masses are in a correct range, they would possess properties that are cosmologically desirable (see Section 3.2). The name axion does not describe a particular kind of particle, but is generally taken to be a light pseudo-Goldstone boson from a global chiral symmetry, or more generally in cosmology an axion-like particle (ALP) is a particle which has similar cosmological properties to the axion. The QCD axion is the axion, corresponding to the Peccei-Quinn symmetry, which solves the strong CP problem.

3.1 QCD Axions

The Peccei-Quinn symmetry is one of the most popular, if not the most popular, solutions to the strong CP problem. The strong CP problem is an open problem in particle physics, where the CP symmetry is, in principle, violated by strong interactions, but measurements of the neutron dipole moment bound this violation to be tiny. The value of the CP violation can thus be considered unnatural, especially since weak interactions violate CP measurably. A consequence of the breaking of this symmetry is the appearance of QCD axions (henceforth called axions), which have garnered much interest in their own right. They are the light scalar particles, which correspond to the pseudo-Goldstone bosons of the PQ symmetry [15].

3.1.1 The Strong CP Problem

To understand the strong CP problem, it is easiest to look at the QCD Lagrangian in an isolated fashion. This Lagrangian is

$$\mathcal{L}_{QCD} = -\frac{1}{4}G_{\mu\nu}^a G_a^{\mu\nu} + \sum_q \bar{q}(i\gamma^\mu D_\mu - m_q)q, \quad (3.1)$$

where $G_{\mu\nu}^a$ (and $a = 1, \dots, 8$ since $G_{\mu\nu}^a$ is in the adjoint representation of $SU(3)_c$) is the gluon strength tensor defined in Eq. (2.5), q are the quarks and D_μ is the covariant derivative from Eq. (2.8), though only including the $SU(3)_c$ terms. Unlike the SM, pure QCD is not a chiral theory, i.e. left- and right-handed quarks are treated in the same way.

The strong CP problem arises from the inclusion of the term

$$\theta \frac{g_s^2}{32\pi^2} G_{\mu\nu}^a \tilde{G}_a^{\mu\nu} \quad (3.2)$$

to the QCD Lagrangian. Here θ is a free parameter of the SM. The gluon strength tensor dual, $\tilde{G}_a^{\mu\nu}$, is defined as

$$\tilde{G}_a^{\mu\nu} = \frac{1}{2}\epsilon^{\mu\nu\rho\sigma} G_{a\rho\sigma}, \quad (3.3)$$

$\epsilon_{\mu\nu\rho\sigma}$ is the totally antisymmetric tensor. The gluon strength tensor transforms as a pseudotensor, this means that contracting it with the strength tensor will lead to a term that is not P-invariant, but is C-invariant nonetheless. A direct evaluation of the indices shows that $G_{\mu\nu}^a \tilde{G}_a^{\mu\nu} \propto \mathbf{E}_a \cdot \mathbf{B}^a$, which is the product of a vector with an axial vector and therefore not P invariant. Thus, the term in (3.2) is not CP-invariant. Including it in the QCD Lagrangian leads to

$$\mathcal{L}_{QCD} = -\frac{1}{4}G_{\mu\nu}^a G_a^{\mu\nu} + \sum_q \bar{q}(i\gamma^\mu D_\mu - m_q)q + \theta \frac{g_s^2}{32\pi^2} G_{\mu\nu}^a \tilde{G}_a^{\mu\nu}. \quad (3.4)$$

The factor θ has now a clear interpretation, it quantifies how strong CP is broken by the inclusion of this term. As will be seen later, this is not a physical parameter. Although it might seem unfounded, the CP-violating term can be included at the classical level, since this term is a total divergence, in fact it is very similar to the divergence of the anomalous chiral current (also called the chiral anomaly)

$$\partial_\mu J_5^\mu = N_f \frac{g_s^2}{16\pi^2} G_{\mu\nu}^a \tilde{G}_a^{\mu\nu}, \quad (3.5)$$

where N_f is the number flavours. This symmetry is the chiral analogue of the baryon



(a) Electromagnetic chiral anomaly.

(b) QCD chiral anomaly.

Figure 3.1: Chiral anomalies due to triangle diagrams.

number, but is not conserved in the SM, as it is broken by chiral anomalies and the quarks' masses. The triangle diagrams, corresponding to the chiral anomaly can be seen in Fig. 3.1. This means that its inclusion has no effect on the classical equations of motion and that the effect this term has will not be seen at any order in perturbation theory. Therefore, the CP-violating term will contribute at most non-perturbatively. Since QCD is asymptotically free and perturbative after a phase transition at about 200 MeV, CP violation should manifest more strongly at low energies, while becoming irrelevant at high energies. In Appendix C.1 it is shown that the inclusion of this term arises naturally from the topology of the gauge group.

To get the physical parameter for CP violation it is necessary to look at a more complete model, in particular it is important to remember that a phase in the quark masses will also lead to CP violation. Writing quark mass phases, θ_q , explicitly in (3.4) leads to the Lagrangian

$$\mathcal{L}_{QCD} = -\frac{1}{4}G_{\mu\nu}^a G_a^{\mu\nu} + \sum_q \bar{q}(i\gamma^\mu D_\mu - m_q e^{i\theta_q})q + \theta \frac{g_s^2}{32\pi^2} G_{\mu\nu}^a \tilde{G}_a^{\mu\nu}, \quad (3.6)$$

where m_q are real. These phases contribute to weak CP violation, which is parameterized by the phase CKM matrix. Chiral transformations of the quarks

$$q \rightarrow e^{i\gamma_5 \frac{\alpha}{2}} q, \quad (3.7)$$

where α is a transformation parameter, lead to mixing of the CP violating term and the masses' phases. The quark masses also break the chiral global symmetry explicitly,

this leads to the a divergence to the chiral current of

$$\partial_\mu J_5^\mu = \sum_q 2m_q \bar{q} i \gamma_5 q + N_f \frac{g_s^2}{16\pi^2} G_{\mu\nu}^a \tilde{G}_a^{\mu\nu}. \quad (3.8)$$

Under the chiral transformation of Eq. (3.7), the quark mass term transforms as

$$\bar{q} m_q e^{i\theta_q} q \rightarrow \bar{q} m_q e^{i(\theta_q + \alpha)} q, \quad (3.9)$$

This means that under the chiral transformation $\theta_q \rightarrow \theta_q + \alpha$. On the other hand, because of the chiral anomaly the quark measure transforms as [28]

$$\mathcal{D}q \mathcal{D}\bar{q} \rightarrow \mathcal{D}q \mathcal{D}\bar{q} e^{-i\alpha \frac{g_s^2}{32\pi^2} \int d^4x G_{\mu\nu}^a \tilde{G}_a^{\mu\nu}}. \quad (3.10)$$

Since this enters the action by means of the path integral, it can be taken as a transformation property of θ , such that $\theta \rightarrow \theta - \alpha$. The physical parameter of strong CP violation must be invariant under these transformations. For only one quark flavour it is $\bar{\theta} = \theta + \theta_q$. In the more general case of multiple quark flavours (for example the SM) it can be shown that (see [28], for example) the invariant CP violating parameter can be written as

$$\bar{\theta} = \theta + \text{Arg} \left(\text{Det}(M^u M^d) \right), \quad (3.11)$$

where $M^{u/d}$ are the quark mass matrices. This leads to a final Lagrangian

$$\mathcal{L}_{QCD} = -\frac{1}{4} G_{\mu\nu}^a G_a^{\mu\nu} + \sum_q \bar{q} (i\gamma^\mu D_\mu - m_q e^{i\theta_q}) q + \bar{\theta} \frac{g_s^2}{32\pi^2} G_{\mu\nu}^a \tilde{G}_a^{\mu\nu}. \quad (3.12)$$

CP violation would lead to an asymmetrical charge distribution in the neutron, giving it an electrical dipole moment. Measurements of this moment are very small, and constrain the CP violating parameter to be $\bar{\theta} < 10^{-10}$ [26]. This leads to the statement of the strong CP problem: *If CP is clearly/badly broken by weak interactions, why is CP violation so small, if at all present, in strong interactions?*

3.1.2 Solving the Strong CP Problem: Axions and the Peccei-Quinn Symmetry

An anomalous, global, chiral $U(1)$ symmetry, called the *Peccei-Quinn Symmetry* (PQ), $U(1)_{PQ}$, is introduced to QCD (and thus to the SM). This symmetry is also spontaneously broken, and the axion, a , is its Goldstone boson. Under PQ, the axion transforms additively, like

$$a \rightarrow a + \alpha f_a. \quad (3.13)$$

Here, f_a is an energy scale called the *axion decay constant*, associated to the breaking of the aforementioned symmetry, and α is a free (real) transformation parameter. The axion decay constant plays a central role in determining the axion's dynamics and is a free parameter of the theory. The fact that this solves the strong CP problem was first noted by Peccei and Quinn [44, 45], hence the name. The axion as a Goldstone mode of the was noticed shortly afterwards by both Weinberg and Wilczek (see Appendix C.2).

The axion effective Lagrangian is given by [28]

$$\mathcal{L}_a = \frac{1}{2}(\partial_\mu a)(\partial^\mu a) + \mathcal{L}_Y(\partial_\mu a, \Psi) + \frac{g_{a\gamma}}{4}aF^{\mu\nu}\tilde{F}_{\mu\nu} + \frac{a}{f_a}\frac{g_s^2}{32\pi^2}G_{\mu\nu}^a\tilde{G}_a^{\mu\nu}. \quad (3.14)$$

Here $g_{a\gamma}$ is the axion-photon coupling constant, and is model dependent, while

$$\tilde{F}^{\mu\nu} = \frac{1}{2}\epsilon^{\mu\nu\rho\sigma}F_{\rho\sigma} \quad (3.15)$$

is the electromagnetic dual strength tensor. This means that the axion also couples to the electromagnetic chiral anomaly. The terms in the axion-fermion couplings are of the form

$$\mathcal{L}_Y(\partial_\mu a, \Psi) \supset \frac{\partial_\mu a}{2f_a}C_{a\Psi}\bar{\Psi}\gamma^\mu\gamma_5\Psi, \quad (3.16)$$

where $C_{a\Psi}$ is a model dependent coupling constant. The last term in the Lagrangian (3.14) ensures that the PQ symmetry possesses a chiral anomaly

$$\partial_\mu J_{PQ}^\mu \propto \frac{g_s^2}{32\pi^2}G_{\mu\nu}^a\tilde{G}_a^{\mu\nu}, \quad (3.17)$$

while also breaking the translation symmetry explicitly. This means the axion is actually a pseudo-Goldstone boson and will acquire mass. The term $\mathcal{L}_Y(\partial_\mu a, \Psi)$ represents Yukawa couplings between the axion and fermions.

There are two arguments to give on why the PQ symmetry and the axion solve the strong CP problem. The first argument is that is possible to absorb $\bar{\theta}$ in the axion by choosing α properly. This is because the full Lagrangian contains a coupling of the form

$$\mathcal{L} \supset \left(\frac{a}{f_a} + \bar{\theta}\right)\frac{g_s^2}{32\pi^2}G_{\mu\nu}^a\tilde{G}_a^{\mu\nu}. \quad (3.18)$$

Thus, it can be seen that the effect of the CP-violating term becomes unphysical, since it become a consequence of the transformation properties of the broken PQ symmetry. The problem with this argument is that $\bar{\theta}$ also transforms under the chiral symmetry as

$$\bar{\theta} \rightarrow \bar{\theta} - \alpha, \quad (3.19)$$

prohibiting the elimination of $\bar{\theta}$ by the correct choice of α , unless somehow a and $\bar{\theta}$

shift differently. Nevertheless, it can be eliminated by the axion's acquisition of a vev . Here

$$a \rightarrow a_p + \langle a \rangle, \quad (3.20)$$

where a_p is the physical axion with $\langle a_p \rangle = 0$. If

$$\langle a \rangle = -f_a \bar{\theta}, \quad (3.21)$$

the $\bar{\theta}$ term disappears, solving the strong CP problem [28, 46].

The coupling of the axion to the PQ anomalous current also generates an effective potential for the action

$$V_{eff} = -\frac{a}{f_a} \frac{g_s^2}{32\pi^2} G_{\mu\nu}^a \tilde{G}_a^{\mu\nu}. \quad (3.22)$$

From this potential one can deduce that the vev of Eq. (3.21) is in fact the minimum of the effective potential, i.e.

$$\left\langle \frac{\partial V_{eff}}{\partial a} \right\rangle = -\frac{1}{f_a} \frac{g_s^2}{32\pi^2} \langle G_{\mu\nu}^a \tilde{G}_a^{\mu\nu} \rangle |_{\langle a \rangle = -f_a \bar{\theta}} = 0. \quad (3.23)$$

Also, the axion mass can be extrapolated from this potential, giving

$$m_a^2 = \left\langle \frac{\partial^2 V_{eff}}{\partial a^2} \right\rangle = -\frac{1}{f_a} \frac{g_s^2}{32\pi^2} \frac{\partial}{\partial a} \langle G_{\mu\nu}^a \tilde{G}_a^{\mu\nu} \rangle |_{\langle a \rangle = -f_a \bar{\theta}}. \quad (3.24)$$

To do the precise calculation in (3.23) and (3.24) it is necessary to employ some low-energy approximation of QCD (perturbative or non-perturbative), for example in Section 3.1.3 chiral Lagrangian techniques are employed.

A UV completion of this theory was done independently by Weinberg [47] and Wilczek [48], this axion model is often referred to as the *Peccei-Quinn-Weinberg-Wilczek* (PQWW) model [49], by introducing a second Higgs doublet. See Appendix C.2. The problem with this realization of the UV completion is that the axion decay constant and the SM Higgs vev are proportional in this model, predicting a mass and couplings of the axion that are too large. Experiments at KEK, for example [50], during the 1980s could not find any evidence for this particle, thus ruling out its existence. Invisible axion models circumvent this problem by decoupling the PQ breaking scale from the EW breaking scale, the exact form this occurs is presented in Section 3.1.4.

3.1.3 Axion Mass and Couplings

Axion phenomenology presents some peculiarities, many of which rest on the effective Lagrangian of (3.14), which means, many aspects of axion physics can be studied without knowledge of the UV-complete theory. Of particular interest for this work

are the mass of the axion, and the axion-photon coupling. For many applications and calculations involving the effective theory of axions, for example the axion mass, chiral Lagrangian techniques can be employed, where good results are obtained in the axion-pion chiral Lagrangian. Other interesting couplings, which will not be discussed here, are the axion-electron coupling, axion-hadron couplings, and axion-meson couplings, including the axion-pion coupling.

A good starting approximation for the effective theory, following [28], takes only the couplings to the two lightest quarks into account (for a treatment including the strange quark see [51]). The relevant terms in this Lagrangian are

$$\mathcal{L}_a = \frac{1}{2}(\partial_\mu a)(\partial^\mu a) + \frac{\partial_\mu a}{2f_a} \bar{q} C_{aq}^0 \gamma^\mu \gamma_5 q + \frac{g_{a\gamma}^0}{4} a F^{\mu\nu} \tilde{F}_{\mu\nu} + \frac{a}{f_a} \frac{g_s^2}{32\pi^2} G_{\mu\nu}^a \tilde{G}_a^{\mu\nu} - (\bar{q}_L M_q q_r + h.c.), \quad (3.25)$$

where $q = (u, d)^T$, $M_q = \text{diag}(m_u, m_d)$, and $C_{aq} = \text{diag}(C_{au}, C_{ad})$. The quark mass term has been included as it will be relevant in the future. Performing an axion dependent chiral rotation of the quarks

$$q \rightarrow e^{i\gamma_5 \frac{a}{2f_a} Q_a} q, \quad (3.26)$$

with Q_a a 2×2 matrix acting on q . Multiple terms will arise in the Lagrangian as a consequence of this transformation, which is similar to the transformation of Eq. (3.7). Importantly the term

$$-g_s^2 \frac{\text{Tr}(Q_a)}{32\pi^2} \frac{a}{f_a} G_{\mu\nu}^a \tilde{G}_a^{\mu\nu}, \quad (3.27)$$

which will cancel the topological term in the Lagrangian, provided $\text{Tr}(Q_a) = 1$. This term originates from the chiral anomaly of the quark measure, like Eq. (3.10). Defining

$$\begin{aligned} g_{a\gamma} &= g_{a\gamma}^0 - (2N_c) \frac{e^2}{8\pi^2 f_a} \text{Tr}(Q_a Q^2), \\ C_{aq} &= C_{aq}^0 - Q_a, \\ M_a &= e^{i\frac{a}{2f_a} Q_a} M_q e^{i\frac{a}{2f_a} Q_a}, \end{aligned} \quad (3.28)$$

where $Q = \text{diag}(\frac{2}{3}, -\frac{1}{3})$ is the electric charge matrix for the quarks and N_c is the number of colours, 3 in most models. The resulting Lagrangian is

$$\mathcal{L}_a = \frac{1}{2}(\partial_\mu a)(\partial^\mu a) + \frac{\partial_\mu a}{2f_a} \bar{q} C_{aq} \gamma^\mu \gamma_5 q + \frac{g_{a\gamma}}{4} a F^{\mu\nu} \tilde{F}_{\mu\nu} - (\bar{q}_L M_q q_r + h.c.). \quad (3.29)$$

3.1.3.1 Axion Mass

A relatively simple way to obtain the low energy values for the masses and couplings is to couple the axion to the chiral Lagrangian. In this case interactions are restricted to mesons composed of the two lightest quarks, but will further be constrained to only account for pions. This can be done by coupling the chiral quark current

$$\bar{q}C_{aq}\gamma^\mu\gamma_5q = \frac{1}{2}\text{Tr}(C_{aq})\bar{q}\gamma^\mu\gamma_5q + \frac{1}{2}\text{Tr}(C_{aq}\sigma^b)\bar{q}\gamma^\mu\gamma_5\sigma_bq, \quad (3.30)$$

where $\sigma^b = \sigma_b$ are the Pauli matrices, to the pion chiral Lagrangian. Since only pions are of interest in this case, the isosinglet term (corresponding to the η') can be neglected. This gives the effective Lagrangian

$$\mathcal{L}_a^\chi = \frac{f_\pi^2}{4} \left(\text{Tr} \left((D^\mu U)^\dagger (D_\mu U) \right) + 2B_0 \text{Tr}(UM_a^\dagger + M_a U^\dagger) \right) + \frac{\partial^\mu a}{4f_a} \text{Tr}(C_{aq}\sigma^b)J_{b\mu}, \quad (3.31)$$

where

$$J_\mu^b = \frac{i}{2}f_\pi^2 \text{Tr} \left(\sigma^b (UD_\mu U^\dagger - U^\dagger D_\mu U) \right) \quad (3.32)$$

is the pion current coupled to the axion. The pion decay constant f_π is approximately 92.3 MeV [8]¹, and B_0 is a factor associated to quark condensation. The covariant derivative of U is

$$D^\mu = \partial^\mu U + ieA^\mu[Q, U], \quad (3.33)$$

where U is a pion-dependent $SU(2)$ transformation, defined as

$$U = e^{i\frac{\sigma_a\pi^a}{f_\pi}} = \cos\left(\frac{\pi}{f_\pi}\right) + i\frac{\sigma^a\pi_a}{f_\pi} \sin\left(\frac{\pi}{f_\pi}\right), \quad (3.34)$$

and $\pi^2 = \pi^a\pi_a = (\pi^0)^2 + 2\pi^+\pi^-$, with $\pi^\pm = \frac{1}{\sqrt{2}}(\pi^1 \mp i\pi^2)$ and $\pi^0 = \pi^3$.

The effective potential generated by the term

$$-V(a, \pi^a) = B_0 \frac{f_\pi^2}{2} \text{Tr} \left(UM_a^\dagger + M_a U^\dagger \right), \quad (3.35)$$

in the Lagrangian of (3.31), can be used as a starting point to obtain the axion mass. It is possible to estimate B_0 from this potential². The terms in the potential not

¹The value reported by the PDG is about 130 MeV, which is $\sqrt{2}$ times the value cited, since they do not normalize this parameter by $\frac{1}{\sqrt{2}}$.

²This will only give contributions due to the condensation of up- and down-quarks, which is enough for the approximations taken.

containing the axion (i.e. the pion self interactions) are

$$V(0, \pi^a) = -B_0 f_\pi^2 \cos\left(\frac{\pi}{f_\pi}\right) (m_u + m_d), \quad (3.36)$$

since $\text{Tr}(\sigma^a) = 0$. Thus, the two lowest order terms in this potential are

$$V(0, \pi^a) = -B_0 f_\pi^2 (m_u + m_d) + \frac{1}{2} B_0 (m_u + m_d) \pi^2 + \mathcal{O}\left(\frac{\pi^4}{f_\pi^2}\right). \quad (3.37)$$

The second term is the mass term for the pion. Requiring it to be canonically normalized leads to $B_0 = \frac{m_\pi^2}{m_u + m_d}$, where $m_\pi \approx 137.27 \text{ MeV}$ is the mass average of the pion [8].

Q_a can be conveniently chosen to be $\frac{M_q^{-1}}{\text{Tr}(M_q^{-1})}$, as this eliminates mass mixings between the axion and π^0 , and also simplifies the algebra. Doing the aforementioned algebra, the potential takes the form

$$\begin{aligned} V(a, \pi^a) = & -f_\pi^2 \frac{m_\pi^2}{m_u + m_d} \\ & \left[\left(m_u \cos\left(\frac{m_d}{m_u + m_d} \frac{a}{f_a}\right) + m_d \cos\left(\frac{m_u}{m_u + m_d} \frac{a}{f_a}\right) \right) \cos\left(\frac{\pi}{f_\pi}\right) \right. \\ & \left. + \frac{\pi^0}{\pi} \left(m_u \sin\left(\frac{m_d}{m_u + m_d} \frac{a}{f_a}\right) - m_d \sin\left(\frac{m_u}{m_u + m_d} \frac{a}{f_a}\right) \right) \sin\left(\frac{\pi}{f_\pi}\right) \right]. \quad (3.38) \end{aligned}$$

The axion mass can be obtained from the quadratic axion term. Proceeding in analogy with the estimation of B_0 ,

$$V(a, 0) = -2f_\pi^2 \frac{m_\pi^2}{m_u + m_d} + \frac{1}{2} \frac{m_\pi^2 m_u m_d}{(m_u + m_d)^2} \frac{f_\pi^2}{f_a^2} a^2 + \mathcal{O}\left(\frac{a^3}{f_a^3}\right), \quad (3.39)$$

consequently the axion mass is given by

$$m_a^2 = \frac{m_\pi^2 m_u m_d}{(m_u + m_d)^2} \frac{f_\pi^2}{f_a^2}. \quad (3.40)$$

Taking the square root and substituting for the masses and the pion decay constant (see Table 2.2 for the quark masses) the authors of [52] obtain

$$m_a \approx 5.70 \left(\frac{10^{12} \text{ GeV}}{f_a} \right) \mu\text{eV}, \quad (3.41)$$

This is the value that will be used in this work. Using the numbers of Table 2.2 one gets

$m_a \approx 5.89 \left(\frac{10^{12} \text{ GeV}}{f_a} \right) \mu\text{eV}$. This difference, though not large, is important. It stems from the fact that the masses cited in Table 2.2 are not reported at the same energy scale. For a consistent result the masses should be run to the same scale. The mass cited has the parameters run to 2 GeV.

3.1.3.2 Axion-Photon Coupling

The axion-photon coupling is given in Eq. (3.28) as

$$g_{a\gamma} = g_{a\gamma}^0 - \frac{3e^2}{4\pi^2 f_a} \text{Tr}(Q_a Q^2), \quad (3.42)$$

which depends on the model-dependent coupling $g_{a\gamma}^0$, as well as on the Q_a , though the choice of Q_a should not matter for the final result. N_c has been fixed to 3. This warrants a brief discussion on the nature of the model dependent couplings. Essentially, they arise from the PQ chiral anomaly

$$\partial^\mu J_\mu^{PQ} = \frac{g_s^2 N}{16\pi^2} G_{\mu\nu}^a \tilde{G}_a^{\mu\nu} + \frac{e^2 E}{16\pi^2} F_{\mu\nu} \tilde{F}^{\mu\nu}, \quad (3.43)$$

where N and E are the colour and electromagnetic anomaly coefficients, respectively and are given by [53]

$$N = \sum_i X_i T(R_i), \quad E = \sum_i X_i Q_i^2 D(R_i), \quad (3.44)$$

where the sums run over all fermions, X_i is the PQ charge, and $T(R_i)$ ¹ is the index of the $SU(3)_C$ representation R_i of the i -th fermion. Also, Q_i represent the electric charge of the i -th fermion, and $D(R_i)$ the dimension of R_i .

The anomalous current of Eq. (3.43) will couple to the axion in the following manner

$$\mathcal{L}_a \supset \frac{a}{v_a} \frac{g_s^2 N}{16\pi^2} G_{\mu\nu}^a \tilde{G}_a^{\mu\nu} + \frac{a}{v_a} \frac{e^2 E}{16\pi^2} F_{\mu\nu} \tilde{F}^{\mu\nu} + \frac{\partial^\mu a}{v_a} J_\mu^{PQ}, \quad (3.45)$$

through a process similar to the one described in Section C.1. Requiring this Lagrangian to be normalized like (3.14) leads to

$$v_a = \frac{f_a}{2N}, \quad (3.46)$$

which in turn sets the Lagrangian as

$$\mathcal{L}_a \supset \frac{a}{f_a} \frac{g_s^2}{32\pi^2} G_{\mu\nu}^a \tilde{G}_a^{\mu\nu} + \frac{a}{f_a} \frac{e^2}{32\pi^2} \frac{E}{N} F_{\mu\nu} \tilde{F}^{\mu\nu} + \frac{\partial^\mu a}{f_a} \frac{1}{2N} J_\mu^{PQ}. \quad (3.47)$$

¹For most calculations it is enough to know $T(3) = 1/2$, $T(6) = 5/2$, and $T(8) = 3$.

From this Lagrangian it can be seen that

$$g_{a\gamma}^0 = \frac{e^2}{8\pi^2 f_a} \frac{E}{N} = \frac{\alpha}{2\pi f_a} \frac{E}{N}. \quad (3.48)$$

In the same way as for the axion mass, the matrix Q_a is chosen as $\frac{Q_M^{-1}}{\text{Tr}(Q_M^{-1})}$, which is equal to $\frac{m_u m_d}{m_u + m_d} \text{diag}(m_u^{-1}, m_d^{-1})$. Substituting for this in (3.42) gives

$$g_{a\gamma} = \frac{\alpha}{2\pi f_a} \left(\frac{E}{N} - \frac{2}{3} \frac{m_u + 4m_d}{m_u + m_d} \right) \approx \frac{\alpha}{2\pi f_a} \left(\frac{E}{N} - 1.92 \right). \quad (3.49)$$

The axion couplings to fermions can be briefly obtained from Eq. (3.47). To exemplify this, the PQ current can be supposed to contain only a single (left- and right-handed) fermion species, f , since the contribution of more fermions will be of the same form. Considering this,

$$\frac{\partial^\mu a}{f_a} \frac{1}{2N} J^{\text{PQ}} = \frac{\partial^\mu a}{f_a} \frac{1}{2N} (\bar{f}_L X_{f_L} \gamma_\mu f_L + \bar{f}_R X_{f_R} \gamma_\mu f_R) = \frac{\partial^\mu a}{f_a} \frac{1}{2N} C_{f_a}^0 \bar{f} \gamma_\mu \gamma_5 f, \quad (3.50)$$

where $X_{f_{L/R}}$ is the charge of the left- or right-handed quark. By identifying terms the axion-fermion coupling takes the form

$$C_{f_a}^0 = \frac{X_{f_L} - X_{f_R}}{2N}. \quad (3.51)$$

The existence of Yukawa terms in the SM also gives sets the PQ charge of the Higgs doublet as $X_H = X_{f_L} - X_{f_R}$.

3.1.4 Invisible Axion Models

To fix the problems with the PQWW axion, the axion decay constant must decouple from the EW vev , so that it is no longer true that $f_a \propto v$, like in (C.23). These are called *invisible axion models* since they are built with $f_a \gg v$, thus giving the axion a very small mass and interaction. There are two main frameworks to achieve this, the *Kim-Shifman-Vainshtein-Zakharov* (KSVZ) [54, 55] type and the *Dine-Fischler-Srednicki-Zhitnitsky* (DFSZ) [56, 57] type. KSVZ-type models achieve the UV-completion by introducing heavy vector-like fermions, an example of the simplest realization of this is given in Appendix C.3. DFSZ-style models keep the two Higgs doublets from the PQWW model, but add an extra singlet scalar field, σ . The model in Chapter 4 is a DFSZ-type model. The general theory of the DFSZ axions is presented below.

Unlike the KSVZ model, the DFSZ model keeps the two Higgs doublets from the PQWW model, but adds a SM singlet complex scalar, σ . Again, this scalar carries PQ

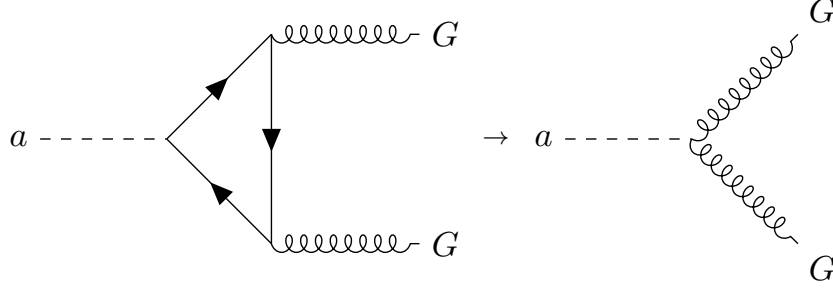


Figure 3.2: Passing from the axion-anomaly coupling in the UV-complete theory to the effective axion-gluon coupling. The same applies to the axion-photon coupling.

charge. Its scalar potential can be written as

$$V(H_u, H_d, \sigma) = \tilde{V}(H_u^\dagger H_u, H_d^\dagger H_d, H_u^\dagger H_d, \sigma^\dagger \sigma) + \lambda H_u H_d \sigma^{\dagger 2} + h.c., \quad (3.52)$$

where \tilde{V} is a potential containing all the possible moduli of the scalars. The last term in the potential ensures that a global $U(1)$ for each of the scalars breaks explicitly into $U(1)_Y \times U(1)_{PQ}$. There are two types of DFSZ models, the difference being on how the leptons couple to the Higgs doublets. The difference can be seen in their Yukawa Lagrangians

$$\begin{aligned} \mathcal{L}_Y^{DFSZ-I} &= y_{ij}^u \bar{Q}^i H_u u_R^j + y_{ij}^d \bar{Q}^i H_d d_R^j + y_{ij}^e \bar{L}^i H_d e_R^j + h.c. \\ \mathcal{L}_Y^{DFSZ-II} &= y_{ij}^u \bar{Q}^i H_u u_R^j + y_{ij}^d \bar{Q}^i H_d d_R^j + y_{ij}^e \bar{L}^i \tilde{H}_u e_R^j + h.c. \end{aligned} \quad (3.53)$$

After PQ and EW symmetry breaking, there will be multiple uncharged scalars, in fact there will be two more than in the PQWW model. By counting these fields it can be seen that there will be three uncharged polar fields, instead of one, i.e. all of these, or a combination of them, could be the axion. This is because there will be an uncharged Goldstone boson for each of the scalars left after symmetry breaking, i.e.

$$\begin{aligned} H_u &\supset \frac{v_u}{\sqrt{2}} e^{i \frac{\alpha_u}{v_u}} \begin{pmatrix} 1 \\ 0 \end{pmatrix}, \\ H_d &\supset \frac{v_d}{\sqrt{2}} e^{i \frac{\alpha_d}{v_d}} \begin{pmatrix} 0 \\ 1 \end{pmatrix}, \\ \sigma &\supset \frac{v_\sigma}{\sqrt{2}} e^{i \frac{\alpha_\sigma}{v_\sigma}}. \end{aligned} \quad (3.54)$$

The axion will couple to these fields exclusively through the PQ current

$$J_\mu^{PQ} = -X_{H_u} H_u^\dagger i \overleftrightarrow{\partial}_\mu H_u - X_{H_d} H_d^\dagger i \overleftrightarrow{\partial}_\mu H_d - X_\sigma \sigma^\dagger i \overleftrightarrow{\partial}_\mu \sigma + J_\mu^{PQ}(\Psi), \quad (3.55)$$

where $J_\mu^{PQ}(\Psi)$ contains the fermionic part of the current and X_ϕ are the PQ charges of the fields, with $\phi = u, d, \sigma$. From the derivatives in the current the terms containing only the the axion components, a_ϕ , can be written as

$$J_\mu^{PQ}(a_\phi) = \sum_\phi X_\phi v_\phi \partial_\mu a_\phi = v_a \partial_\mu a. \quad (3.56)$$

This fixes the axion and its vev as

$$a = \frac{1}{v_a} \sum_\phi X_\phi v_\phi a_\phi, \quad v_a^2 = \sum_\phi X_\phi^2 v_\phi^2. \quad (3.57)$$

The scalar PQ charges in this kind of model are not free, in fact there are two constraints, so that they are fixed up to normalization. The first constraint comes from having the term $H_u H_d \sigma^{\dagger 2}$ PQ invariant, which implies

$$X_{H_u} + X_{H_d} - 2X_\sigma = 0. \quad (3.58)$$

The second constraint comes from avoiding kinetic mixing between the axion and the Z boson, this constraint comes from a hypercharge current similar to Eq. (3.56) and puts the constrain as

$$\sum_\phi 2Y_\phi X_\phi v_\phi^2 = -X_{H_u} v_u^2 + X_{H_d} v_d^2 = 0, \quad (3.59)$$

where Y_ϕ is the hypercharge of the scalar field ϕ . Thus choosing a unit charge for σ fixes the PQ charges as

$$X_\phi = 1, \quad X_{H_u} = 2 \cos^2(\beta), \quad X_{H_d} = 2 \sin^2(\beta), \quad (3.60)$$

again with $\tan(\beta) = \frac{v_u}{v_d}$, i.e. $v_u^2 + v_d^2 = v^2$ and v the EW vev . Finally, this leads to the axion vev from Eq. (3.57)

$$v_a^2 = v_\sigma^2 + v^2 (\sin(2\beta))^2. \quad (3.61)$$

If $v_\sigma \gg v$, the desired result of $v_a \approx v_\sigma$. To integrate out σ , a field dependent chiral transformation, in terms of the axion, is done

$$\Omega \rightarrow e^{-i\gamma_5 \frac{\sigma}{2v_a}} \Omega, \quad (3.62)$$

which uncouples the axion from the radial PQ field and the fermions (see Appendix C.3 for the explicit construction of the radial field). Fig. 3.2 shows diagrammatically how the axion-gluon coupling appears after the integration. Here,

$$\begin{aligned} N &= 3 \left(\frac{1}{2} X_{H_u} + \frac{1}{2} X_{H_d} \right) = 3, \\ E &= 3 \left(3 \left(\frac{2}{3} \right)^2 X_{H_u} + 3 \left(-\frac{1}{3} \right)^2 X_{H_d} + (-1)^2 X_{H_d} \right), \end{aligned} \quad (3.63)$$

for a type-I DFSZ model. In type-II DFSZ models, the PQ charge in the last term in E has to be changed to X_{H_u} . See Eq. (3.44) for the expression of these factors. An equivalent, but more direct way of applying similar constraints is used and explained in the model of Chapter 4, since these constraints are relaxed by the introduction of a second σ field.

3.2 Axions as Dark Matter Candidates

Axions and ALPs can be DM candidates, provided they are light enough to conform with particle physics observations (or rather the lack thereof), but heavy enough such that they were not overproduced in the early Universe. The mass range for a DM axion corresponds to $10^{-12} \text{ eV} \lesssim m_a \lesssim 1 \text{ MeV}$ [15]. Since many axion couplings are model dependent, some of the DM properties also depend on the specific axion model. Luckily, most of them can also be treated at the level of the effective axion Lagrangian (as given in (3.14)) and are independent of the specifics of the UV-complete theory. The favoured mechanism to produce cold axions is the *Misalignment mechanism* (also called *vacuum misalignment*) [58], nevertheless there is also the possibility (though very strongly disfavored) of thermal axion production [15], and of axion production by the decay of cosmic strings and domain walls [49].

The Misalignment Mechanism (for QCD axions) explains the production of cold axions in the early universe by recognizing that the *axion angle*

$$\theta(x) = \frac{a(x)}{f_a}, \quad (3.64)$$

where $a(x)$ is the axion field (or more precisely its *vev*), will begin in the early Universe at a value θ_i , the misalignment angle, which does not necessarily minimize the axion potential. As the Universe expands, this angle approaches and then begins to oscillate around the potential's minimum. While this occurs, an excess of axions is produced by the fields' oscillation. Other particles can also be produced through axion decay. When the field reaches the minimum, all of its kinetic energy has dissipated due to the

oscillation, and the number density per comoving volume of the axions turns out to be constant. Making some assumptions about the adiabaticity of the fields' evolution, the relic density can be found to be

$$\Omega_a^{mis} h^2 \approx 2 \times 10^4 \left(\frac{f_a}{10^{16} \text{ GeV}} \right)^{\frac{7}{6}} \langle \theta_i^2 \rangle, \quad (3.65)$$

with $h = \frac{H_0}{100}$, the reduced Hubble constant. A detailed derivation of this relic density is found in Appendix B.2. In scenarios where domain walls or cosmic strings are present, the estimation of the relic density changes considerably [28, 49].

A Flavourful Axion Model

In this chapter a model is presented, where the PQ symmetry is identified with the FN symmetry, i.e.

$$U(1)_{FN} = U(1)_{PQ}, \quad (4.1)$$

which can be called the Peccei-Quinn-Froggatt-Nielsen (PQFN) symmetry. Axions arising from flavour symmetries are known under different names, such as *flaxions* [59, 60], *axiflavons* [61, 62, 63], and *flavourful axions* [64, 65, 66]¹. A feature of these kind of models is that the mass hierarchy, as well as the Strong CP Problem are solved by the same extension of the SM. Particularly, the model discussed here is a type-II DFSZ model, and has a Nearest-Neighbour-Interaction texture (NNI) [67] for the quark mass matrices and an A_2 texture [68] for the neutrino mass matrices. Furthermore, some aspects of the phenomenology of this model will be discussed, either directly or after a precise χ^2 fit of the masses and mixing parameters of the SM fermions. This model [69] was proposed and developed in collaboration with Dr. Eduardo Peinado, Dr. Newton Nath, and M.Sc. León García.

4.1 The Model

The flavourful axion model will be presented from a theoretical standpoint in this section. First a brief overview of the model is presented, leading to a detailed description of the quark sector and its UV-completion, as well as the lepton sector. Finally, the scalar sector, including the physical axion, is discussed.

4.1.1 Overview of the Model

The SM is extended by the inclusion of two Higgs doublets, H_u and H_d , and two complex scalar $SU(2)_L$ singlets, σ and σ' , which are the flavons for quarks and leptons,

¹Flavourful axion is the preferred term in this work, mainly because it translates nicely to Spanish as *axión sabroso*.

respectively. In the neutrino sector three heavy right-handed fermions, N_i , where $i = 1, 2, 3$, are added as well, which will be similar to sterile neutrinos in a type-I seesaw scenario. The inclusion of the two Higgs doublets signifies that the axion in question will be of the DFSZ type, as a matter of fact a type-II DFSZ axion, as can be seen from the Lagrangian in (4.20). Breaking of the PQFN symmetry (which henceforth will only be called the PQ symmetry) will also lead to a physical axion, which will be a linear combination of the Goldstone bosons of the scalars.

Although there exist some constraints on the PQ charges, as was pointed in Sec. 3.1.3 and Sec. 3.1.4, these are not strong enough to determine the PQ charges of the theory completely. In order to do this, the FN mechanism can be introduced in such a way that the mass matrices for quarks and neutrinos arise from the charge assignment and operators of dimension greater than 4. The NNI texture for the quark masses will be required to arise at next-to-leading order, likewise the A_2 texture will arise for the neutrinos. The NNI texture has the same zeros as the Fritzsch texture [70, 71], but unlike the Fritzsch texture, is not necessarily hermitic. This structure has the non-zero elements in $i = j + 1$, and here $i = N = j$, leading to

$$M^{u/d} = \begin{pmatrix} 0 & \times & 0 \\ \times & 0 & \times \\ 0 & \times & \times \end{pmatrix}. \quad (4.2)$$

The A_2 texture is similar in the sense that $i = j + 1$, but here has $i = N, N - 1 = j$, and is also symmetrical, this translates as

$$m_\nu = m_\nu^T = \begin{pmatrix} 0 & \times & 0 \\ \times & \times & \times \\ 0 & \times & \times \end{pmatrix}. \quad (4.3)$$

Both of these textures are chosen, since they are phenomenologically viable. This means that they are able to give observables, masses and mixing parameters, well in agreement with results from experiments and global fits. How good these are is quantified in Sec. 4.2.1. In particular, the NNI texture is chosen over the Fritzsch texture, since the Fritzsch texture has trouble replicating the small value of V_{cb} in the CKM matrix, simultaneously with the large value of m_t [72, 73].

The lepton sector, through the inclusion of the N_i fermions will be renormalizable, whereas for the quark sectors two possible UV-completions are discussed. The first UV-completion will include heavy coloured, weak isospin singlet, fermions, F_{ij} , corresponding to a scenario analogous to the type-I seesaw mechanism. The second UV-completion is done through the inclusion of two heavy weak isospin doublet scalars, $\Phi_{u/d}$, corresponding to a type-II seesaw mechanism.

4.1.2 The Quark Sector

The PQ charges of the quarks are chosen in such a manner that the (3, 3) term in the up- and down-quark mass matrices are generated at dimension 5, while all the others are generated at higher dimensions. The strong constraint comes from the requirement that at order 5 the mass matrices have a NNI structure. Following the convention of DFSZ models that the Higgs doublets have unit PQ charge (positive or negative) and requiring PQ invariance of the SM Lagrangian leads to the PQ charges in Table 4.1. It can be noticed that the charge of the flavon, σ , does not require special treatment and is determined by the aforementioned constraints. It can be noticed that the PQ charge of the down-type quarks is opposite to that of the up-type quarks.

Fields/Symmetry	Q_{iL}	u_{iR}	d_{iR}	H_u	H_d	σ
$SU(2)_L \times U(1)_Y$	(2, 1/6)	(1, 2/3)	(1, -1/3)	(2, -1/2)	(2, 1/2)	(1, 0)
$U(1)_{PQ}$	(9/2, -5/2, 1/2)	(-9/2, 5/2, -1/2)	(-9/2, 5/2, -1/2)	1	1	1

Table 4.1: Field content and transformation properties of the PQ-symmetry under the DFSZ type-I seesaw model, where $i = 1, 2, 3$ represent families of three quarks. The PQ charges of the quarks are given in the order of the families' masses, with the lightest as the first.

The lowest order terms in the effective Lagrangian, invariant under PQ and the SM gauge symmetries as given by Table 4.1, coupling every combination of up-type quarks to the flavon are the following

$$\begin{aligned}
-\mathcal{L} \supset & \frac{C_{11}^u}{\Lambda^8} \bar{Q}_{1L} H_u u_{1R} \sigma^8 + \frac{C_{12}^u}{\Lambda} \bar{Q}_{1L} H_u u_{2R} \sigma + \frac{C_{13}^u}{\Lambda^4} \bar{Q}_{1L} H_u u_{3R} \sigma^4 + \frac{C_{21}^u}{\Lambda} \bar{Q}_{2L} H_u u_{1R} \sigma \\
& + \frac{C_{22}^u}{\Lambda^4} \bar{Q}_{2L} \tilde{H}_d u_{2R} \sigma^{*4} + \frac{C_{23}^u}{\Lambda} \bar{Q}_{2L} \tilde{H}_d u_{3R} \sigma^* + \frac{C_{31}^u}{\Lambda^4} \bar{Q}_{3L} H_u u_{1R} \sigma^4 + \frac{C_{32}^u}{\Lambda} \bar{Q}_{3L} \tilde{H}_d u_{2R} \sigma^* \\
& + y_{33}^u \bar{Q}_{3L} H_u u_{3R} ,
\end{aligned} \tag{4.4}$$

where C_{ij}^u represents coupling constant of each term and Λ is the FN cut-off scale of the model. These terms are analogous for the down sector, owing to the fact that the PQ charges of the down-type quarks are the negative of the up-type quarks, and reads as

$$\begin{aligned}
-\mathcal{L} \supset & \frac{C_{11}^d}{\Lambda^8} \bar{Q}_{1L} H_d d_{1R} \sigma^8 + \frac{C_{12}^d}{\Lambda} \bar{Q}_{1L} H_d d_{2R} \sigma + \frac{C_{13}^d}{\Lambda^4} \bar{Q}_{1L} H_d d_{3R} \sigma^4 + \frac{C_{21}^d}{\Lambda} \bar{Q}_{2L} H_d d_{1R} \sigma \\
& + \frac{C_{22}^d}{\Lambda^4} \bar{Q}_{2L} \tilde{H}_u d_{2R} \sigma^{*4} + \frac{C_{23}^d}{\Lambda} \bar{Q}_{2L} \tilde{H}_u d_{3R} \sigma^* + \frac{C_{31}^d}{\Lambda^4} \bar{Q}_{3L} H_d d_{1R} \sigma^4 + \frac{C_{32}^d}{\Lambda} \bar{Q}_{3L} \tilde{H}_u d_{2R} \sigma^* \\
& + y_{33}^d \bar{Q}_{3L} H_d d_{3R} ,
\end{aligned} \tag{4.5}$$

with C_{ij}^d as the coupling constant and Λ as the cut-off scale. It is worth noting that the Higgs doublets couple to both sectors, i.e. not exclusively to their subscript's sector.

After PQ symmetry breaking hierarchical mass terms arise from the FN mechanism.

The corresponding mass matrices are, up to dimension 7 or equivalently up to $\frac{\langle\sigma\rangle^3}{\Lambda^3}$,

$$M^{u/d} = \begin{pmatrix} 0 & \epsilon v_{u/d} C_{12}^{u/d} & 0 \\ \epsilon v_{u/d} C_{21}^{u/d} & 0 & \epsilon v_{d/u} C_{23}^{u/d} \\ 0 & \epsilon v_{d/u} C_{32}^{u/d} & y_{33}^{u/d} v_{u/d} \end{pmatrix}, \quad (4.6)$$

where $\epsilon = \frac{v_\sigma}{\Lambda} = \frac{\langle\sigma\rangle^*}{\Lambda}$, and $v_{u/d}$ is the vev of the up- or down-sector Higgs doublet. It can be noticed that these are NNI-type mass matrices. Since typical values of ϵ are of the order of 0.2 [43], the mass matrices can for most purposes be taken at this order. Alternatively, an extra symmetry can be introduced to the model, prohibiting higher order terms, although for simplicity this was not done here. It is also worth noting that the mass hierarchy between the up- and down-sector is not explicitly generated by the ϵ powers, especially between m_t and m_b , as is typical in FN models. Nevertheless, it can be explained by a hierarchy between v_u and v_d .

4.1.3 UV-Completion of the Quark Sector

Two UV-completions of the quark sector are presented, following the style of a type-I and type-II seesaw mechanism.

4.1.3.1 Type-I Seesaw

As the name of this UV-completion suggests, this is analogous to the Type-I seesaw UV-completion for neutrinos, but with some differences. Unlike the UV completion in the case of neutrinos, the heavy fermions will carry colour charge (as an $SU(3)_C$ triplet), and will be vector-like. Otherwise they are analogous, i.e. will be an $SU(2)_L$ singlet, but will carry PQ charge and weak hypercharge. These fermions, F_q^{ij} , will couple to the left-handed quarks and the Higgs doublets with a Yukawa coupling \mathcal{Y}_{ij}^q , these fields will mix through the mass terms \mathcal{M}_{ij}^q , and finally will couple to the flavon and the right-handed quarks with a different Yukawa coupling, \mathcal{Y}'_{ij}^q . The UV-complete Lagrangian in the up-quark sector, corresponding to Eq. (4.4), is

$$\begin{aligned} -\mathcal{L}_u^{UV} \supset & \mathcal{Y}_{12}^u \bar{Q}_{1L} H_u F_{uR}^{12} + \mathcal{M}_{12}^u \bar{F}_{uR}^{12} F_{uL}^{12} + \mathcal{Y}'_{12}^u \bar{F}_{uL}^{12} \sigma u_{2R} \\ & + \mathcal{Y}_{21}^u \bar{Q}_{2L} H_u F_{uR}^{21} + \mathcal{M}_{21}^u \bar{F}_{uR}^{21} F_{uL}^{21} + \mathcal{Y}'_{21}^u \bar{F}_{uL}^{21} \sigma u_{1R} \\ & + \mathcal{Y}_{23}^u \bar{Q}_{2L} \tilde{H}_d F_{uR}^{23} + \mathcal{M}_{23}^u \bar{F}_{uR}^{23} F_{uL}^{23} + \mathcal{Y}'_{23}^u \bar{F}_{uL}^{23} \sigma^* u_{3R} \\ & + \mathcal{Y}_{32}^u \bar{Q}_{3L} \tilde{H}_d F_{uR}^{32} + \mathcal{M}_{32}^u \bar{F}_{uR}^{32} F_{uL}^{32} + \mathcal{Y}'_{32}^u \bar{F}_{uL}^{32} \sigma^* u_{2R}. \end{aligned} \quad (4.7)$$

Fields/Symmetry	F_{uC}^{12}	F_{uC}^{21}	F_{uC}^{23}	F_{uC}^{32}	F_{dC}^{12}	F_{dC}^{21}	F_{dC}^{23}	F_{dC}^{32}
$U(1)_Y$	2/3	2/3	2/3	2/3	-1/3	-1/3	-1/3	-1/3
$U(1)_{PQ}$	7/2	-7/2	-3/2	3/2	7/2	-7/2	-3/2	3/2

Table 4.2: Vector like fermions and their transformation properties of the PQ-symmetry under the DFSZ type-I seesaw model, where $C = L, R$.

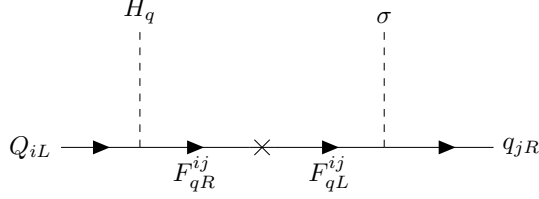


Figure 4.1: UV-complete diagram within the DFSZ type-I seesaw framework from Eqs. (4.7) and (4.8).

The down-quark sector of Eq. (4.5) has a similar UV-completion, which is

$$\begin{aligned}
-\mathcal{L}_d^{UV} \supset & \mathcal{Y}_{12}^d \bar{Q}_{1L} H_d F_{dR}^{12} + \mathcal{M}_{12}^d \overline{F_{dR}^{12}} F_{dL}^{12} + \mathcal{Y}'_{12} \overline{F_{dL}^{12}} \sigma d_{2R} \\
& + \mathcal{Y}_{21}^d \bar{Q}_{2L} H_d F_{dR}^{21} + \mathcal{M}_{21}^d \overline{F_{dR}^{21}} F_{dL}^{21} + \mathcal{Y}'_{21} \overline{F_{dL}^{21}} \sigma d_{1R} \\
& + \mathcal{Y}_{23}^d \bar{Q}_{2L} \tilde{H}_u F_{dR}^{23} + \mathcal{M}_{23}^d \overline{F_{dR}^{23}} F_{dL}^{23} + \mathcal{Y}'_{23} \overline{F_{dL}^{23}} \sigma^* d_{3R} \\
& + \mathcal{Y}_{32}^d \bar{Q}_{3L} \tilde{H}_u F_{dR}^{32} + \mathcal{M}_{32}^d \overline{F_{dR}^{32}} F_{dL}^{32} + \mathcal{Y}'_{32} \overline{F_{dL}^{32}} \sigma^* d_{2R}. \tag{4.8}
\end{aligned}$$

The charges of the heavy fermions can be read from Table 4.2, while Fig. 4.1 shows the Feynman diagram corresponding to Eq. (4.7) and Eq. (4.8).

The quarks will acquire mass after PQ and EW symmetry breaking, that is after the three scalars acquire their corresponding vev . The resulting mass matrices (up and down) take the form

$$M^{u/d} = \begin{pmatrix} M_{QLqR} & M_{QLFR} \\ M_{FLqR} & M_{FLFR} \end{pmatrix}_{7 \times 7}, \tag{4.9}$$

which are 7×7 matrix expressed in the $(\bar{Q}_L, F_{(u/d)L}) \times (q_R, F_{(u/d)R})$. Its entries are the following submatrices

$$M_{Q_L Q_R} = \begin{pmatrix} 0 & 0 & 0 \\ 0 & 0 & 0 \\ 0 & 0 & y_{33}^{u/d} v_{u/d} \end{pmatrix}, \quad (4.10)$$

$$M_{Q_L F_R} = \begin{pmatrix} y_{12}^{u/d} v_{u/d} & 0 & 0 & 0 \\ 0 & y_{21}^{u/d} v_{u/d} & y_{23}^{u/d} v_{d/u} & 0 \\ 0 & 0 & 0 & y_{32}^{u/d} v_{d/u} \end{pmatrix}, \quad (4.11)$$

$$M_{F_L Q_R} = \begin{pmatrix} 0 & y_{12}^{r/d} v_\sigma & 0 \\ y_{21}^{r/d} v_\sigma & 0 & 0 \\ 0 & 0 & y_{23}^{r/d} v_\sigma^* \\ 0 & y_{32}^{r/d} v_\sigma^* & 0 \end{pmatrix}, \quad (4.12)$$

$$M_{F_L F_R} = \text{diag}(\mathcal{M}_{12}^{u/d}, \mathcal{M}_{21}^{u/d}, \mathcal{M}_{23}^{u/d}, \mathcal{M}_{32}^{u/d}). \quad (4.13)$$

This scenario works like a type-I seesaw, which was discussed in Section 2.2.2, if the masses of the heavy fermions are much greater than that of the quarks. A small difference is that the particles will be Dirac particles, unlike the neutrino seesaw. Therefore, the mass matrix for the SM quarks can be approximated as

$$m^{u/d} \approx M_{Q_L Q_R} - M_{Q_L F_R} M_{F_L F_R}^{-1} M_{F_L Q_R}. \quad (4.14)$$

Another difference is the appearance of an extra term in the seesaw formula, $M_{Q_L Q_R}$, this would correspond to a left-handed neutrino majorana mass in the neutrino sector, and since it is prohibited by the SM symmetries (a left-handed Majorana mass term would violate weak hypercharge, see Section 2.2.1) is set to 0. The approximate mass matrices are

$$\begin{aligned} m^{u/d} &= \begin{pmatrix} 0 & \frac{y_{12}^{u/d} y_{12}^{r/d}}{\mathcal{M}_{12}} v_{u/d} v_\sigma & 0 \\ \frac{y_{21}^{u/d} y_{21}^{r/d}}{\mathcal{M}_{21}} v_{u/d} v_\sigma & 0 & \frac{y_{23}^{u/d} y_{23}^{r/d}}{\mathcal{M}_{23}} v_{d/u}^* v_\sigma^* \\ 0 & \frac{y_{32}^{u/d} y_{32}^{r/d}}{\mathcal{M}_{32}} v_{d/u}^* v_\sigma^* & y_{33}^{u/d} v_{u/d} \end{pmatrix}, \\ &= \begin{pmatrix} 0 & \mathbf{A}_{u/d} & 0 \\ \mathbf{B}_{u/d} & 0 & \mathbf{C}_{u/d} \\ 0 & \mathbf{D}_{u/d} & \mathbf{E}_{u/d} \end{pmatrix}, \end{aligned} \quad (4.15)$$

where $\mathbf{A}_{u/d}$, $\mathbf{B}_{u/d}$, $\mathbf{C}_{u/d}$, $\mathbf{D}_{u/d}$, and $\mathbf{E}_{u/d}$ are complex entries. As was expected from the low-energy theory, these matrices possess a NNI texture. It is also worth noting that the suppressing role played by $\frac{1}{\Lambda}$ in the low-energy theory is now taken over by $\frac{1}{\mathcal{M}_{ij}}$,

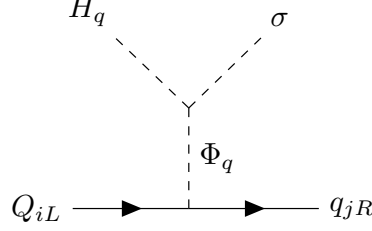


Figure 4.2: UV-complete diagram within the DFSZ type-II seesaw framework from Eqs. (4.16), and (4.17).

setting a natural scale for these masses at $\mathcal{M}_{ij} \sim \Lambda^1$.

4.1.3.2 Type-II Seesaw

A second possible UV-completion introduces two new heavy $SU(2)_L$ doublets, $\Phi_{u/d}$, to the theory. These transform under $SU(2)_L \times U(1)_Y \times U(1)_{PQ}$ in the following representations: Φ_u in $(2, -1/2, 2)$ representation, and Φ_d in the $(2, 1/2, 2)$ representation. The Lagrangian of the up-quark sector (Eq. (4.4)) is UV-completed as

$$-\mathcal{L}_u^{UV} \supset \mathcal{Y}_{12}^u \bar{Q}_{1L} \Phi_u u_{2R} + \mathcal{Y}_{21}^u \bar{Q}_{2L} \Phi_u u_{1R} + \kappa_u H_u \Phi_u^\dagger \sigma + \mathcal{Y}_{23}^u \bar{Q}_{2L} \tilde{\Phi}_d u_{3R} + \mathcal{Y}_{32}^u \bar{Q}_{3L} \tilde{\Phi}_d u_{2R} + \kappa_d \tilde{H}_d \Phi_d \sigma^* . \quad (4.16)$$

In the same vein, the Lagrangian (4.5) becomes

$$-\mathcal{L}_d^{UV} \supset \mathcal{Y}_{12}^d \bar{Q}_{1L} \Phi_d d_{2R} + \mathcal{Y}_{21}^d \bar{Q}_{2L} \Phi_d d_{1R} + \kappa_u H_u \Phi_d^\dagger \sigma + \mathcal{Y}_{23}^d \bar{Q}_{2L} \tilde{\Phi}_d d_{3R} + \mathcal{Y}_{32}^d \bar{Q}_{3L} \tilde{\Phi}_d d_{2R} + \kappa_d \tilde{H}_d \Phi_d \sigma^* . \quad (4.17)$$

The Feynman diagram for this UV-completion can be seen in Fig. 4.2, and has the same topology as the type-II seesaw, hence the name.

After PQ and EW symmetry breaking, the quarks will acquire masses, as was the case in the previous UV-completion and also the IR theory. In this case the mass matrices for the up- and down-quarks will be

$$m^{u/d} = \begin{pmatrix} 0 & \mathcal{Y}_{12}^{u/d} v_{\Phi_{u/d}} & 0 \\ \mathcal{Y}_{21}^{u/d} v_{\Phi_{u/d}} & 0 & \mathcal{Y}_{23}^{u/d} v_{\Phi_{d/u}} \\ 0 & \mathcal{Y}_{32}^{u/d} v_{\Phi_{d/u}} & \mathcal{Y}_{33}^{u/d} v_{u/d} \end{pmatrix} , \quad (4.18)$$

where the *vevs* $v_{\Phi_{u/d}}$ correspond to the newly introduced heavy scalars. At leading order

¹This is to be expected *a priori*, since at low energies the UV completion has to agree with the effective theory. Nevertheless it is a good indication that the UV-completion was done correctly.

these are

$$v_{\Phi_{u/d}} \approx -\frac{\kappa_{u/d} v_\sigma v_{u/d}}{M_{\Phi_{u/d}}^2}, \quad (4.19)$$

with $M_{\Phi_{u/d}}$ as the masses of $\Phi_{u/d}$. These *vevs* can be obtained from the scalar potential in Eqs. (4.31) and (4.32). It is worth noting that the mass matrices, again, possess the NNI structure. Furthermore, they are again suppressed (but now quadratically) by the masses of the heavy fields.

4.1.4 The Lepton Sector

Up until now the second flavon, σ' , has not been needed. But, it will be necessary to include it in the lepton sector, since otherwise the Majorana mass matrix will be singular at leading order, since the 12-term would be prohibited by the PQ symmetry. The Yukawa Lagrangian of this sector is given by

$$\begin{aligned} -\mathcal{L}_y^l \supset & y_e \bar{L}_{eL} H_d \ell_{eR} + y_\mu \bar{L}_{\mu L} \tilde{H}_u \ell_{\mu R} + y_\tau \bar{L}_{\tau L} H_d \ell_{\tau R} \\ & + y_1' \bar{L}_{eL} H_u N_1 + y_2' \bar{L}_{\mu L} \tilde{H}_d N_2 + y_3' \bar{L}_{\tau L} H_u N_3 \\ & + \frac{M_1}{2} \bar{N}_1^c N_1 + \frac{y_{12}^N}{2} \bar{N}_1^c N_2 \sigma' + \frac{y_{13}^N}{2} \bar{N}_1^c N_3 \sigma + \frac{y_{33}^N}{2} \bar{N}_3^c N_3 \sigma'. \end{aligned} \quad (4.20)$$

The first line includes the terms for the charged leptons, the second, the interaction of the left-handed leptons with the heavy neutrinos N_i , and the last line the Majorana terms. From here it can be seen that the charged lepton mass matrix and the neutrino Dirac mass matrix will be diagonal, whereas the right-handed Majorana mass matrix will not. The representations of the new fields can be read from Table 4.3.

Fields/Symmetry	L_{iL}	ℓ_{iR}	N_i	σ'
$SU(2)_L \times U(1)_Y$	(2, -1/2)	(1, -1)	(1, 0)	(1, 0)
$U(1)_{PQ}$	(1, -3, 0)	(0, -2, -1)	(0, -2, -1)	2

Table 4.3: Field content and transformation properties of the leptonic fields and the scalar field σ' , where $i = 1, 2, 3$ represent the three lepton families.

Since the energy at which PQ breaks is taken to be much greater than that of EW symmetry breaking, the seesaw mechanism is naturally realized, as the Majorana masses of the heavy neutrinos will be much larger than the Dirac masses. Explicitly, they can be written as

$$M_R = \begin{pmatrix} M_1 & y_{12}^N v_{\sigma'} & y_{13}^N v_\sigma \\ y_{12}^N v_{\sigma'} & 0 & 0 \\ y_{13}^N v_\sigma & 0 & y_{33}^N v_{\sigma'} \end{pmatrix} \quad (4.21)$$

and

$$M_D = \text{diag}(v_u y_1^\nu, v_u^* y_2^\nu, v_d y_3^\nu). \quad (4.22)$$

The neutrino mass matrix is given by the seesaw formula as

$$m_\nu = -M_D^T M_R^{-1} M_D, \quad (4.23)$$

which is

$$m_\nu = \frac{1}{v_{\sigma'}} \begin{pmatrix} 0 & -\frac{v_u v_d^* y_1^\nu y_2^\nu}{y_{12}^N} & 0 \\ -\frac{v_u v_d^* y_1^\nu y_2^\nu}{y_{12}^N} & \frac{(v_d^* y_2^\nu)^2 (M_1 v_{\sigma'} y_{33}^N - v_\sigma^2 (y_{13}^N)^2)}{v_{\sigma'}^2 y_{33}^N (y_{12}^N)^2} & \frac{v_u v_d^* v_\sigma y_2^\nu y_3^\nu y_{13}^N}{v_{\sigma'} y_{12}^N y_{33}^N} \\ 0 & \frac{v_u v_d^* v_\sigma y_2^\nu y_3^\nu y_{13}^N}{v_{\sigma'} y_{12}^N y_{33}^N} & -\frac{v_u^2 (y_3^\nu)^2}{y_{33}^N} \end{pmatrix} \quad (4.24)$$

and corresponds to the A_2 texture.

The inclusion σ' in this model has the consequence that non-zero terms appear at dimension-6 in the quark sector. The Lagrangian at this dimension takes the form

$$-\mathcal{L}_Y^{d=6} \supset \frac{C_{13}^u}{\Lambda^2} \bar{Q}_{1L} H_u u_{3R} \sigma'^2 + \frac{C_{31}^u}{\Lambda^2} \bar{Q}_{3L} H_u u_{1R} \sigma'^2 + \frac{C_{22}^u}{\Lambda^2} \bar{Q}_{2L} \tilde{H}_d u_{2R} \sigma'^{*2}, \quad (4.25)$$

for up-type quarks, and

$$-\mathcal{L}_Y^{d=6} \supset \frac{C_{13}^d}{\Lambda^2} \bar{Q}_{1L} H_d d_{3R} \sigma'^2 + \frac{C_{31}^d}{\Lambda^2} \bar{Q}_{3L} H_d d_{1R} \sigma'^2 + \frac{C_{22}^d}{\Lambda^2} \bar{Q}_{2L} \tilde{H}_u d_{2R} \sigma'^{*2}, \quad (4.26)$$

for down-type quarks. The UV-completion can be done with the heavy fermions introduced in Section 4.1.3.1, but only for the first term in each Lagrangian. For the other two terms new fermions, with different charges, have to be introduced. Nonetheless, as was stated before, terms of dimension higher than 5 are suppressed strongly by higher orders of ϵ , or can be prohibited by additional symmetries. As such the mass matrices are only considered up to dimension 5. The UV-completion of the first term in (4.25) can be written as

$$-\mathcal{L}_u^{UV} \supset y_{12}^u \bar{Q}_{1L} H_u F_{uR}^{12} + \mathcal{M}_{12}^u \overline{F_{uR}^{12}} F_{uL}^{12} + y_{12}^{u'} \overline{F_{uL}^{12}} \sigma' F_{uR}^{32} + \mathcal{M}_{32}^u \overline{F_{uR}^{32}} F_{uL}^{32} + y_{32}^{u'} \overline{F_{uL}^{32}} \sigma' u_{3R}, \quad (4.27)$$

and for the corresponding term in (4.26)

$$-\mathcal{L}_d^{UV} \supset y_{12}^d \bar{Q}_{1L} H_d F_{dR}^{12} + \mathcal{M}_{12}^d \overline{F_{dR}^{12}} F_{dL}^{12} + y_{12}^{d'} \overline{F_{dL}^{12}} \sigma' F_{dR}^{32} + \mathcal{M}_{32}^d \overline{F_{dR}^{32}} F_{dL}^{32} + y_{32}^{d'} \overline{F_{dL}^{32}} \sigma' d_{3R}. \quad (4.28)$$

The diagram corresponding to these UV-completions can be see in Fig. 4.3.

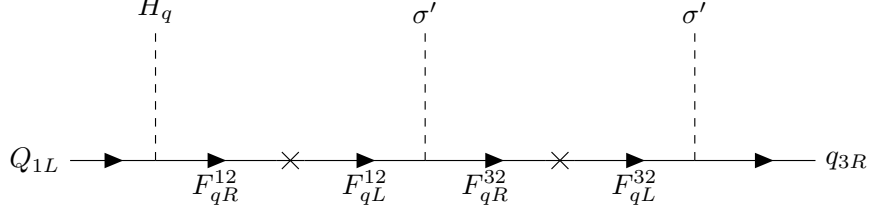


Figure 4.3: UV complete diagram for a dimension-6 operator within the DFSZ type-I seesaw framework in presence of flavon field σ' as follows from Eqs. (4.27), and (4.28).

4.1.5 The Scalar Sector

The complete scalar sector depends on the UV-completion of the theory, as the type-II seesaw UV-completion introduces two new heavy $SU(2)_L$ doublets, in addition to the original four scalar fields, since these are complex or $SU(2)_L$ doublets, the degrees of freedom are more than four. As a matter of fact, the scalars in the first UV-completion can be written as

$$H_u = \begin{pmatrix} h_u^0 + iA_u \\ h_u^- \end{pmatrix}, \quad H_d = \begin{pmatrix} h_d^+ \\ h_d^0 + iA_d \end{pmatrix}, \quad \sigma = S + iA, \quad \sigma' = S' + iA', \quad (4.29)$$

where each term corresponds to a real scalar field. It is worth noting that the fields A_i are the Goldstone bosons of the theory and will contribute to the physical axion. Additionally, the two heavy scalars can be written as

$$\Phi_u = \begin{pmatrix} \phi_u^0 + iA'_u \\ \phi_u^- \end{pmatrix}, \quad \Phi_d = \begin{pmatrix} \phi_d^+ \\ \phi_d^0 + iA'_d \end{pmatrix}. \quad (4.30)$$

The scalar potential, again, will depend on the UV-completion of the theory. Normally, scalar potentials in DFSZ-style models are restricted to have either terms like $\tilde{H}_u H_d \sigma$ or $\tilde{H}_u H_d \sigma^2$ [56, 74]. Since there are two scalar singlets, σ and σ' , both of type of couplings will be present, each with a different flavon, as can be seen from the scalar potential (4.31). This, as well as the quantity of scalar fields present, means that the scalar potential will be quite complicated. For the type-I seesaw UV-completion it reads

$$\begin{aligned} V_1 = & \mu_u^2 H_u^\dagger H_u + \mu_d^2 H_d^\dagger H_d + \mu_1^2 \sigma \sigma^\dagger + \mu_2^2 \sigma' \sigma'^\dagger + \lambda_u (H_u^\dagger H_u)^2 + \lambda_d (H_d^\dagger H_d)^2 + \lambda (\sigma \sigma^\dagger)^2 \\ & + \lambda' (\sigma' \sigma'^\dagger)^2 + \lambda_1 (H_u^\dagger H_d) (H_d^\dagger H_u) + \lambda_2 (H_u^\dagger H_u) (H_d^\dagger H_d) + \lambda_3 (H_u^\dagger H_d) (H_d^\dagger H_u) \\ & + \lambda_4 (\sigma \sigma^\dagger) (H_u^\dagger H_u) + \lambda_5 (\sigma \sigma^\dagger) (H_d^\dagger H_d) + \lambda_6 (\tilde{H}_u^\dagger H_d) (\sigma^\dagger)^2 + \lambda_7 (\sigma' \sigma'^\dagger) (H_u^\dagger H_u) \\ & + \lambda_8 (\sigma' \sigma'^\dagger) (H_d^\dagger H_d) + \lambda_9 (\sigma' \sigma'^\dagger) (\sigma \sigma^\dagger) + \lambda_{10} (\tilde{H}_u^\dagger H_d) \sigma'^\dagger + \kappa (\sigma^2 \sigma'^\dagger + (\sigma^\dagger)^2 \sigma'). \end{aligned} \quad (4.31)$$

In the type-II seesaw scenario the potential becomes even more complicated. Here it can be written as

$$\begin{aligned}
V_2 = & V_1 + \mu_{\Phi_u}^2 \Phi_u^\dagger \Phi_u + \mu_{\Phi_d}^2 \Phi_d^\dagger \Phi_d + \kappa_u (H_u^\dagger \Phi_u) \sigma^\dagger + \kappa_d (H_d^\dagger \Phi_d) \sigma^\dagger + \lambda_{11} (\tilde{\Phi}_d^\dagger \Phi_u) (\sigma'^\dagger)^2 \\
& + \lambda_{12} (\tilde{H}_d^\dagger \Phi_u) (\sigma'^\dagger \sigma^\dagger) + \lambda_{13} (\tilde{H}_u^\dagger \Phi_d) (\sigma'^\dagger \sigma^\dagger) + \lambda_{14} (\Phi_u^\dagger \Phi_u)^2 + \lambda_{15} (\Phi_d^\dagger \Phi_d)^2 \\
& + \lambda_{16} (\Phi_d^\dagger H_d) (H_d^\dagger \Phi_d) + \lambda_{17} (\Phi_u^\dagger H_d) (H_d^\dagger \Phi_u) + \lambda_{18} (\Phi_d^\dagger H_u) (H_u^\dagger \Phi_d) \\
& + \lambda_{19} (\Phi_u^\dagger H_u) (H_u^\dagger \Phi_u) + \lambda_{20} (\Phi_d^\dagger \Phi_u) (\Phi_u^\dagger \Phi_d) + \lambda_{21} (\sigma \sigma^\dagger) (\Phi_u^\dagger \Phi_u) + \lambda_{22} (\sigma \sigma^\dagger) (\Phi_d^\dagger \Phi_d) \\
& + \lambda_{23} (\sigma' \sigma'^\dagger) (\Phi_u^\dagger \Phi_u) + \lambda_{24} (\sigma' \sigma'^\dagger) (\Phi_d^\dagger \Phi_d) .
\end{aligned} \tag{4.32}$$

It is worth mentioning that here, for simplicity (since there are many scalars), the scalar fields after spontaneous symmetry breaking are not normalized by $\sqrt{2}$. This can change some of the values derived in the past chapters by factors of $\sqrt{2}$.

4.1.6 The Axion

To extract the physical axion from the PQ current, as was done in Section 3.1.4, it is useful to begin by writing down the Goldstone boson absorbed by the Z-boson (due to the Higgs mechanism), which is

$$A_Z = \frac{\sum_i Y_i v_i A_i}{\sqrt{\sum_i Y_i^2 v_i^2}} , \tag{4.33}$$

where Y_i is the hypercharge of each scalar field, and v_i its vev . For the type-I seesaw model the relevant Goldstone bosons are $A_i \in \{A, A', A_u, A_d\}$, whereas for the type-II seesaw they are $A_i \in \{A, A', A_u, A_d, A'_u, A'_d\}$. Similarly, the Goldstone boson related to the PQ symmetry is given by

$$A_{PQ} = \frac{\sum_i X_i v_i A_i}{\sqrt{\sum_i X_i^2 v_i^2}} , \tag{4.34}$$

where X_i is the PQ charge of the scalar field, whose Goldstone boson is A_i . Since the axion is orthogonal to the Z-boson Goldstone, it is necessary to subtract A_Z from it [53]. This leads to the axion taking the form

$$a = A_{PQ} - \left[\frac{\sum_i X_i Y_i v_i^2}{\sqrt{\sum_i Y_i^2 v_i^2} \sqrt{\sum_i X_i^2 v_i^2}} \right] A_Z . \tag{4.35}$$

There are some restrictions on the axion of Eq. (4.35). The first one comes from the SM Higgs vev , i.e. $\sqrt{\sum_i Y_i^2 v_i^2} \approx 246$ Gev. The second restriction is that $\sqrt{\sum_i X_i^2 v_i^2}$

is bounded from below by the value of f_a , the possible values of which are discussed in the following sections. For these two restrictions to be simultaneously satisfied a strong hierarchy must exist between the $vevs$ of the flavons and the Higgs doublets, wherein $v_{\sigma/\sigma'} \gg v_{u/d}$. Also, the following hierarchy is chosen $v_\sigma \gg v_{\sigma'}$, since it leads to negligible mixing between A and A' . This also means that the quarks will couple stronger to the axion than the leptons, as well as generating a hierarchy between the masses of quarks and leptons.

Interesting model dependent parameters for this axion are the following: the mass, the axion decay constant, the electromagnetic anomaly factor, the colour anomaly factor, and the axion-photon coupling [28]. Of these parameters, only the axion decay constant is a free parameter, and it is inversely proportional to the mass. For the origin of these parameters see Section 3.1.3. The anomalous factors are given by (3.44) as

$$N = \sum_i X_i T(R_i) = 5, \quad E = \sum_i X_i Q_i^2 D(R_i) = \frac{28}{3}. \quad (4.36)$$

The mass is given by Eq. (3.41)

$$m_a \approx 5.70 \left(\frac{10^{12} \text{ GeV}}{f_a} \right) \mu\text{eV}. \quad (4.37)$$

The axion decay constant can be at most be reduced from $f_a = \frac{v_a}{\sqrt{2N}}$ to

$$f_a \approx \frac{v_\sigma}{\sqrt{2N}}, \quad (4.38)$$

since v_σ is by a significant degree the largest of the $vevs$ in $v_a = \sqrt{\sum X_i^2 v_i^2}$ (the sum runs over all the scalars in the theory). Notice that since the $vevs$ were not normalized by $\sqrt{2}$, $f_a = \frac{v_a}{\sqrt{2N}}$, instead of $\frac{v_a}{2N}$. The axion-photon coupling is given by Eq. (3.49), and is

$$g_{a\gamma} = \frac{\alpha}{2\pi f_a} \left(\frac{E}{N} - \frac{2}{3} \frac{m_u + 4m_d}{m_u + m_d} \right) \approx \frac{\alpha}{2\pi f_a} \left(\frac{E}{N} - 1.92 \right). \quad (4.39)$$

In this model $\frac{E}{N} = \frac{28}{15} \approx 1.87$, which implies $g_{a\gamma}$ will be small and negative. Comparing it to the DFSZ benchmark $SU(5)$ grand unified theory [75], where $\frac{E}{N} = \frac{8}{3}$, the following relationship is found

$$\frac{|g_{a\gamma}^{SU(5)}|}{|g_{a\gamma}^{Flaxion}|} \approx 14. \quad (4.40)$$

Thus it is suppressed by more than an order of magnitude when compared to the benchmark, where

$$g_{a\gamma}^{SU(5)} = \frac{1.53}{10^{16} \text{ GeV}} \left(\frac{m_a}{\mu\text{eV}} \right). \quad (4.41)$$

Even without knowledge of f_a it is possible to discuss part of the phenomenology of the axion-photon interaction. Restricting the discussion to the $(g_{a\gamma} - m_a)$ plane, for $m_a \geq 1$ eV, $g_{a\gamma}$ is mostly constrained from cosmology and astrophysics as can be seen from Fig. 1 of Ref. [76]. Besides this, for $m_a \leq 1$ eV various haloscope detectors put the tightest constraints on the axion mass and axion-photon coupling as has been outlined in Figure 16 of Ref. [28]. For an axion mass of $\mathcal{O}(10^{-6})$ eV, as the reason of interest for the model, the Axion Dark Matter eXperiment (ADMX) [77] searching for cold dark matter axions with a haloscope detector, provides the most stringent bound. It can be seen from Fig. 5 of [77] that the ADMX can explore $2 \times 10^{-6} \leq m_a \leq 3.8 \times 10^{-6}$ eV for the coupling strength of $\mathcal{O}(10^{-15})$ GeV $^{-1}$. On the other hand, the ADMX Phase IIa/Gen-2 can improve their sensitivity to the axion mass to $(1.8, 8) \times 10^{-6}$ eV for $|g_{a\gamma}|$ one order of magnitude smaller compared to the latest ADMX bound, i.e., $\mathcal{O}(10^{-16})$ GeV $^{-1}$, for details see Fig. 9 of [77]. Choosing $f_a \sim 10^{12}$ GeV, and $m_a \sim 10^{-6}$ eV, the axion-photon coupling is $|g_{a\gamma}| \sim 10^{-18}$ GeV $^{-1}$, as given by Eq. (3.49), and hence the suppression of this coupling places this model beyond the reach of projected ADMX Phase IIa/Gen-2 sensitivity [77]. Fig. 4.4 shows many of these bounds in their current form and their projections.

4.2 Numerical Analysis

With the model well established, it is now possible to study some phenomenological properties numerically. The analysis begins with a χ^2 fit to the masses and mixing parameters of the fermions (Section 4.2.1). The best-fit points are later used to study flavour violation, focusing on flavour violating decays with axion in a final state (Section 4.2.2), and flavour violating neutral currents (Section 4.2.3). From these processes constraints on the free parameters of the model can be derived.

4.2.1 Masses and Mixing Parameters of Fermions

A χ^2 fit is conducted to find the parameters of the mass matrices, that lead to the best values according to experiments and global fits. The χ^2 function is defined as follows

$$\chi^2 = \sum \frac{(\mu_{exp} - \mu_{fit})^2}{\sigma_{exp}^2}, \quad (4.42)$$

where the sum runs over all observables. Also, μ_{fit} represent the masses and mixing parameters calculated from the mass matrices. The observable and fitting parameters can be read from Table 4.4 (quarks) and Table 4.5 (leptons), where μ_{exp} and σ_{exp} are the observables to be fitted and their standard deviation [8, 9].

4.2.1.1 Quark Masses and Mixing Parameters

The quark mass matrices are given by Eq. (4.43). It is worth noting that the quark fields can be redefined such that there exist only two non-zero phases (in [78] this was done for four-zero textures of the mass matrices). In the Appendix D, a detailed analysis of the phase redefinition is presented. Thus, the up- and down-quark mass matrices that are used in the fit are given by

$$m^{u/d} = \begin{pmatrix} 0 & A_{u/d} & 0 \\ B_{u/d} e^{-i\alpha_{u/d}} & 0 & C_{u/d} e^{-i\alpha_{u/d}} \\ 0 & D_{u/d} e^{-i\beta_{u/d}} & E_{u/d} e^{-i\beta_{u/d}} \end{pmatrix}. \quad (4.43)$$

Also, as pointed out in Appendix D, it is the difference in the up- and down- quark phase matrices that is relevant for the CKM matrix, therefore, phases α_d and β_d have been fixed to zero. There are 12 parameters that need to be fitted, 10 amplitudes (5 for each matrix) and 2 phases. These 12 parameters are fitted to account for the 10 physical observables related to them, the 6 quark masses, the 3 CKM angles and the CP-violating phase. The observables are obtained from these matrices using the MPT package [79]. The fit is done at the energy scale M_Z [9]. The initial values for the fitting procedure are randomized, while the rest of the procedure is based on a deterministic minimization algorithm. The results from the best fit are given in Table 4.4, where $\chi_q^2 = 0.0355$. It is worth noting that χ_q^2 is not normalized by the number of free parameters.

Unsurprisingly, χ^2 is very small, as the number of free parameters is larger than the number of observables. Nonetheless, this shows that the NNI texture is capable of reproducing observations with great accuracy.

4.2.1.2 Lepton Masses and Mixing Parameters

Following a similar approach to the quark sector, the masses and mixing angles of the leptonic sector are fitted. In this case only the elements of the neutrino mass matrix are fitted, since the charged lepton matrix is already diagonal. The neutrino mass matrix has the A_2 -texture and takes the form

$$m_\nu = \begin{pmatrix} 0 & a e^{i\phi_a} & 0 \\ a e^{i\phi_a} & b e^{i\phi_b} & c e^{i\phi_c} \\ 0 & c e^{i\phi_c} & d e^{i\phi_d} \end{pmatrix}. \quad (4.44)$$

It is not necessary to redefine the phases of this matrix, as there are more observables than degrees of freedom. Nevertheless, the phases can be redefined, leaving only two of them non-zero. The fitting procedure was done in for both cases, finding exactly

Parameter	Best fit	
$A_u/(10^{-2} \text{ GeV})$	1.493	
$B_u/(10^{-2} \text{ GeV})$	-5.531	
C_u/GeV	-3.008	
$D_u/(10^1 \text{ GeV})$	3.562	
$E_u/(10^2 \text{ GeV})$	1.679	
$A_d/(10^{-2} \text{ GeV})$	-1.241	
$B_d/(10^{-2} \text{ GeV})$	1.228	
$C_d/(10^{-1} \text{ GeV})$	-3.083	
$D_d/(10^{-1} \text{ GeV})$	-4.774	
E_d/GeV	-2.797	
$\alpha_u/^\circ$	96.64	
$\beta_u/^\circ$	98.34	

Observable	Global-fit value		Model best-fit
	Best-fit value	1σ range	
$\theta_{12}^q/^\circ$	13.03	12.98 \rightarrow 13.07	12.988
$\theta_{13}^q/^\circ$	0.209	0.201 \rightarrow 0.216	0.2085
$\theta_{23}^q/^\circ$	2.41	2.37 \rightarrow 2.45	2.411
$\delta^q/^\circ$	69.21	66.12 \rightarrow 72.31	68.516
$m_u/(10^{-3} \text{ GeV})$	1.288	0.766 \rightarrow 1.550	1.2889
$m_c/(10^{-1} \text{ GeV})$	6.268	6.076 \rightarrow 6.459	6.2677
m_t/GeV	171.68	170.17 \rightarrow 173.18	171.684
$m_d/(10^{-3} \text{ GeV})$	2.751	2.577 \rightarrow 3.151	2.7507
$m_s/(10^{-2} \text{ GeV})$	5.432	5.153 \rightarrow 5.728	5.4328
m_b/GeV	2.854	2.827 \rightarrow 2.880	2.8536
χ_q^2			0.0355

Table 4.4: Best-fit values of the model parameters in the quark sector are shown in the upper table. The global best-fit as well as their 1σ error [8, 9] for the various observables are given in the second and third columns of the lower table. Also, the best-fit values of the various observables are listed in the last column of the lower table.

the same values for all observables, therefore only one of them, the one without phase redefinition, is presented here.

The χ^2 function is identical as in (4.42), the only differences being the observables and their standard deviations. The leptonic masses and mixings obtained from the fit, which are compatible with the latest global fit data, can be seen in Table 4.5 at $\chi_l^2 = 2.0053$. As was the case with the quark sector, χ_l^2 is not normalized by the number of free parameters.

The only parameter in Table 4.5 that falls out of the 1σ range is δ^l (it falls in the 1.07σ range). Nevertheless, considering that $\chi_l^2 \approx 2$ is unnormalized, the fit is still very good. The PDG [8] gives four global fits for the neutrino masses and mixings, of these the most recent [7] was chosen. While most parameters vary relatively little between the fits, there is significant deviation of δ^l from the last fit to the first three. Also, in all cases the uncertainty of δ^l is by far the largest. With this in mind, the that fact best-fit point for the model falls slightly outside the 1σ range is not very worrying, as in all the other global fits it falls inside of this range. Interestingly, in all cases it is bigger than the central value of the fit, suggesting that the A_2 texture favours values of δ^l near the maximal CP-violating phase of 270° .

Parameter	Best fit	
$a/(10^{-3} \text{ eV})$	9.933	
$b/(10^{-2} \text{ eV})$	2.646	
$c/(10^{-2} \text{ eV})$	2.475	
$d/(10^{-2} \text{ eV})$	2.264	
$\phi_a/^\circ$	29.87	
$\phi_b/^\circ$	91.88	
$\phi_c/^\circ$	3.03	
$\phi_d/^\circ$	-109.97	

Observable	Global-fit value		Model best-fit
	Best-fit value	1σ range	
$\theta_{12}^l/^\circ$	34.5	33.5 \rightarrow 35.7	34.85
$\theta_{13}^l/^\circ$	8.45	8.31 \rightarrow 8.61	8.432
$\theta_{23}^l/^\circ$	47.7	46.0 \rightarrow 48.9	48.11
$\delta^l/^\circ$	218	191 \rightarrow 256	258.8
$\alpha/^\circ$			65.27
$\beta/^\circ$			265.08
$\Delta m_{21}^2/(10^{-5} \text{ eV}^2)$	7.55	7.39 \rightarrow 7.75	7.571
$\Delta m_{32}^2/(10^{-3} \text{ eV}^2)$	2.424	2.394 \rightarrow 2.454	2.4221
$\sum m_\nu/(10^{-2} \text{ eV})$			6.453
m_e/MeV	0.4865763	0.4865735 \rightarrow 0.4865789	-
m_μ/GeV	0.10271897	0.10271866 \rightarrow 0.10271931	-
m_τ/GeV	1.74618	1.74602 \rightarrow 1.74633	-
χ_I^2			2.0053

Table 4.5: Best-fit values of the model parameters in the lepton sector are shown in the upper table. The global best-fit as well as their 1σ error [7, 8, 9] for the various observables are given in the second and third columns of the lower table. Also, the best-fit values of the various observables are listed in the last column of the lower table.

4.2.2 Flavour Violating Decays with Axions

The model contains flavour violating Yukawa couplings. Flavour violating processes containing quarks are particularly interesting, as they can have an axion in the final state [80], i.e.

$$q_i \rightarrow q_j a, \quad (4.45)$$

where the quark q_i can decay to the quark q_j and an axion. These processes can be studied through meson decays and are independent of the UV-completion of the theory, and thus are the same in both models.

The starting point of this analysis is the Lagrangian of the quark-flavon interaction, of Eq. (4.4) and Eq. (4.5). In the interaction basis, the Yukawa couplings of the quarks to σ can be written as

$$\mathcal{L}_{\sigma q} = y_{ij}^u \overline{u_{jL}} \sigma u_{iR} + y_{ij}^{\prime u} \overline{u_{jL}} \sigma^\dagger u_{iR} + y_{ij}^d \overline{d_{jL}} \sigma d_{iR} + y_{ij}^{\prime d} \overline{d_{jL}} \sigma^\dagger d_{iR}, \quad (4.46)$$

where the Yukawa coupling matrices $y_{ij}^{u^{(\prime)}}$ and $y_{ij}^{d^{(\prime)}}$ are

$$y^{u/d} = \frac{1}{v_\sigma} \begin{pmatrix} 0 & \mathbf{A}_{u/d} & 0 \\ \mathbf{B}_{u/d} & 0 & 0 \\ 0 & 0 & 0 \end{pmatrix}, \quad y^{u'/d'} = \frac{1}{v_\sigma} \begin{pmatrix} 0 & 0 & 0 \\ 0 & 0 & \mathbf{C}_{u/d} \\ 0 & \mathbf{D}_{u/d} & 0 \end{pmatrix}, \quad (4.47)$$

and $\mathbf{A}_{u/d}$, $\mathbf{B}_{u/d}$, $\mathbf{C}_{u/d}$, and $\mathbf{D}_{u/d}$ are the (complex) parameters of the quark mass matrices. Transforming the quarks to the mass basis (see Section 2.1.6), the quark-flavon Yukawa Lagrangian becomes

$$\begin{aligned} \mathcal{L}_{\sigma q'} &= y_{ij}^u U_{ikL}^\dagger \overline{u'_{kL}} \sigma U_{jLR} u'_{lR} + y_{ij}^{u'} U_{ikL}^\dagger \overline{u'_{kL}} \sigma^\dagger U_{jLR} u'_{lR} \\ &+ y_{ij}^d V_{ikL}^\dagger \overline{d'_{kL}} \sigma V_{jLR} d'_{lR} + y_{ij}^{d'} V_{ikL}^\dagger \overline{d'_{kL}} \sigma^\dagger V_{jLR} d'_{lR}, \end{aligned} \quad (4.48)$$

where u'/d' denote quark mass eigenstates, U_L^u and U_R^u diagonalize the up quark mass matrix and U_L^d and U_R^d diagonalize the down quark mass matrix, respectively. Writing the Yukawa couplings in the mass basis as $\lambda^{u^{(\prime)}} = U_L^\dagger y^{u^{(\prime)}} U_R^u$ and $\lambda^{d^{(\prime)}} = V_L^\dagger y^{d^{(\prime)}} U_R^d$, Eq. (4.48) can be written more compactly as

$$\mathcal{L}_{\sigma q'} = \lambda_{ij}^u \overline{u'_{iL}} \sigma u'_{jR} + \lambda_{ij}^{u'} \overline{u'_{iL}} \sigma^\dagger u'_{jR} + \lambda_{ij}^d \overline{d'_{iL}} \sigma d'_{jR} + \lambda_{ij}^{d'} \overline{d'_{iL}} \sigma^\dagger d'_{jR}. \quad (4.49)$$

Finally, by neglecting axion mixing with other scalars, the Lagrangian describing the coupling of the axion to the quarks

$$\mathcal{L}_{aq'} = ia(\epsilon_{ij}^u \overline{u'_i} u'_j + \epsilon_{ij}^d \overline{d'_i} d'_j + \epsilon_{ij}^{u'} \overline{u'_i} \gamma_5 u'_j + \epsilon_{ij}^{d'} \overline{d'_i} \gamma_5 d'_j), \quad (4.50)$$

where $\epsilon_{ij}^{u,d} = (\lambda_{ij} - \lambda_{ij}^\dagger)/2$ and $\epsilon_{ij}^{u',d'} = (\lambda_{ij} + \lambda_{ij}^\dagger)/2$. From these couplings the branching ratio of flavor violating decays with axions can be calculated.

The most sensitive test of neutral flavor violation with a final state axion is the $K^+ \rightarrow \pi^+ a$ process [80]. The decay ratio for the Kaon decay to axion and pion is given in [81],

$$\Gamma(K^+ \rightarrow \pi^+ a) \approx \frac{m_K}{64\pi} |\epsilon_{21}^d|^2 B_S^2 \left(1 - \frac{m_\pi^2}{m_K^2}\right), \quad (4.51)$$

where B_S is a non-perturbative parameter and is calculated in lattice to $B_S \approx 4.6$ [81]. To estimate the Kaon decay the best-fit point, as tabulated in Table 4.4, is evaluated in Eq. (4.48) and Eq. (4.49), to find $|\epsilon_{21}^d|^2$. This leads to

$$\Gamma(K^+ \rightarrow \pi^+ a) \approx \frac{1.9 \times 10^{-9} \text{GeV}^3}{v_\sigma^2}. \quad (4.52)$$

Using the latest constraint of the branching ratio for the Kaon decay from the E949

Collaboration [82] i.e.,

$$\text{BR}(K^+ \rightarrow \pi^+ a) = \frac{\Gamma(K^+ \rightarrow \pi^+ a)}{\Gamma_{\text{Total}}(K^+)} < 7.3 \times 10^{-11} , \quad (4.53)$$

the following constraint on v_σ is $v_\sigma \geq 2.5 \times 10^{10}$ GeV. For the models described above, where $v_\sigma \approx \sqrt{2} f_a N$ with $N = 5$, the bounds on v_σ can be shifted to the axion decay constant, f_a , where

$$f_a \geq 7 \times 10^9 \text{ GeV} . \quad (4.54)$$

Current measurements from the NA62 collaboration [83] give a similar, and in some cases smaller, limit to the branching ratio. A smaller branching ratio would also make the bound on v_σ more stringent, but in this case not very significantly. The smallest branching ratio coming from NA62 is $\text{BR}(K^+ \rightarrow \pi^+ a) < 5 \times 10^{-11}$, although it would require an axion mass of about (160–225) MeV [83], since the axion mass must be significantly smaller, the actual constraint imposed by NA62 is not as strong. Nevertheless, the sensitivity of NA62 to this decay channel is $\text{BR}(K^+ \rightarrow \pi^+ a) < 1.0 \times 10^{-12}$ [65, 84]. If future measurements were to reach this limit, the bound on v_σ would become $v_\sigma \geq 2.1 \times 10^{11}$ GeV, or equivalently, $f_a \geq 3 \times 10^{10}$ GeV. These bounds are an order of magnitude smaller than those coming from the E949 experiment.

Another meson decay that can constrain the axion decay constant is the $B^+ \rightarrow K^+ a$ decay, where the bottom to strange quark transition is probed. The decay width of this process is given by [81] as

$$\Gamma(B^+ \rightarrow K^+ a) \approx \frac{m_B}{64\pi} |\epsilon_{32}^d|^2 (f_0^K(0))^2 \left(\frac{m_B}{m_b - m_s} \right)^2 \left(1 - \frac{m_K^2}{m_B^2} \right)^3 , \quad (4.55)$$

with $f_0^K(0) \sim 0.33$ [85]. The experiment Belle-II constrains the branching ratio of this process to $\text{BR}(B^+ \rightarrow K^+ a) < 10^{-6} - 10^{-8}$ [61], which leads

$$v_\sigma \geq 1.8 \times (10^7 - 10^8) \text{ GeV} . \quad (4.56)$$

Since $v_\sigma \approx \sqrt{2} N f_a$, the bound above translates into

$$f_a \geq 6 \times (10^6 - 10^7) \text{ GeV} . \quad (4.57)$$

This bound is smaller than that coming from Kaon decays, as such, the former is taken.

Concluding this section, the axion decay constant $f_a > 7 \times 10^9$ GeV bound translates to the bounds $m_a < 0.7 \times 10^{-3}$ eV, and $|g_{a\gamma}(\text{GeV}^{-1})| < 0.8 \times 10^{-14}$, for the axion mass and axion-photon coupling, respectively. These bounds are two orders of magnitude stronger than the limits from astrophysics (see Figure 1 of [76]). It is worth noting that

these bounds are obtained by neglecting $\sigma - \sigma'$ mixing. When this mixing is sizable the bounds on f_a are relaxed, and consequently those on m_a and $|g_{a\gamma}|$ as well. On the other hand, the bounds would at most become stronger by about an order of magnitude in the case where the branching ratio of NA62 is as low as its sensitivity. See Fig. 4.4 for the limits imposed by Kaon decay and different experiments.

4.2.3 Flavour Violating Higgs Couplings

The two Higgs doublets present in this model allow for the existence of flavour changing neutral currents (FCNCs). These currents are relevant for this model, since natural flavour conservation¹ is difficult to implement here, since it would require the imposition of discrete symmetries or the inclusion of more Higgs doublets, deviating from minimality. FCNCs are strongly constrained through some decays, like the Kaon-to-muon decay $K_L \rightarrow \mu^- \mu^+$, or top decays such as $t \rightarrow hc, hu$ [87]. This can be used to the advantage of furthering the constraints of the model, by setting limits to the scalars' masses and couplings to the Higgs bosons.

The high scale of PQ breaking induces a decoupling of the components of H_u and H_d from the components of σ_i . This simplifies the expression for the Higgs bosons, which at leading order are $h \approx h_0^u \cos \alpha + h_0^d \sin \alpha$, and $H \approx -h_0^u \sin \alpha + h_0^d \cos \alpha$, where one identifies h as the 125 GeV boson observed at LHC, and H as an additional heavy scalar. The couplings of these two particles to the SM fermions may be obtained from the effective Lagrangian of (4.4) and (4.5) and read as follows

$$\mathcal{L} \supset \frac{C_1^u}{v_u} \overline{u_L} u_R h_0^u + \frac{C_2^u}{v_d} \overline{u_L} u_R h_0^d + \frac{C_1^d}{v_d} \overline{d_L} d_R h_0^d + \frac{C_2^d}{v_u} \overline{d_L} d_R h_0^u, \quad (4.58)$$

where the matrices $C_i^{u/d}$ are given by

$$C_1^{u/d} = \begin{pmatrix} 0 & \mathbf{A}_{u/d} & 0 \\ \mathbf{B}_{u/d} & 0 & 0 \\ 0 & 0 & \mathbf{E}_{u/d} \end{pmatrix}, \quad C_2^{u/d} = \begin{pmatrix} 0 & 0 & 0 \\ 0 & 0 & \mathbf{C}_{u/d} \\ 0 & \mathbf{D}_{u/d} & 0 \end{pmatrix}, \quad (4.59)$$

whose entries are the parameters of the quark mass matrices. Writing this in terms of the bosons h and H , and the quarks in the mass basis, the Lagrangian becomes

$$\mathcal{L} \supset h \overline{u'_L} u'_R \left(\frac{C_1^{uu}}{v_u} \cos \alpha - \frac{C_2^{uu}}{v_d} \sin \alpha \right) + H \overline{u'_L} u'_R \left(\frac{C_1^{uu}}{v_u} \sin \alpha + \frac{C_2^{uu}}{v_d} \cos \alpha \right) + (u \rightarrow d), \quad (4.60)$$

¹The authors of [86] define natural flavour conservation as *the assumption that only one Higgs field can couple to a given quark species.*

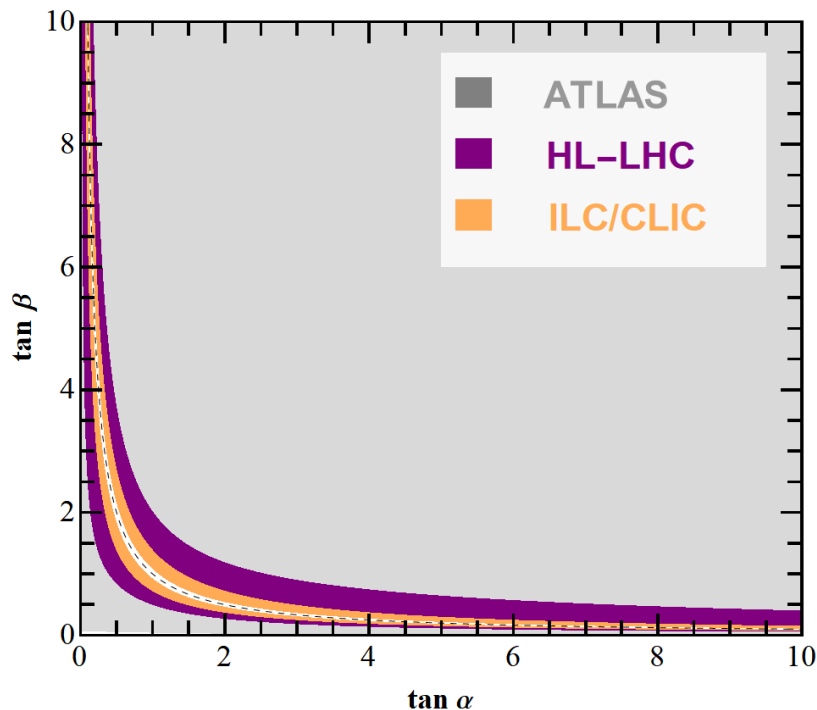


Figure 4.5: Exclusion region plot in the $(\tan \alpha - \tan \beta)$ plane obtained from the non-observation of the $t \rightarrow hc$ flavor violating decay. The gray colored region is excluded by ATLAS data [4], the purple colored region is expected to be probed in the future by the HL-LHC experiment [5] and the orange region will be further probed by ILC or CLIC [6]. The uncolored region (see white thin band) predicts a branching ratio beyond the sensitivity of these experiments. The dashed line indicates limit of no flavor violation in light Higgs Yukawa couplings.

where the matrices $C_i^{u/d}$ are defined as

$$C_i^{u} = U_L^{u\dagger} C_i^u U_R^u \quad , \quad C_i^{d} = U_L^{d\dagger} C_i^d U_R^d . \quad (4.61)$$

Besides α , the other free parameter for studying flavour violation is β , which is through the relationship

$$v_{SM} = v_u \sin \beta + v_d \cos \beta, \quad (4.62)$$

where v_{SM} is the SM Higgs vev .

In the limit $v_u/v_d = \cot \alpha$ the Yukawa couplings of h are proportional to the up- and down-quark mass matrices, while the couplings of H are not. After the transformation of the fermion states to the mass basis, the couplings of h are diagonal, while the couplings of H are not, thus this will be called the flavour conserving limit (for h), since the diagonal nature of the coupling matrix prohibits mixing between the flavours. This limit does not affect the couplings of the axion, which means that the processes

discussed in the previous section do not vanish. A deviation of α from the flavor conserving limit will introduce flavor violating couplings of the light Higgs boson, which can be probed with observables such as $t \rightarrow hc$ in the up-sector and $h \rightarrow bs$ in the down sector. The $t \rightarrow hc$ decay channel currently has an upper bound set by ATLAS [4]

$$\text{BR}(t \rightarrow hc)_{\text{LHC}} < 1.1 \times 10^{-3}, \quad (4.63)$$

while future experiments HL-LHC [5], ILC and CLIC [6] project the following sensitivities to this process

$$\text{BR}(t \rightarrow hc)_{\text{HL-LHC}} < 2 \times 10^{-4}, \quad (4.64)$$

$$\text{BR}(t \rightarrow hc)_{\text{ILC/CLIC}} < 10^{-5}. \quad (4.65)$$

With this in mind, the branching ratio can be calculated from (4.60) following [88]

$$\Gamma_{t \rightarrow hc} = \frac{C_{tc}^2 m_t}{16\pi} \sqrt{[1 - (R_c - R_h)^2][1 - (R_c + R_h)^2]} [(R_c + 1)^2 - R_h^2], \quad (4.66)$$

where the coupling C_{tc} is defined as

$$C_{tc} = \frac{[(C_1^{tu})_{23} + (C_1^{tu})_{32}] \cos \alpha}{v_{SM} \sin \beta} - \frac{[(C_2^{tu})_{23} + (C_2^{tu})_{32}] \sin \alpha}{v_{SM} \cos \beta}, \quad (4.67)$$

m_t is the top quark mass, R_h is the Higgs to top mass ratio, $R_h = m_h/m_t$, and R_c is the charm to top mass ratio, $R_c = m_c/m_t$. Using the experimental value for the total width of the top quark [8] the constraints on the free parameters $\tan \alpha$ and $\tan \beta$ are derived, and illustrated in Fig. 4.5. From the best fit point given in Table 4.4, a numerical value of Eq. (4.66) is obtained, giving the following approximate constraint on the free parameters

$$\left| \frac{\cos \alpha}{\sin \beta} (1 - \tan \alpha \tan \beta) \right| \leq 17 \frac{\Gamma_{t \rightarrow hc}^{Exp}}{[GeV]}, \quad (4.68)$$

for a given experimental input of the decay width $\Gamma_{t \rightarrow hc}^{Exp}$. Fig. 4.5 shows that small values of $\tan \beta$ allow only large values of $\tan \alpha$ and small values of $\tan \alpha$ allow only large values of $\tan \beta$, which is also implied by Eq. (4.68). It can also be seen that ATLAS data has already ruled out a large portion of the parameter space (gray-region) and HL-LHC (purple-region) and CLIC (orange-region) will leave only a small region around the $\tan \beta = \cot \alpha$ limit unprobed [6].

It is also worth noting that the $t \rightarrow hu$ and $h \rightarrow cu$ decays can also place constraints

on α and β , however these are not as strong as those coming from $t \rightarrow hc$, since the hierarchy in the mass matrices is inherited by the coupling matrices $C_i^{u/d}$ (see Eq. (4.59)), which in turn is passed down to the physical coupling matrices $C_i^{tu/d}$ (see Eq. (4.61)). Accordingly the constraints imposed by the aforementioned processes are found to be numerically much weaker than those coming from $t \rightarrow hc$.

4.2.4 Flavourful Axion as a Dark Matter Candidate

The flavourful axion can be a good dark matter candidate, provided a sufficient amount of them was produced in the early universe. Its cosmological properties are not altered significantly by the fact that the PQ symmetry is taken to be a flavour symmetry as well, thus a standard analysis can be performed. The main contribution to the axion relic density is produced by the misalignment mechanism (see Appendix B.2), which is

$$\Omega_a h^2 \approx 2 \times 10^4 \left(\frac{f_a}{10^{16} \text{GeV}} \right)^{7/6} \langle \theta_i^2 \rangle, \quad (4.69)$$

where θ_i is the initial misalignment angle of the cosmological axion field and takes values in the range $[0, 2\pi)$. For the axion breaking scale $5 \times 10^{10} < f_a < 1 \times 10^{15}$ (GeV), one can match the axion relic density to the observed dark matter relic abundance $\Omega_{DM} h^2 \sim 0.12$ without fine tuning θ . It is worthwhile to mention that the $N > 1$ prediction of DFSZ models induce the formation of stable domain walls in the universe, which is incompatible with the standard cosmology [89]. One way to avoid the effect of domain walls on the observed universe is to embed this type of models in a cosmological model where inflation happens after the formation of these walls, thereby inflating away the density of the walls (see Appendix B.2 for a brief explanation). Another possible resolution of the domain wall problem is to destabilize the walls with a dynamical breaking of the PQ symmetry [90, 91].

Conclusion

A flavourful axion model was constructed and some of its phenomenological aspects were studied. This model aims to solve multiple problems at once. Mainly, to explain the fermion mass hierarchy, including the neutrinos, and provide a solution to the strong CP problem using the Peccei-Quinn symmetry and its axion. Additionally, axions are popular and well motivated dark matter candidates, and the flavourful axion from this model is no exception. Before this, the theoretical framework regarding the masses and mass hierarchies in the Standard Model (Chapter 2), and axions (Chapter 3), were presented.

The model itself is constructed first by identifying the Froggatt-Nielsen and Peccei-Quinn symmetries, thus treating the Peccei-Quinn symmetry as a flavour symmetry. The charges of the fermions under this symmetry are such that the up- and down-quark mass matrices have the NNI structure, with only the (3, 3) term being generated at tree level and the hierarchy between the mass matrices being explained by a hierarchy between the *vevs* of the two Higgs doublets, that appear in the DFSZ-style axion model. The lepton masses are realized in a type-I seesaw scenario, obtaining the A_2 structure for the neutrinos' masses, implying they are Majorana particles. In the quark sector two UV-completions, following the type-I and type-II seesaw topologies in the diagrams, are given, whose quark mass matrices also possess the NNI structure. In the scalar sector, the axion is extracted from the Goldstone bosons of the flavons and Higgs doublets. The axion and its decay constant are obtained from the scalars' Goldstone bosons and the scalars' Peccei-Quinn charges and *vevs*. Using the $SU(5)$ grand unified theory as a benchmark, it can be seen that the flavourful axion's coupling to the photon is about 14 times weaker than the $SU(5)$ axion.

The masses and mixing parameters of the quarks and leptons were obtained by means of a χ^2 fit, and can be seen in Table 4.4 and Table 4.5, respectively. Using the parameters found in the fit it is possible to put constraints on the flavourful axion's free parameter f_a , by analyzing flavour violating decays with the axion as a final state. The constraint found is $f_a \geq 7 \times 10^9$ GeV, implying $m_a < 0.7 \times 10^{-3}$ eV, and $|g_{a\gamma}(\text{GeV}^{-1})| <$

0.8×10^{-14} . The two Higgs doublets present in the model raise the possibility of the existence of flavour changing neutral currents, where the $t \rightarrow hc$ decay channel is the most constraining. These constraints, obtained through the branching ratio of the decay, are summarized in Fig. 4.5, where the latest bounds of ATLAS, as well as the limits of future experiments (HL-LHC, ILC and CLIC), are shown. Lastly, the flavourful axion can also be a cold dark matter candidate, where it can explain the dark matter relic density for any initial misalignment angle provided the axion decay constant takes a value between 5×10^{10} GeV and 1×10^{15} GeV, and the axions were produced by the misalignment mechanism.

These results show that it is possible to construct relatively simple (regarding extra fields and symmetries) extensions of the Standard Model, that can explain many of the problems present in it at the same time, in this case the fermion mass hierarchy, the strong CP problem, and the neutrino masses, while also providing a dark matter candidate. Since there are more free parameters than observables in the quark sector, future studies in this model could also focus on trying to eliminate some of them, for example by finding or imposing symmetries. Through a phenomenological analysis, it is possible to constrain these models, whereby they can be made to conform to current observations, while also distinguishing them from the Standard Model.

Why a New Particle?

A question that can (and should) be asked before contemplating the introduction of a new particle, is the more fundamental question *why dark matter?* Is there no other explanation for the phenomena mentioned in Sec. 1.2? The short answer is yes, with some caveats. For instance, there are theories like *Modified Newtonian Dynamics* (MOND) [92] and its relativistic offspring *Tensor-Vector-Scalar gravity* (TeVeS) [93], that attempt to explain phenomena attributed to DM by other means. In this case by modifying gravitational dynamics. MOND in particular modifies Newtonian dynamics (hence the name) in the small acceleration limit, explaining the rotation curves of some galaxies. Since this is non-relativistic, MOND fails to explain gravitational lensing. TeVeS is a relativistic generalization of MOND, where MOND arises in the weak field limit, as Newtonian dynamics does for General Relativity. This theory can explain gravitational lensing. Nonetheless, most alternatives to DM have trouble in other areas. One very important area where the standard cosmological model, Λ CDM (Lambda Cold Dark Matter), holds an acute advantage is in explaining the history and evolution of the Universe.

Numerical simulations based on Λ CDM can replicate the Cosmic Microwave Background (CMB), and importantly its anisotropies, while many theories based on TeVeS fail in this task (as with most contested theories, there are exemptions, see [94] for an in-depth discussion). Furthermore, the structure and evolution of the CMB helps discriminate between DM candidates. The argument against modified gravity and in general a dark-matterless Universe given in [15] rests on the CMB anisotropies and the formation of large scale structures. In the early Universe, before recombination¹, the baryonic density fluctuations and the photon thermal fluctuations (i.e. the thermal fluctuations in the CMB) were proportional, since baryons and photons were tightly coupled. As such, the baryonic density fluctuations in the early Universe can be con-

¹This means the formation of hydrogen atoms from free protons and electrons that occurred as the Universe cooled down.

strained by the anisotropies of the CMB to be

$$\frac{\delta\rho}{\rho} < 10^{-4}. \quad (\text{A.1})$$

Nowadays, large scale, non-linear structures exist, which is related to large baryonic density fluctuations

$$\frac{\delta\rho}{\rho} \gg 1. \quad (\text{A.2})$$

However, the baryonic density fluctuations should grow like matter (in the linear regime, which is valid in the early Universe), in other words

$$\frac{\delta\rho}{\rho} \sim a, \quad (\text{A.3})$$

where a is the scale factor. This factor would grow due to redshift by about three orders of magnitude from the value it took on recombination to the present value. This would imply that the fluctuations are much smaller than what can be seen today. In turn, this discrepancy suggests that there must exist matter, that decoupled from baryons and photons earlier than recombination, thus creating inhomogenities, which interact with the rest of the matter gravitationally, that could later grow and explain the non-linear structures present nowadays.

Disregarding modifications to gravity still does not assure that DM is a new particle. The last argument showed that it is hard to account for structure formation with only baryons. Another argument against baryonic DM is that Big Bang Nucleosynthesis [8] predicts a baryon density

$$\Omega_b h^2 \approx 0.02, \quad (\text{A.4})$$

which is in agreement, for example the results of the Planck 2018 Review [95] show $\Omega_b h^2 = 0.0224 \pm 0.0001$. Compelling as these arguments are, they are bound to cosmological scales. For a long time it was thought that at the galactic scale the dark halos could be composed of massive, macroscopic objects composed of baryons, called MACHOs (Massive Compact Halo Objects), like brown dwarfs and gas balls (Jupiter-like planets). Consistent with the cosmological estimates, these objects were not found at the rates. Experiments like EROS-2 [96] observed the dark halo of the Magellanic Clouds, expecting to find about 39 microlensing events, but could only observe one. While this does not mean MACHOs do not exist, it does strongly constrain their contribution to the total amount of DM to at most 8%.

Derivation of some Cosmological Quantities

B.1 Virial Mass of the Coma Cluster

A brief overview of the derivation of the virial mass of the galaxies is given, following [15]. First summing the forces applied to every galaxy in the cluster and then taking the time-average of these forces times the position of the galaxy, i.e of the virial

$$\text{Vir} = \sum_i \mathbf{F}_i \cdot \mathbf{r}_i. \quad (\text{B.1})$$

Under the assumption that the cluster is stationary, the time derivative of the polar moment of inertia, defined as

$$\Theta = \sum_i M_i r_i^2 \quad (\text{B.2})$$

vanishes. From this follows that the time average of the virial is

$$\overline{\text{Vir}} = -2\overline{T}, \quad (\text{B.3})$$

where T is the kinetic energy of the cluster. In the Newtonian limit the inverse square law holds for the gravitational potential, thus

$$\text{Vir} = U = -\frac{1}{2} \sum_{i \neq j} G_N \frac{M_i M_j}{|\mathbf{r}_i - \mathbf{r}_j|}, \quad (\text{B.4})$$

where M_i is the mass of the i -th galaxy and G_N the gravitational constant. The galaxies can be taken as uniformly distributed in a sphere of radius R_c and of total mass M_c , this leads to

$$\overline{U} = -G_N \frac{3M_c}{5R_c}. \quad (\text{B.5})$$

The kinetic energy average is thus the kinetic energy of a body with mass M_c and speed given by the average of the individual galaxies' kinetic energies, where Zwicky used $\overline{v^2}$ for the double average. Taking this and Eq. (B.3) into account it follows that

$$M_c = \frac{5R_c \overline{v^2}}{3G_N}. \quad (\text{B.6})$$

Considering non-uniform spherical distributions Zwicky took this as an upper limit to the cluster mass, which is about

$$M_c > 9 \times 10^{43} \text{ kg}. \quad (\text{B.7})$$

B.2 Misalignment Mechanism

Axion self-interactions are given by a potential. Since the interest here is to understand how axions were formed in the early Universe it will be important to write a temperature-dependent effective potential,

$$V\left(\frac{a}{f_a}, T\right). \quad (\text{B.8})$$

Defining the *axion angle*

$$\theta(x) = \frac{a(x)}{f_a}, \quad (\text{B.9})$$

it can be noticed that θ possesses the following periodic symmetry

$$\theta = \theta + 2\pi, \quad (\text{B.10})$$

since it relates to the strong CP-violating phase. The potential should respect this symmetry, thus

$$V(\theta, T) \sim \cos(\theta). \quad (\text{B.11})$$

As a matter of fact, calculations based on the Dilute Instanton Gas Approximation (DIGA) [97] find the potential as

$$V(\theta, T)|_{T \gg T_C} = \chi(T) (1 - \cos(\theta)), \quad (\text{B.12})$$

where $T_C \approx 200 \text{ MeV}$ is the QCD critical temperature, where the phase transition from the confined to the free regime occurs, i.e. where QCD becomes perturbative. The other parameter, $\chi(T)$ is the QCD topological susceptibility, and is given by

$$\chi(T) = f_a^2 m_a^2(T). \quad (\text{B.13})$$

The temperature dependence of the mass (and also other parameters) is a complication that arises in finite temperature QFT, after the phase transition the mass can be given by a power law

$$m_a(T)|_{T \gg T_c} \simeq \beta m_a(T=0) \left(\frac{T_c}{T} \right)^\gamma, \quad (\text{B.14})$$

with β is a QCD dependent proportionality constant. The power $\gamma \approx 3.7$, while β is of the order $\mathcal{O}(-2)$.

The axion angle has a Klein-Gordon (in a potential) equation of motion

$$\square\theta + \frac{\partial V(\theta, T)}{\partial\theta} = 0. \quad (\text{B.15})$$

In an expanding (and flat) universe a scalar field satisfies

$$\square\theta(x) = \left(\partial_t^2 + 3H(t)\partial_t - \frac{1}{R^2(t)}\nabla^2 \right) \theta(x), \quad (\text{B.16})$$

where H the Hubble rate, defined as $H(t) = \frac{\dot{R}(t)}{R(t)}$. The axion potential takes the form (from Eq. (B.12) and Eq. (B.13))

$$V(\theta, T)|_{T \gg T_c} = f_a^2 m_a^2(T) \sum_{n=1}^{\infty} \frac{(-1)^{n+1} \theta^{2n}}{(2n+1)!}. \quad (\text{B.17})$$

Keeping only the quadratic term in the potential and doing a spatial Fourier transform ($\nabla^2 \rightarrow -k^2$) Eq. (B.16) becomes

$$\ddot{\theta} + 3H(t)\dot{\theta} + \frac{k^2}{R^2(t)}\theta + m_a^2(T)\theta = 0. \quad (\text{B.18})$$

Each wavevector \mathbf{k} characterizes the (Fourier) modes of the axion angle field. The full solution to Eq. (B.18) will include an integral over all the modes. The zero modes of the field ($k=0$) are the main contributors to the number density. Since higher frequency modes become relevant when $k \gtrsim H(t)R(t)$, their number density is suppressed in comparison to that of the zero modes¹ [28].

The equation of motion can be taken therefore as

$$\ddot{\theta} + 3H(t)\dot{\theta} + m_a^2(T)\theta = 0. \quad (\text{B.19})$$

It is worth noting that temperature is time varying, this means $T = T(t)$ and therefore $m_a(T) = m_a(t)$.

¹In a more formal treatment of the subject, it would be necessary to discuss the relationship between the wavelength, λ , k , and R in order to reach this conclusion.

The equation of motion Eq. (B.19), is similar to the equation of motion of a dampened oscillator (it would be exactly this equation if the coefficients were constant). There are two important regimes for the qualitative behaviour of θ . The first regime happens at high temperatures. Eq. (B.14) shows that at temperatures far greater than T_{QCD} , $m_a \sim 0$, which is the case for this regime. The second regime occurs when the mass term starts to become relevant. In this regime the field will start to oscillate, as such a time, t_{osc} , can be defined, which signals the onset of this behaviour. This time can be defined implicitly by

$$T_{osc} = T(t_{osc}), \quad (\text{B.20})$$

where the oscillation temperature, T_{osc} , is given by

$$m_a(T_{osc}) = 3H(T_{osc}). \quad (\text{B.21})$$

Therefore, the first regime happens at $t \ll t_{osc}$, and the second at $t \gtrsim t_{osc}$.

For the first regime

$$\ddot{\theta} + 3H(t)\dot{\theta} = 0. \quad (\text{B.22})$$

and $R(t) \propto t^{\frac{1}{2}}$, as at this time it can be assumed that the Universe is radiation dominated, which implies

$$3H(t) = 3 \frac{1}{2} \frac{t^{-\frac{1}{2}}}{t^{\frac{1}{2}}} = \frac{3}{2t}. \quad (\text{B.23})$$

This gives the equation of motion in this regime as

$$\ddot{\theta} + \frac{3}{2t}\dot{\theta} = 0. \quad (\text{B.24})$$

A natural initial condition is given at time PQ breaks, t_{PQ} , i.e.

$$\begin{aligned} \theta(t_{PQ}) &= \theta_{PQ} \\ \dot{\theta}(t_{PQ}) &= \dot{\theta}_{PQ}. \end{aligned} \quad (\text{B.25})$$

The solution can be thus found by integrating twice, giving

$$\begin{aligned} \theta(t) &= \theta_{PQ} - 2\dot{\theta}_{PQ} t_{PQ}^{\frac{3}{2}} \left(t^{-\frac{1}{2}} - t_{PQ}^{-\frac{1}{2}} \right) = \theta_{PQ} + \frac{\dot{\theta}_{PQ}}{H_{PQ}} \left(1 - \frac{R_{PQ}}{R(t)} \right) \\ \dot{\theta}(t) &= \dot{\theta}_{PQ} \frac{t_{PQ}^{\frac{3}{2}}}{t^{\frac{3}{2}}} = \dot{\theta}_{PQ} \left(\frac{R_{PQ}}{R(t)} \right)^3, \end{aligned} \quad (\text{B.26})$$

where $H_{PQ} = H(t_{PQ})$ and $R_{PQ} = R(t_{PQ})$. This solution goes from θ_{PQ} at t_{PQ} to $\theta_{PQ} + \frac{\dot{\theta}_{PQ}}{H_{PQ}}$ as t grows.

Unless $t \sim t_{PQ}$, which would be significantly earlier than t_{osc} , the aforementioned solution is approximately as a constant. Therefore, in the second regime the angle from Eq. (B.26) can be taken as a constant. This angle is called the *(initial) misalignment angle*

$$\theta_i = \theta_{PQ} + \frac{\dot{\theta}_{PQ}}{H_{PQ}}, \quad (\text{B.27})$$

since it is not necessarily aligned (meaning of the same value) with the angle that minimizes the axion potential. From Eq. (B.26) it can also be seen that

$$\dot{\theta}_i \approx 0, \quad (\text{B.28})$$

since $t_{osc} \gg t_{PQ}$. The value of the misalignment angle will depend on cosmological factors, but will also be important to determine the axion relic density, which is the reason for the name of this mechanism.

During inflation the value of θ will change by of the order of $H(T)$, this will repeatedly happen in a period corresponding to the Hubble time, thus given enough time, θ will take every possible value, much like a random walk [98]. The standard scenarios occur under the assumption that the PQ symmetry remains unbroken, in other words the Universe's final temperature is lower than the PQ-temperature, and depend on whether this symmetry is broken during or after inflation¹ [28]. This distinction is necessary due to the possibility of domain walls and other topological effects [15, 49] existing for axions. If PQ-breaking occurs during inflation the domain walls will be negligible, as they will be inflated away. In this case the misalignment angle will take a homogeneous value. On the other hand, if it occurs after inflation domain walls will be present and important. Also, the misalignment angle could take different values in causally disconnected regions, but in the present only one of these might be contained in our Hubble volume. A first estimation of the misalignment angle for this case can be made by averaging the squared angle over the interval $[-\pi, \pi)$, such that

$$\theta_i \equiv \sqrt{\langle \theta_i^2 \rangle} = \left(\frac{1}{2\pi} \int_{-\pi}^{\pi} f(\theta) \theta^2 d\theta \right)^{\frac{1}{2}}, \quad (\text{B.29})$$

where $f(\theta)$ is a distribution, dependent on the axion potential's form. In the harmonic approximation, as was used before ($V(\theta, T) \approx \frac{\theta^2}{2}$), the distribution is uniform, $f(\theta) \approx 1$. This approximation leads to the misalignment angle being

$$\theta_i = \frac{\pi}{\sqrt{3}}. \quad (\text{B.30})$$

¹More precisely, this condition is that the axion decay constant is larger than the Hubble rate at the end of inflation.

Now it is useful to return from the angle $\theta(t)$ to the axion field $a(t)$, in order to calculate the axion relic density. The effective equation of state for the axion field is

$$w_a = \left\langle \frac{\frac{1}{2}\dot{a} - V(a, T)}{\frac{1}{2}\dot{a} + V(a, T)} \right\rangle, \quad (\text{B.31})$$

where w_a is called the scale factor, and the average, signified by the brackets, is done over a time larger than the oscillation period. There is a clear distinction in the scale factor between the regimes before and after t_{osc} . Before this time

$$\frac{1}{2}\dot{a}|_{t \ll t_{osc}} \approx 0, \quad (\text{B.32})$$

since it is proportional to $\dot{\theta}$. This means that

$$w_a|_{t \ll t_{osc}} = -1. \quad (\text{B.33})$$

This behaviour is dark energy-like, this means the axion field is frozen at this time, and corresponds to the approximately constant solution obtained in Eq. (B.26). After the field begins to oscillate, the kinetic and potential energies will be the same over a period of oscillation, leading to

$$w_a|_{t > t_{osc}} = 0. \quad (\text{B.34})$$

Although the axion field is no longer frozen, the axion number density in a comoving volume will freeze out, assuming there is no entropy injection in the evolution of the Universe, this implies that

$$\frac{n_a(T)}{s(T)} = \text{const}, \quad (\text{B.35})$$

where n_a is the (axion) number density and s the entropy density. This also implies that

$$n_a(T) = n_a(T_{osc}) \frac{s(T)}{s(T_{osc})}. \quad (\text{B.36})$$

To continue, it is useful to start with the axion energy density and its derivative

$$\begin{aligned} \rho_a &= f_a^2 \left(\frac{\dot{\theta}}{2} + m_a(T)^2 \frac{\theta^2}{2} \right) \\ \dot{\rho}_a &= f_a^2 \left(\frac{\ddot{\theta}}{2} + \dot{m}_a(T) m_a(T) \theta^2 + m_a(T)^2 \theta \dot{\theta} \right), \end{aligned} \quad (\text{B.37})$$

where the spatial derivatives have been neglected. After some algebra, the equation of

motion, Eq. (B.16), can be rewritten in terms of the new variables as

$$\dot{\rho}_a = \left(\frac{\dot{m}_a(T)}{m_a(T)} - 3H(t) \right) \rho_a. \quad (\text{B.38})$$

To roughly obtain the energy density for the asymptotic value of the axion field, where it has settled on the minimum of the potential, a quick calculation can be performed. Assuming that the equation evolves adiabatically¹, this means that $\frac{\dot{m}_a}{m_a}, H \ll m_a(T)$, and that entropy will be conserved in the comoving volume. The solution in this case can be obtained straightforwardly by integrating, giving

$$\rho_a = C \frac{m_a(T)}{R(t)^3}, \quad (\text{B.39})$$

with C being a constant. Since $\rho_a \propto R(T)^{-3}$, it can be inferred that the axion field describes non-relativistic matter.

Since matter will dominate the axions energy density can be expressed as

$$\rho_a(T) = m_a(T)n_a(T). \quad (\text{B.40})$$

Using Eq. (B.14) for the mass and Eq. (B.36), the energy density becomes

$$\rho_a(T) = m_a \beta n_a(T_{osc}) \frac{s(T)}{s(T_{osc})} \left(\frac{T_C}{T} \right)^\gamma. \quad (\text{B.41})$$

Averaging Eq. (B.37) at T_{osc} , and dividing by the axion mass, an expression for the number density can be obtained

$$n_a(T_{osc}) = b f_a^2 \frac{m_a^2(T_{osc}) \langle \theta_i^2 \rangle}{2}. \quad (\text{B.42})$$

The constant b is of the order $\mathcal{O}(1)$, and is included to account for the approximations taken in previous steps. The entropy density, in a radiation dominated Universe, can be written as

$$s(T) = \frac{2\pi^2}{45} g_s(T) T^3, \quad (\text{B.43})$$

where $g_s(T) = \sum_p \eta_p g_p \left(\frac{T_p}{T} \right)^3$ represents the effective number of entropy relativistic degrees of freedom; the sum runs over all p particle species, T_p is the species' temperature, g_p its internal degrees of freedom, and $\eta_p = 1, \frac{7}{8}$ the statistical factor for bosons and

¹This approximation is not always valid [99].

fermions, respectively. Combining the last two equations, the energy density becomes

$$\rho_a(T) = \frac{\beta b}{2} m_a^2 f_a^2 \langle \theta_i^2 \rangle \frac{g_s(T)}{g_s(T_{osc})} \frac{T^3 T_C^\gamma}{T_{osc}^{3+\gamma}}. \quad (\text{B.44})$$

The axion relic density, from misalignment, takes the form

$$\Omega_a^{mis} = \frac{\rho_a}{\rho_{crit}}, \quad (\text{B.45})$$

where

$$\rho_{crit} = \frac{3m_{Pl}^2 H_0^2}{8\pi}, \quad (\text{B.46})$$

m_{Pl} is the Planck mass, and $H_0 = H(T_{today})$ is the Hubble constant. A better result takes anharmonic terms in the axion potential into account. Also, in the presence of domain walls the axion population can significantly change, for example due to vibrations or decay of the domain walls. A benchmark, which will be used later, for the relic density is given by [49] as

$$\Omega_a^{mis} h^2 \approx 2 \times 10^4 \left(\frac{f_a}{10^{16} \text{ GeV}} \right)^{\frac{7}{6}} \langle \theta_i \rangle^2, \quad (\text{B.47})$$

with $h = \frac{H_0}{100}$, the reduced Hubble constant.

The Origin of the Strong CP Problem and two Axion Models

C.1 From the $U(1)$ Problem to the Strong CP Problem

The strong CP problem arose historically by a solution of another problem, *the $U(1)$ problem* [46]. The $U(1)$ problem was a significant problem with QCD in the 70s, where an apparent axial $U(1)$ symmetry was broken inconsistently with experimental results. The problem follows from an observation that in the massless limit, QCD possess global $U(N)_L \times U(N)_R$ symmetries for the N left and right handed quarks. The symmetry is equivalent to a vector times an axial symmetry, i.e. $U(N)_V \times U(N)_A$. This symmetry is a good approximate symmetry for the three lightest quarks, the up, down, and strange quark, as well as just the up and down quark, the two lightest quarks. As $U(N) = U(1) \times SU(N)$, the aforementioned symmetry, with $N = 2$ can be rewritten as

$$U(2)_L \times U(2)_R = SU(2)_L \times SU(2)_R \times U(1)_V \times U(1)_A. \quad (\text{C.1})$$

The symmetry is spontaneously broken as quark condensates acquire a vev , in other words $\langle \bar{u}u \rangle = \langle \bar{d}d \rangle \neq 0$. After symmetry breaking the group is reduced to

$$SU(2)_I \times U(1)_B \times U(1)_A. \quad (\text{C.2})$$

The subgroup $SU(2)_I = SU(2)_V$ is the vector $SU(2)$ (and a diagonal subgroup of $U(2)_L \times U(2)_R$) corresponding to isospin, $U(1)_B$ is the baryon number, this symmetry is exact in the SM Lagrangian, but anomalous, the $U(1)_A$ is the problematic group. The broken symmetry corresponds to an axial $SU(2)_A$. The Goldstone bosons associated with the breaking of the symmetry are the three pions π^0 , π^+ , and π^- . These are not massless, since the quark masses also break the symmetry explicitly, giving them mass, i.e. they are pseudo-Goldstone bosons. The problem now is that the $U(1)_A$ symmetry is not observed in nature. If it were also spontaneously broken, there would

be a massive pseudo-Goldstone boson in the meson spectrum. The η and η' are the next lightest mesons after the pion, but group theoretical considerations constrain the masses to be $m_{\eta'} < \sqrt{3}m_{\pi^0}$ [19]. The masses of the η mesons are, $m_\eta \approx 548$ MeV and $m_{\eta'} \approx 958$ MeV, compared to $m_{\pi^0} \approx 135$ MeV [8], which violate the aforementioned constraint by about 4 times. In consequence, the $U(1)_A$ symmetry appears to be no symmetry at all.

In 1976 t'Hooft gave a solution to the $U(1)$ problem by showing that introduction of the CP violating term (also called the topological term) broke the $U(1)_A$ symmetry [100]. Essentially, a non-trivial vacuum structure, emerging from the topology of the QCD gauge group, breaks the $U(1)_A$ symmetry further, also giving rise to the topological term in the QCD Lagrangian. A quick summary of the solution [46], will be presented.

It is useful to return to the anomalous chiral current from Eq. (3.5). The fact that this current is anomalous is not apparent from the Lagrangian or in the classical theory, as a matter of fact it is not zero due to contributions by triangle diagrams like those of Fig. 3.1 (see Eq. 3.44 for the expression of these factors and [101] for a complete review on anomalies). This divergence is associated with the chiral symmetry, $U(1)_A$. If it also were to contribute to the action, the symmetry would not be a symmetry of the Lagrangian, solving the $U(1)$ problem. Under the chiral symmetry the quarks transform like in Eq. (3.7). The divergence of the current contributes to the action like

$$\delta S_5^{QCD} = \alpha \int d^4x \partial_\mu J_5^\mu, \quad (\text{C.3})$$

since this is a total divergence it can be written as a surface integral, which is formally done in Euclidean 4-space after a Wick rotation, i.e. by mapping $x_0 \rightarrow ix_0$. This ensures that the action is actually finite, the end result must be taken back to spacetime (Minkowski space). Since this is a rather informal summary of the solution it will not be necessary to take this step explicitly, a more formal treatment of the topic is given in Chapter 5 of [102].

The divergence can be explicitly written as

$$\delta S_5^{QCD} = \alpha \frac{N_f g_s^2}{16\pi^2} \int d^4x G_{\mu\nu}^a \tilde{G}_a^{\mu\nu}. \quad (\text{C.4})$$

The divergence must be in the functional part of the equation, i.e. it must come from the gluon strength tensors, therefore

$$G_{\mu\nu}^a \tilde{G}_a^{\mu\nu} = \partial_\mu K^\mu. \quad (\text{C.5})$$

The current K^μ is called a topological current or *Chern-Simons current* and can be

expressed as

$$K^\mu = \epsilon^{\mu\nu\rho\sigma} G_\nu^a \left(G_{a\rho\sigma} - \frac{g_s}{3} f_{abc} G_\rho^b G_\sigma^c \right). \quad (\text{C.6})$$

Using Stokes' Theorem Eq. (C.4) can be expressed as a surface integral

$$\delta S_5^{QCD} = \alpha \frac{N_f g_s^2}{16\pi^2} \int d\sigma_\mu K^\mu, \quad (\text{C.7})$$

where the surface integral is over boundary the hypersphere S_3 (again, formally in Euclidean space). Naively, since $K^\mu \propto G_a^\mu$ one would expect $K^\mu \rightarrow 0$ at the boundary, as one expects $G_a^\mu \rightarrow 0$ at the boundary. This is not exactly true, it is true that G_a^μ can be 0 at the boundary, but it can also be a gauge transformation of 0, what is known as a *pure gauge* configuration¹.

The question that arises then is if it is possible to have non-zero contributions to the action from the pure gauge configurations. If this is the case, $U(1)_A$ is not a symmetry of QCD, solving the $U(1)$ problem. These configurations are best studied by writing the gluons as a $\mathfrak{su}(3)$ vector, i.e.

$$G_\mu = \frac{\lambda_a}{2} G_\mu^a, \quad (\text{C.8})$$

where $\frac{\lambda_a}{2}$ are the $\mathfrak{su}(3)$ generators. The usefulness of this comes from the fact that under a gauge transformation

$$G_\mu \rightarrow U^\dagger G_\mu U + \frac{i}{g_s} U^\dagger \partial_\mu U, \quad (\text{C.9})$$

with $U \in SU(3)$, therefore $U^\dagger = U^{-1}$. In a pure gauge configuration the gauge field takes the form

$$G_\mu = \frac{i}{g_s} U^\dagger \partial_\mu U. \quad (\text{C.10})$$

To continue, it is enough to restrict the problem to a subgroup of $SU(3)$, namely $SU(2)$. The pure gauge configurations can be classified by how U maps to the identity element, specifically they can be classified by how they fail to be continuously deformed to the identity element². As $\mathbf{x} \rightarrow \infty$ the gauge group element U can tend to unity as

$$U_n \rightarrow e^{2\pi i n}, \quad (\text{C.11})$$

where n is an integer, called the winding number. This integer is related to the Jacobian of $S_3 \rightarrow S_3$ maps. To simplify the following expressions a gauge, sometimes called the

¹To get a finite contribution to the action the proper boundary condition is $G_{\mu\nu}^a \rightarrow 0$, allowing the possibility of non-zero configurations of G_μ^a .

²Formally these are the homotopy classes of the gauge group.

temporal gauge, can be chosen. In this gauge $G_0^a = 0$, while the spatial components are unconstrained, consequently $K^0 \neq 0$. In this gauge, n results from the following integral

$$n = i \frac{g_s^3}{24\pi^2} \int d^3\mathbf{x} \operatorname{Tr}(\epsilon_{ijk} G_{(n)}^i G_{(n)}^j G_{(n)}^k), \quad (\text{C.12})$$

where $G_{(n)}^i$ is a pure gauge configuration satisfying Eq. (C.11). This is also related to the current K^μ , that in the chosen gauge simplifies to

$$K^0 = -\frac{g_s}{3} \epsilon^{ijk} \epsilon_{abc} G_i^a G_j^b G_k^c = \frac{4}{3} i g_s \epsilon^{ijk} \operatorname{Tr}(G_i G_j G_k). \quad (\text{C.13})$$

The pure gauge configurations are associated with different vacua, $|n\rangle$ ¹. These vacua are not physical, since K^μ is not gauge invariant. The physical vacuum is a superposition of the $|n\rangle$ vacua,

$$|\theta\rangle = \sum_n e^{in\theta} |n\rangle, \quad (\text{C.14})$$

known as the θ -vacuum. This relates to the contribution to the action δS_5^{QCD} by considering vacuum transitions. The transition from the vacuum at $t = +\infty$ to $t = -\infty$ can be expressed as

$$\langle \theta_+ | \theta_- \rangle = \sum_{n, m} e^{-im\theta} e^{in\theta} \langle m_+ | n_- \rangle. \quad (\text{C.15})$$

Defining the winding number difference $\nu = n - m$, the vacuum transition becomes

$$\langle \theta_+ | \theta_- \rangle = \sum_\nu e^{i\nu\theta} \sum_m \langle m_+ | (m + \nu)_- \rangle. \quad (\text{C.16})$$

On the other hand it can be seen from Eq. (C.12) and Eq. (C.13) that the winding number difference can be expressed as

$$\nu = n|_{t=+\infty} - n|_{t=-\infty} = \frac{g_s^2}{32\pi^2} \int d^4\mathbf{x} \partial_0 K^0(t, \mathbf{x}) = \frac{g_s^2}{32\pi^2} \int d^3\mathbf{x} K^0(t, \mathbf{x})|_{t=-\infty}^{t=+\infty}. \quad (\text{C.17})$$

Now, it is possible to write the transition as a path for fixed ν , this means that $\sum_m \langle m_+ | (m + \nu)_- \rangle$ can be expressed as an integral. Doing this results in the following expression

$$\langle \theta_+ | \theta_- \rangle = \int \mathcal{D}G \sum_\nu e^{iS_{QCD}} e^{i\nu\theta} \delta\left(\nu - \frac{g_s^2}{32\pi^2} \int d^4\mathbf{x} G_{\mu\nu}^a \tilde{G}_a^{\mu\nu}\right). \quad (\text{C.18})$$

¹These correspond to classical solutions of the action in Euclidean 4-space, called *instantons*. An explicit construction is given in [103].

The QCD action is $S_{QCD} = \int d^4x \mathcal{L}_{QCD}$, while the δ assures that ν is fixed. The expression for ν comes from transforming Eq. (C.17) to the form of Eq. (C.4). Substituting ν in the exponential leads to the final form of the vacuum transition

$$\langle \theta_+ | \theta_- \rangle = \int \mathcal{D}G \sum_{\nu} e^{i \left(S_{QCD} + \int d^4x \theta \frac{g_s^2}{32\pi^2} G_{\mu\nu}^a \tilde{G}_a^{\mu\nu} \right)} \delta \left(\nu - \frac{g_s^2}{32\pi^2} \int d^4x G_{\mu\nu}^a \tilde{G}_a^{\mu\nu} \right). \quad (\text{C.19})$$

The exponential now contains the QCD action plus the topological term, from this follows the effective action

$$S_{eff} = S_{QCD} + \int d^4x \theta \frac{g_s^2}{32\pi^2} G_{\mu\nu}^a \tilde{G}_a^{\mu\nu} \quad (\text{C.20})$$

and hence the topological correction to the QCD Lagrangian from Eq. (3.6). This is called a *superselection rule*, since the topological term enters the Lagrangian by the choice of a θ -vacuum.

By doing this, it is shown that the topological term arises naturally from the complicated vacuum structure of QCD. This solves the $U(1)$ problem, since $U(1)_A$ is not a real symmetry of the QCD Lagrangian. A consequence is the introduction of another problem, the strong CP problem.

C.2 PQWW Axion

The PQWW axion was first described in 1977 by Weinberg and Wilczek [47, 48]. A scalar $SU(2)_L$ doublet is introduced, acting as a second Higgs doublet, there is then a Higgs doublet for up-type quarks, H_u , and a Higgs doublet for down-type quarks H_d . These scalars are charged under $U(1)_{PQ}$, as well as the quarks. The scalar sector (excluding lepton couplings) of the UV-complete Lagrangian takes the form

$$\mathcal{L}_H = (\partial_\mu H_u)^\dagger (\partial^\mu H_u) + (\partial_\mu H_d)^\dagger (\partial^\mu H_d) - V(H_u, H_d), \quad (\text{C.21})$$

where $V(H_u, H_d)$ is a potential including quadratic and quartic interactions between the scalars. When the scalars acquire a vev , $v_{u/d}$, $SU(2)_L \times U(1)_Y \times U(1)_{PQ}$ breaks down spontaneously. This will give mass to the fermions coupled to the doublets like

$$y_{ij}^u \bar{Q}^i H_u u_R^j, \quad \text{or} \quad y_{ij}^d \bar{Q}^i \widetilde{H}_d u_R^j, \quad (\text{C.22})$$

where the terms for the down- and lepton sector are analogous (there is no extra Higgs doublet for the charged leptons). This gives the SM particles masses, but unlike the SM with one Higgs doublet, there are four neutral real scalars. Like the SM, one gives

the Z boson its mass, the other one is the Higgs boson and the last two can form a complex scalar Φ . The axion decay constant is associated to the vev of Φ , which breaks the PQ symmetry and is given by

$$f_a = \frac{v}{6} \sin(2\beta), \quad (\text{C.23})$$

with $\tan(\beta) = \frac{v_u}{v_d}$ and v the EW vev .

The axion shows up as the radial part of Φ [98]. This field acquires a vev

$$\langle \Phi \rangle = \frac{f_a}{\sqrt{2}}, \quad (\text{C.24})$$

it can then be written as

$$\Phi = \frac{1}{\sqrt{2}}(f_a + r_a)e^{i\frac{a}{f_a}}, \quad (\text{C.25})$$

where r_a is a radial (real scalar) field and the axion appears as the Goldstone boson in the exponential. It also couples to the, now massive, quarks as (in the diagonal basis)

$$\mathcal{L}_{\Phi q} = \sum_q m_q \bar{q}_R q_L \Phi + h.c. \quad (\text{C.26})$$

The axion-anomaly coupling will arise from terms like

$$\bar{q}_R e^{i\frac{a}{f_a}} q_L, \quad (\text{C.27})$$

where the radial field and the quarks can be integrated out. A diagrammatic explanation of this process can be seen in Fig. 3.2.

C.3 KSVZ Axion

In KSVZ [54, 55] models, heavy vector-like fermions, \mathcal{Q} , are added to the SM, whose charges and representations can be completely arbitrary, as long as at least one of the fermions transforms non-trivially under $SU(3)_C$. Besides the fermions, a complex scalar Φ is added to the theory. This scalar will play the role of the PQWW σ and the following theory is similar. Since σ is unrelated to the Higgs doublet this framework allows for $f_a \gg v$. It is also unnecessary to include two Higgs doublets.

As an example of the implementation of a KSVZ-type axion suppose that only a heavy fermion, \mathcal{Q} , and the scalar σ are added to the SM. The scalar is an SM singlet, while \mathcal{Q} is an $SU(3)_C$ triplet, but otherwise uncharged. The Lagrangian for this model

looks like

$$\mathcal{L}_{KSVZ} = (\partial_\mu \sigma)^\dagger (\partial^\mu \sigma) + \bar{Q} i \gamma^\mu D_\mu Q - (Y_Q \bar{Q}_L Q_R \sigma + h.c.) - V(\sigma). \quad (\text{C.28})$$

Under PQ they transform as

$$\sigma \rightarrow e^{i\alpha} \sigma, \quad Q \rightarrow e^{-i\gamma_5 \frac{\alpha}{2}} Q, \quad (\text{C.29})$$

this means that the left- and right-handed components of the fermion transform as $Q_{L/R} \rightarrow e^{\pm i \frac{\alpha}{2}} Q_{L/R}$. The scalar potential $V(\sigma)$ contains quadratic and quartic terms, and can be written in terms of the scalar's vev , $\frac{v_a}{2}$ like

$$V = \lambda_\sigma \left(\sigma^\dagger \sigma - \frac{v_a^2}{2} \right)^2. \quad (\text{C.30})$$

In terms of a radial field and the Goldstone boson, i.e. the axion, this scalar takes the form of Eq. (C.25)

$$\sigma = \frac{1}{\sqrt{2}} (v_a + r_a) e^{i \frac{a}{v_a}}. \quad (\text{C.31})$$

The fermion and radial field acquire a mass given by

$$m_Q = Y_Q \frac{v_a}{\sqrt{2}}, \quad m_r = \sqrt{2\lambda_\sigma} v_a. \quad (\text{C.32})$$

To integrate out these fields, a field dependent chiral transformation, in terms of the axion, is done

$$Q \rightarrow e^{-i\gamma_5 \frac{a}{2v_a}} Q \quad (\text{C.33})$$

this uncouples the axion from the fermions and the radial field. As it is anomalous (due to triangle diagrams) it also introduces the axion-anomaly coupling to the Lagrangian (see Fig. 3.2), i.e.

$$\delta S_{KSVZ} = \int d^4x \frac{g_s^2}{32\pi^2} \frac{a}{v_a} G_{\mu\nu}^a \tilde{G}_a^{\mu\nu}. \quad (\text{C.34})$$

In this simple model v_a can be readily identified with f_a , in other words $N = \frac{1}{2}$, since $f_a = \frac{1}{2N}$.

Redefinition of Phases in Mass Matrices

The procedure of redefining the phases of mass matrices will be exemplified here with the quark mass matrices of Eq. (4.15). These matrices can be written as

$$m^{u/d} = \begin{pmatrix} 0 & A_{u/d} e^{i\alpha_{u/d}} & 0 \\ B_{u/d} e^{i\beta_{u/d}} & 0 & C_{u/d} e^{i\gamma_{u/d}} \\ 0 & D_{u/d} e^{i\delta_{u/d}} & E_{u/d} e^{i\epsilon_{u/d}} \end{pmatrix}, \quad (\text{D.1})$$

where $A_{u/d}, B_{u/d}, C_{u/d}, D_{u/d}, E_{u/d}, \alpha_{u/d}, \beta_{u/d}, \gamma_{u/d}, \delta_{u/d}$, and $\epsilon_{u/d}$ are real parameters. These matrices can be diagonalized by bi-unitary transformations. It can be noticed that the superscript (u/d) can be dropped, since the procedure is identical in the up- and down- sector (and also in general).

$$m^{diag} = U_L^\dagger m U_R = O_L^T P_L^\dagger m P_R O_R, \quad (\text{D.2})$$

where L and R depict the left- and right-chiral fields, respectively, and $O_{L/R} \in SO(3)$. Also, $U_L = P_L O_L$ and $U_R = P_R O_R$ are the unitary matrices that diagonalize $m^\dagger m$ and $m m^\dagger$, respectively, and $P_L = \text{diag}(1, e^{i\alpha}, e^{i\beta})$, $P_R = \text{diag}(e^{i\rho_1}, e^{i\rho_2}, e^{i\rho_3})$ are the diagonal phase matrices. Thus transforming the left- and right-handed fermions by P_L and P_R , respectively, it is possible to get a completely real mass matrix

$$m = \begin{pmatrix} 0 & A & 0 \\ B & 0 & C \\ 0 & D & E \end{pmatrix}, \quad (\text{D.3})$$

where the phases have been shifted from $P_L^\dagger m P_R$ to the fields.

Since only $U_L^{u/d}$ contribute to the CKM matrix, which is defined as

$$\begin{aligned} V_{CKM} &= (U_L^u)^\dagger (U_L^d) = ((O_L^u)^T (P_L^u)^\dagger) (P_L^d O_L^d), \\ &= (O_L^u)^T \text{diag}(1, e^{-i(\alpha_u - \alpha_d)}, e^{-i(\beta_u - \beta_d)}) O_L^d, \end{aligned} \quad (\text{D.4})$$

one can see that the right-handed phases will not contribute to the masses and mixing parameters, and can therefore be set to 0 in the fit. It is also worth noting that only the phase differences appear in V_{CKM} , this means that two phases can be set to 0. Finally, the phase-redefined mass matrices take the form

$$P_L^\dagger m = \begin{pmatrix} 0 & A & 0 \\ B e^{-i\alpha} & 0 & C e^{-i\alpha} \\ 0 & D e^{-i\beta} & E e^{-i\beta} \end{pmatrix}, \quad (\text{D.5})$$

where in either the top- or down-quark matrix the phases can be set to 0 (or one in each). An analogous procedure can be carried out for the neutrino mass matrix, where hermitian conjugation has to be changed for transposition.

Bibliography

- [1] V. C. Rubin, N. Thonnard, and W. K. Ford, Jr., “Rotational properties of 21 SC galaxies with a large range of luminosities and radii, from NGC 4605 /R = 4kpc/ to UGC 2885 /R = 122 kpc/,” *Astrophys. J.* **238** (1980) 471. xi, 4
- [2] C. Collaboration, “Public plots for Higgs $\rightarrow \mu\mu$.” CMS Collection., Aug, 2020. xi, 17
- [3] C. O’HARE, “cajohare/axionlimits: Axionlimits,” July, 2020. <https://doi.org/10.5281/zenodo.3932430>. xi, 58
- [4] **ATLAS** Collaboration, M. Aaboud *et al.*, “Search for top-quark decays $t \rightarrow Hq$ with 36 fb^{-1} of pp collision data at $\sqrt{s} = 13 \text{ TeV}$ with the ATLAS detector,” *JHEP* **05** (2019) 123, [arXiv:1812.11568](https://arxiv.org/abs/1812.11568) [hep-ex]. xii, 65, 66
- [5] **ATLAS** Collaboration, “Expected sensitivity of ATLAS to FCNC top quark decays $t \rightarrow Zu$ and $t \rightarrow Hq$ at the High Luminosity LHC,”. xii, 65, 66
- [6] M. Vos *et al.*, “Top physics at high-energy lepton colliders,” [arXiv:1604.08122](https://arxiv.org/abs/1604.08122) [hep-ex]. xii, 65, 66
- [7] P. de Salas, D. Forero, C. Ternes, M. Tortola, and J. Valle, “Status of neutrino oscillations 2018: 3σ hint for normal mass ordering and improved CP sensitivity,” *Phys.Lett.* **B782** (2018) 633–640, [arXiv:1708.01186](https://arxiv.org/abs/1708.01186) [hep-ph]. xiii, 26, 60, 61
- [8] **Particle Data Group** Collaboration, P. Zyla *et al.*, “Review of Particle Physics,” *PTEP* **2020** no. 8, (2020) 083C01. xiii, 19, 20, 24, 26, 37, 38, 57, 60, 61, 66, 71, 81
- [9] S. Antusch and V. Maurer, “Running quark and lepton parameters at various scales,” *JHEP* **11** (2013) 115, [arXiv:1306.6879](https://arxiv.org/abs/1306.6879) [hep-ph]. xiii, 57, 59, 60, 61
- [10] B. Pontecorvo, “Mesonium and anti-mesonium,” *Sov. Phys. JETP* **6** (1957) 429. 2

- [11] **Super-Kamiokande** Collaboration, S. Fukuda *et al.*, “Determination of solar neutrino oscillation parameters using 1496 days of Super-Kamiokande I data,” *Phys. Lett. B* **539** (2002) 179–187, [arXiv:hep-ex/0205075](#). 2
- [12] **SNO** Collaboration, J. Boger *et al.*, “The Sudbury neutrino observatory,” *Nucl. Instrum. Meth. A* **449** (2000) 172–207, [arXiv:nucl-ex/9910016](#). 2
- [13] S. Andriolo, S. Y. Li, and S. H. H. Tye, “String Landscape and Fermion Masses,” *Phys. Rev. D* **101** no. 6, (2020) 066005, [arXiv:1902.06608](#) [hep-th]. 2
- [14] F. Zwicky, “On the Masses of Nebulae and of Clusters of Nebulae,” *Astrophys. J.* **86** (1937) 217–246. 3
- [15] S. Profumo, *An Introduction to Particle Dark Matter*. World Scientific, 1st. ed., 2017. 3, 5, 30, 43, 70, 72, 76
- [16] J. Oort, “The force exerted by the stellar system in the direction perpendicular to the galactic plane and some related problems,” *Bulletin of the Astronomical Institutes of the Netherlands* **6** (1932) 249–286. 3
- [17] R. H. Sanders, *The dark matter problem: A historical perspective*. CUP, draft ed., 2009. 3
- [18] W. J. Quirk, “Numerical experiments in spiral structure,” in *Gravitational N-Body Problem*, M. Lecar, ed., pp. 250–253. Springer Netherlands, Dordrecht, 1972. 5
- [19] M. D. Schwartz, *Quantum Field Theory And The Standard Model*. Cambridge University Press, 1st. ed., 2014. 7, 18, 81
- [20] P. Langacker, *The Standard Model and Beyond, Second Edition*. Series in High Energy Physics, Cosmology and Gravitation. CRC Press, 2nd. ed., 2017. 7, 18
- [21] Y. Nambu, “Quasi-particles and gauge invariance in the theory of superconductivity,” *Phys. Rev.* **117** (Feb, 1960) 648–663. <https://link.aps.org/doi/10.1103/PhysRev.117.648>. 11
- [22] J. Goldstone, “Field theories with \ll superconductor \gg solutions,” *Il Nuovo Cimento* **117** (Jan, 1961) 154–164. https://link.springer.com/article/10.1007%2F978-94-007-2812-7_22. 11
- [23] J. Goldstone, A. Salam, and S. Weinberg, “Broken symmetries,” *Phys. Rev.* **127** (Aug, 1962) 965–970. <https://link.aps.org/doi/10.1103/PhysRev.127.965>. 11

- [24] N. Cabibbo, “Unitary Symmetry and Leptonic Decays,” *Phys. Rev. Lett.* **10** (1963) 531–533. 19
- [25] M. Kobayashi and T. Maskawa, “CP Violation in the Renormalizable Theory of Weak Interaction,” *Prog. Theor. Phys.* **49** (1973) 652–657. 19
- [26] **MuLan** Collaboration, D. M. Webber *et al.*, “Measurement of the Positive Muon Lifetime and Determination of the Fermi Constant to Part-per-Million Precision,” *Phys. Rev. Lett.* **106** (2011) 041803, [arXiv:1010.0991 \[hep-ex\]](#). 20, 33
- [27] **nEDM** Collaboration, C. Abel *et al.*, “Measurement of the permanent electric dipole moment of the neutron,” *Phys. Rev. Lett.* **124** no. 8, (2020) 081803, [arXiv:2001.11966 \[hep-ex\]](#). 20
- [28] L. Di Luzio, M. Giannotti, E. Nardi, and L. Visinelli, “The landscape of QCD axion models,” *Phys. Rept.* **870** (2020) 1–117, [arXiv:2003.01100 \[hep-ph\]](#). 20, 33, 34, 35, 36, 44, 56, 57, 74, 76
- [29] **Super-Kamiokande** Collaboration, Y. Fukuda *et al.*, “Evidence for oscillation of atmospheric neutrinos,” *Phys. Rev. Lett.* **81** (1998) 1562–1567, [arXiv:hep-ex/9807003](#). 21
- [30] V. A. Novikov, L. B. Okun, A. N. Rozanov, and M. I. Vysotsky, “Theory of Z boson decays,” *Rept. Prog. Phys.* **62** (1999) 1275–1332, [arXiv:hep-ph/9906465](#). 21
- [31] M. Ibe, A. Kusenko, and T. T. Yanagida, “Why three generations?,” *Phys. Lett. B* **758** (2016) 365–369, [arXiv:1602.03003 \[hep-ph\]](#). 21
- [32] J. W. F. Romão, Jorge; Valle, *Neutrinos in high energy and astroparticle physics*. Wiley, 2015. 21
- [33] C. W. K. Carlo Giunti, *Fundamentals of Neutrino Physics and Astrophysics*. Oxford University Press, USA, illustrated edition ed., 2007. 21
- [34] S. Weinberg, “Baryon and Lepton Nonconserving Processes,” *Phys. Rev. Lett.* **43** (1979) 1566–1570. 22
- [35] M. Escudero, J. Lopez-Pavon, N. Rius, and S. Sandner, “Relaxing Cosmological Neutrino Mass Bounds with Unstable Neutrinos,” *JHEP* **12** (2020) 119, [arXiv:2007.04994 \[hep-ph\]](#). 23

- [36] S. Roy Choudhury and S. Choubey, “Updated Bounds on Sum of Neutrino Masses in Various Cosmological Scenarios,” *JCAP* **09** (2018) 017, [arXiv:1806.10832 \[astro-ph.CO\]](#). 23
- [37] A. Loureiro *et al.*, “On The Upper Bound of Neutrino Masses from Combined Cosmological Observations and Particle Physics Experiments,” *Phys. Rev. Lett.* **123** no. 8, (2019) 081301, [arXiv:1811.02578 \[astro-ph.CO\]](#). 23
- [38] M. Aker *et al.*, “First direct neutrino-mass measurement with sub-eV sensitivity,” *arXiv Preprint* (2021) , [arXiv:2105.08533 \[hep-ex\]](#). 23
- [39] B. Pontecorvo, “Inverse beta processes and nonconservation of lepton charge,” *Zh. Eksp. Teor. Fiz.* **34** (1957) 247. 25
- [40] Z. Maki, M. Nakagawa, and S. Sakata, “Remarks on the unified model of elementary particles,” *Prog. Theor. Phys.* **28** (1962) 870–880. 25
- [41] Z.-z. Xing and Z.-h. Zhao, “The effective neutrino mass of neutrinoless double-beta decays: how possible to fall into a well,” *Eur. Phys. J. C* **77** no. 3, (2017) 192, [arXiv:1612.08538 \[hep-ph\]](#). 26
- [42] C. Froggatt and H. B. Nielsen, “Hierarchy of Quark Masses, Cabibbo Angles and CP Violation,” *Nucl. Phys. B* **147** (1979) 277–298. 26
- [43] K. Babu, “TASI Lectures on Flavor Physics,” in *Theoretical Advanced Study Institute in Elementary Particle Physics: The Dawn of the LHC Era*, pp. 49–123. 2010. [arXiv:0910.2948 \[hep-ph\]](#). 26, 27, 28, 48
- [44] R. Peccei and H. R. Quinn, “CP Conservation in the Presence of Instantons,” *Phys.Rev.Lett.* **38** (1977) 1440–1443. 34
- [45] R. D. Peccei and H. R. Quinn, “Constraints Imposed by CP Conservation in the Presence of Instantons,” *Phys. Rev. D* **16** (1977) 1791–1797. 34
- [46] R. D. Peccei, “The Strong CP problem and axions,” *Lect. Notes Phys.* **741** (2008) 3–17, [arXiv:hep-ph/0607268](#). 35, 80, 81
- [47] S. Weinberg, “A New Light Boson?,” *Phys.Rev.Lett.* **40** (1978) 223–226. 35, 84
- [48] F. Wilczek, “Problem of Strong P and T Invariance in the Presence of Instantons,” *Phys.Rev.Lett.* **40** (1978) 279–282. 35, 84
- [49] D. J. E. Marsh, “Axion Cosmology,” *Phys. Rept.* **643** (2016) 1–79, [arXiv:1510.07633 \[astro-ph.CO\]](#). 35, 43, 44, 76, 79

-
- [50] Y. Asano, E. Kikutani, S. Kurokawa, T. Miyachi, M. Miyajima, Y. Nagashima, T. Shinkawa, S. Sugimoto, and Y. Yoshimura, “Search for a Rare Decay Mode $K^+ \rightarrow \pi^+ \text{ Neutrino anti-neutrino and Axion}$,” [35](#)
- [51] M. Bauer, M. Neubert, S. Renner, M. Schnubel, and A. Thamm, “Consistent treatment of axions in the weak chiral Lagrangian,” [arXiv:2102.13112 \[hep-ph\]](#). [36](#)
- [52] G. Grilli di Cortona, E. Hardy, J. Pardo Vega, and G. Villadoro, “The QCD axion, precisely,” *JHEP* **01** (2016) 034, [arXiv:1511.02867 \[hep-ph\]](#). [38](#)
- [53] M. Srednicki, “Axion Couplings to Matter. 1. CP Conserving Parts,” *Nucl.Phys.* **B260** (1985) 689–700. [39](#), [55](#)
- [54] J. E. Kim, “Weak Interaction Singlet and Strong CP Invariance,” *Phys. Rev. Lett.* **43** (1979) 103. [40](#), [85](#)
- [55] M. A. Shifman, A. I. Vainshtein, and V. I. Zakharov, “Can Confinement Ensure Natural CP Invariance of Strong Interactions?,” *Nucl. Phys.* **B166** (1980) 493–506. [40](#), [85](#)
- [56] M. Dine, W. Fischler, and M. Srednicki, “A Simple Solution to the Strong CP Problem with a Harmless Axion,” *Phys.Lett.* **B104** (1981) 199–202. [40](#), [54](#)
- [57] A. Zhitnitsky, “On Possible Suppression of the Axion Hadron Interactions. (In Russian),” *Sov.J.Nucl.Phys.* **31** (1980) 260. [40](#)
- [58] P. Fox, A. Pierce, and S. D. Thomas, “Probing a QCD string axion with precision cosmological measurements,” [arXiv:hep-th/0409059](#). [43](#)
- [59] Y. Ema, K. Hamaguchi, T. Moroi, and K. Nakayama, “Flaxion: a minimal extension to solve puzzles in the standard model,” *JHEP* **01** (2017) 096, [arXiv:1612.05492 \[hep-ph\]](#). [45](#)
- [60] C. D. Carone and M. Merchand, “ T models with high quality flaxions,” *Phys. Rev. D* **101** no. 11, (2020) 115032, [arXiv:2004.02040 \[hep-ph\]](#). [45](#)
- [61] L. Calibbi, F. Goertz, D. Redigolo, R. Ziegler, and J. Zupan, “Minimal axion model from flavor,” *Phys. Rev. D* **95** no. 9, (2017) 095009, [arXiv:1612.08040 \[hep-ph\]](#). [45](#), [63](#)
- [62] F. Arias-Aragon and L. Merlo, “The Minimal Flavour Violating Axion,” *JHEP* **10** (2017) 168, [arXiv:1709.07039 \[hep-ph\]](#). [Erratum: *JHEP* 11, 152 (2019)]. [45](#)
-

- [63] M. Linster and R. Ziegler, “A Realistic $U(2)$ Model of Flavor,” *JHEP* **08** (2018) 058, [arXiv:1805.07341 \[hep-ph\]](#). 45
- [64] F. Björkeröth, E. J. Chun, and S. F. King, “Accidental Peccei–Quinn symmetry from discrete flavour symmetry and Pati–Salam,” *Phys. Lett. B* **777** (2018) 428–434, [arXiv:1711.05741 \[hep-ph\]](#). 45
- [65] F. Björkeröth, E. J. Chun, and S. F. King, “Flavourful Axion Phenomenology,” *JHEP* **08** (2018) 117, [arXiv:1806.00660 \[hep-ph\]](#). 45, 63
- [66] Q. Bonnefoy, E. Dudas, and S. Pokorski, “Chiral Froggatt-Nielsen models, gauge anomalies and flavourful axions,” *JHEP* **01** (2020) 191, [arXiv:1909.05336 \[hep-ph\]](#). 45
- [67] G. Branco, L. Lavoura, and F. Mota, “Nearest Neighbor Interactions and the Physical Content of Fritzsch Mass Matrices,” *Phys. Rev. D* **39** (1989) 3443. 45
- [68] P. H. Frampton, S. L. Glashow, and D. Marfatia, “Zeroes of the neutrino mass matrix,” *Phys. Lett. B* **536** (2002) 79–82, [arXiv:hep-ph/0201008](#). 45
- [69] L. M. G. de la Vega, N. Nath, S. Nellen, and E. Peinado, “Flavored axion in the UV-complete Froggatt-Nielsen models,” [arXiv:2102.03631 \[hep-ph\]](#). 45
- [70] H. Fritzsch, “Weak Interaction Mixing in the Six - Quark Theory,” *Phys. Lett. B* **73** (1978) 317–322. 46
- [71] H. Fritzsch, “Quark Masses and Flavor Mixing,” *Nucl. Phys. B* **155** (1979) 189–207. 46
- [72] H. Ishimori, T. Kobayashi, H. Ohki, Y. Shimizu, H. Okada, and M. Tanimoto, “Non-Abelian Discrete Symmetries in Particle Physics,” *Prog. Theor. Phys. Suppl.* **183** (2010) 1–163, [arXiv:1003.3552 \[hep-th\]](#). 46
- [73] H. Fritzsch, Z.-z. Xing, and Y.-L. Zhou, “Non-Hermitian Perturbations to the Fritzsch Textures of Lepton and Quark Mass Matrices,” *Phys. Lett. B* **697** (2011) 357–363, [arXiv:1101.4272 \[hep-ph\]](#). 46
- [74] D. Espriu, F. Mescia, and A. Renau, “Axion-Higgs interplay in the two Higgs-doublet model,” *Phys. Rev. D* **92** no. 9, (2015) 095013, [arXiv:1503.02953 \[hep-ph\]](#). 54
- [75] H. Georgi and S. L. Glashow, “Unity of All Elementary Particle Forces,” *Phys. Rev. Lett.* **32** (1974) 438–441. 56

- [76] I. G. Irastorza and J. Redondo, “New experimental approaches in the search for axion-like particles,” *Prog. Part. Nucl. Phys.* **102** (2018) 89–159, [arXiv:1801.08127 \[hep-ph\]](#). 57, 63
- [77] I. Stern, “ADMX Status,” *PoS ICHEP2016* (2016) 198, [arXiv:1612.08296 \[physics.ins-det\]](#). 57
- [78] Z.-z. Xing and Z.-h. Zhao, “On the four-zero texture of quark mass matrices and its stability,” *Nucl. Phys. B* **897** (2015) 302–325, [arXiv:1501.06346 \[hep-ph\]](#). 59
- [79] S. Antusch, J. Kersten, M. Lindner, M. Ratz, and M. A. Schmidt, “Running neutrino mass parameters in see-saw scenarios,” *JHEP* **03** (2005) 024, [arXiv:hep-ph/0501272](#). 59
- [80] L. Di Luzio, “Flavour Violating Axions,” *EPJ Web Conf.* **234** (2020) 01005, [arXiv:1911.02591 \[hep-ph\]](#). 61, 62
- [81] J. F. Kamenik and C. Smith, “FCNC portals to the dark sector,” *JHEP* **03** (2012) 090, [arXiv:1111.6402 \[hep-ph\]](#). 62, 63
- [82] **E949, E787** Collaboration, S. Adler *et al.*, “Measurement of the $K^+ \rightarrow \pi^+ \nu \bar{\nu}$ branching ratio,” *Phys. Rev. D* **77** (2008) 052003, [arXiv:0709.1000 \[hep-ex\]](#). 63
- [83] **NA62** Collaboration, E. Cortina Gil *et al.*, “Search for a feebly interacting particle X in the decay $K^+ \rightarrow \pi^+ X$,” *JHEP* **03** (2021) 058, [arXiv:2011.11329 \[hep-ex\]](#). 63
- [84] **NA62** Collaboration, T. Spadaro, “The NA62 experiment at CERN: status and perspectives,” in *6th International Workshop on the CKM Unitarity Triangle*. 1, 2011. [arXiv:1101.5631 \[hep-ex\]](#). 63
- [85] P. Ball and R. Zwicky, “New results on $B \rightarrow \pi, K, \eta$ decay formfactors from light-cone sum rules,” *Phys. Rev. D* **71** (2005) 014015, [arXiv:hep-ph/0406232](#). 63
- [86] A. J. Buras, M. V. Carlucci, S. Gori, and G. Isidori, “Higgs-mediated FCNCs: Natural Flavour Conservation vs. Minimal Flavour Violation,” *JHEP* **10** (2010) 009, [arXiv:1005.5310 \[hep-ph\]](#). 64
- [87] J. Herrero-Garcia, M. Nebot, F. Rajec, M. White, and A. G. Williams, “Higgs Quark Flavor Violation: Simplified Models and Status of General

- Two-Higgs-Doublet Model,” *JHEP* **02** (2020) 147, [arXiv:1907.05900 \[hep-ph\]](#). 64
- [88] D. Atwood, S. K. Gupta, and A. Soni, “Constraining the flavor changing Higgs couplings to the top-quark at the LHC,” *JHEP* **10** (2014) 057, [arXiv:1305.2427 \[hep-ph\]](#). 66
- [89] P. Sikivie, “Of Axions, Domain Walls and the Early Universe,” *Phys. Rev. Lett.* **48** (1982) 1156–1159. 67
- [90] S. M. Barr and J. E. Kim, “New Confining Force Solution of the QCD Axion Domain-Wall Problem,” *Phys. Rev. Lett.* **113** no. 24, (2014) 241301, [arXiv:1407.4311 \[hep-ph\]](#). 67
- [91] M. Reig, “On the high-scale instanton interference effect: axion models without domain wall problem,” *JHEP* **08** (2019) 167, [arXiv:1901.00203 \[hep-ph\]](#). 67
- [92] M. Milgrom, “A modification of the Newtonian dynamics as a possible alternative to the hidden mass hypothesis.,” *American Physical Journal* **270** (July, 1983) 365–370. 70
- [93] J. D. Bekenstein, “Relativistic gravitation theory for the modified newtonian dynamics paradigm,” *Phys. Rev. D* **70** (Oct, 2004) 083509. <https://link.aps.org/doi/10.1103/PhysRevD.70.083509>. 70
- [94] K. Pardo and D. N. Spergel, “What is the price of abandoning dark matter? Cosmological constraints on alternative gravity theories,” *Phys. Rev. Lett.* **125** no. 21, (2020) 211101, [arXiv:2007.00555 \[astro-ph.CO\]](#). 70
- [95] **Planck** Collaboration, N. Aghanim *et al.*, “Planck 2018 results. VI. Cosmological parameters,” [arXiv:1807.06209 \[astro-ph.CO\]](#). 71
- [96] **EROS-2** Collaboration, P. Tisserand *et al.*, “Limits on the Macho Content of the Galactic Halo from the EROS-2 Survey of the Magellanic Clouds,” *Astron. Astrophys.* **469** (2007) 387–404, [arXiv:astro-ph/0607207](#). 71
- [97] D. J. Gross, R. D. Pisarski, and L. G. Yaffe, “QCD and Instantons at Finite Temperature,” *Rev. Mod. Phys.* **53** (1981) 43. 73
- [98] A. Hook, “TASI Lectures on the Strong CP Problem and Axions,” *PoS TASI2018* (2019) 004, [arXiv:1812.02669 \[hep-ph\]](#). 76, 85
- [99] K. J. Bae, J.-H. Huh, and J. E. Kim, “Update of axion CDM energy,” *JCAP* **09** (2008) 005, [arXiv:0806.0497 \[hep-ph\]](#). 78

- [100] G. 't Hooft, "Symmetry Breaking Through Bell-Jackiw Anomalies," *Phys. Rev. Lett.* **37** (1976) 8–11. [81](#)
- [101] J. A. Harvey, "TASI 2003 lectures on anomalies," 9, 2005.
[arXiv:hep-th/0509097](#). [81](#)
- [102] M. Shifman, *Advanced Topics in Quantum Field Theory: A Lecture Course*. Cambridge University Press, 2012. [81](#)
- [103] A. A. Belavin, A. M. Polyakov, A. S. Schwartz, and Y. S. Tyupkin, "Pseudoparticle Solutions of the Yang-Mills Equations," *Phys. Lett. B* **59** (1975) 85–87. [83](#)